Characterizing Humulone Content in Beer Using Differential Mobility Spectrometry

by

Qiuying Zhang

A thesis
presented to the University of Waterloo
in fulfilment of the
thesis requirement for the degree of
Master of Science
in
Chemistry

Waterloo, Ontario, Canada, 2018

© Qiuying Zhang 2018

Author's Declaration

I hereby declare that I am the sole author of this thesis. This is a true copy of the thesis, including any required final revisions, as accepted by my examiners.

I understand that my thesis may be made electronically available to the public.

Abstract

Beer is a complex fermented beverage and several hundreds of components have been identified erenow. Hops are extremely important to beer's organoleptic qualities, especially bitterness. Bitterness, a distinguishing component of beer's taste, is of concern for many beer brewing companies. Chemically, the bitterness of beers is associated with the content of iso-humulone, an isomerization product of tasteless natural humulone present in hops. Thus, it is vital to characterize humulone concentration profiles because brewers can utilize these to adjust desired beer properties. However, until now, there are some uncertainties of the quantitative relation between particular hop-derived compounds and sensory bitterness. In this research, the possibility of differential mobility spectrometry (DMS) technique being employed to separate and identify different humulone isomers has been explored. Results are compared against the UV-Vis spectrometry method, which is the conventional analytical technique used to determine the bitterness level of beer. Influence of external factors on the humulone isomerization and decomposition are also studied with rationalization from theoretical calculations.

Acknowledgements

First and foremost, I would like to acknowledge the help and guidance of my supervisor Dr. W. Scott Hopkins. During the graduate project, it has been over two years with your constant and generous help not only in my studies, but also in my life.

I would also like to thank my committee members Dr. Steven Innocente and Dr. Tadeusz Gorecki for guiding me through my thesis and making time for my presentations.

I would also like to express my gratitude to Hopkins group former and current members for their contributions to my research. I would specially like to thank Ce Zhou for reading my thesis and giving me helpful feedback, and I really appreciate Ce Zhou's efforts in filtering data and programing. Also thanks go to Stephen Walker for helping me with my research, and Ryland Scott for sharing his research results with me.

In addition, I would also like to acknowledge Dr. Jake Fisher for kindly providing UV-Vis spectrophotometer for this research. I would like to send my gratitude to Dr. Steven Innocente who provided all beer samples in this research.

Last, but not least, I would like to thank my family and friends. Special thanks to my parents for their support and encouragement.

Table of Contents

List of Figures

List of Tables

List of Abbreviations

AAU	Alpha Acid Unit
IBU	International Bitterness Unit
LC	Liquid Chromatography
MEKC	Micellar ElectroKinetic Chromatography
MS	Mass Spectrometry
m/z	Mass-to-Charge Ratio
UV-Vis	Ultraviolet-Visible Spectroscopy
ASBC	American Society of Brewing Chemists
DMS	Differential Mobility Spectrometry
PES	Potential Energy Surface
BH	Basin Hopping
MM	Molecular Mechanics
DFT	Density Functional Theory
UFF	Universal Force Fieled
CHelpG	Charges from electrostatic potentials using a grid based method
HF	Hartree-Fock
LDA	Local-Density Approximation
GGA	Generalized Gradient Approximation
B3LYP	Becke, three-parameter, Lee-Yang-Parr
IMS	Ion Mobility Spectrometry
CCS	Collision Cross Section
FAIMS	High Field Asymmetric Ion Mobility Spectrometry
ESI	ElectroSpray Ionization
SV	Separation Voltage
DC	Direct Current
CV	Compensation Voltage
IPA	Isopropanol
MO	Molecular Orbital
T	Transmittance

N_2	Nitrogen
MeOH	Methanol
H_2O	Water
EPI	Enhance Product Ion
EtOH	Ethanol
CS	Conscience
2NS	Two Night Stand
FL	Fling
KO	Kolsch
BS	Bystander
Bat	Batch-5 Dubbel Vision
In	Inn Oslainte
HCl	Hydrochloric Acid
PCM	Polarized Continuum Model

Chapter 1

Introduction

Beer is one of the oldest beverages produced from fermentation.[1] It was a necessity for people in the Middle Ages because water at that time, which was source of contagious diseases like cholera, typhoid fever,[2] could not be sanitized in an economically efficient way. The addition of hops (shown in Figure 1.1), which grow in all temperate climate zones, during the brewing process can be dated from the 6th century.[2] Even in a quantitatively minor composition, hops play a central role of determining the unique flavor of different beers. Although brewing technology has a long history, the correlation between the brewing process and the resulting beer's taste is only partially understood. The bitterness of beer is associated with iso-humulone, a compound formed via thermal isomerization from humulone, which is one of the essential contents of the hops. Hence, quantitation of humulone and iso-humulone in beer is needed not only for better quality control, but also for accurately tuning the bitterness of new beer products for their unique taste.[3]

Figure 1.1. Hops are used in the brewing process to introduce flavours to Beer.[4]

1.1 Isomerization of Humulone

With regard to beer brewing, the essential component in hops is humulone (see Scheme 1.1). Humulone itself is tasteless, but it isomerizes to the very bitter iso-humulone during the boiling stage of the brewing process.[1] The six-membered ring in humulone undergoes an acyloin rearrangement and yields a five-membered ring iso-humulone structure shown in Scheme 1.1.[5] Iso-humulone has two diastereomers, namely *cis* and *trans*, due to the existence of two chiral centers in the ring.[5] Note that two isomers can be derived from two chiral centers, but two of these can quickly interconvert and become racemic mixture in solution (Scheme 1.1). While *trans* iso-humulone can be isolated/purified, minor impurities are typically present in samples of the *cis* derivative.[2,6]

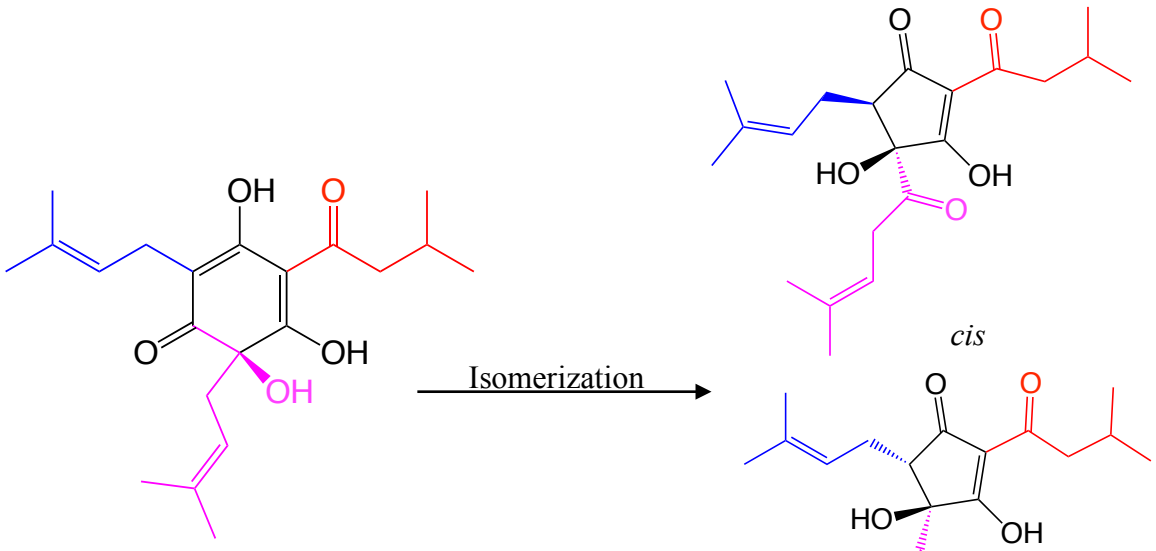

Humulone

Iso-humulone

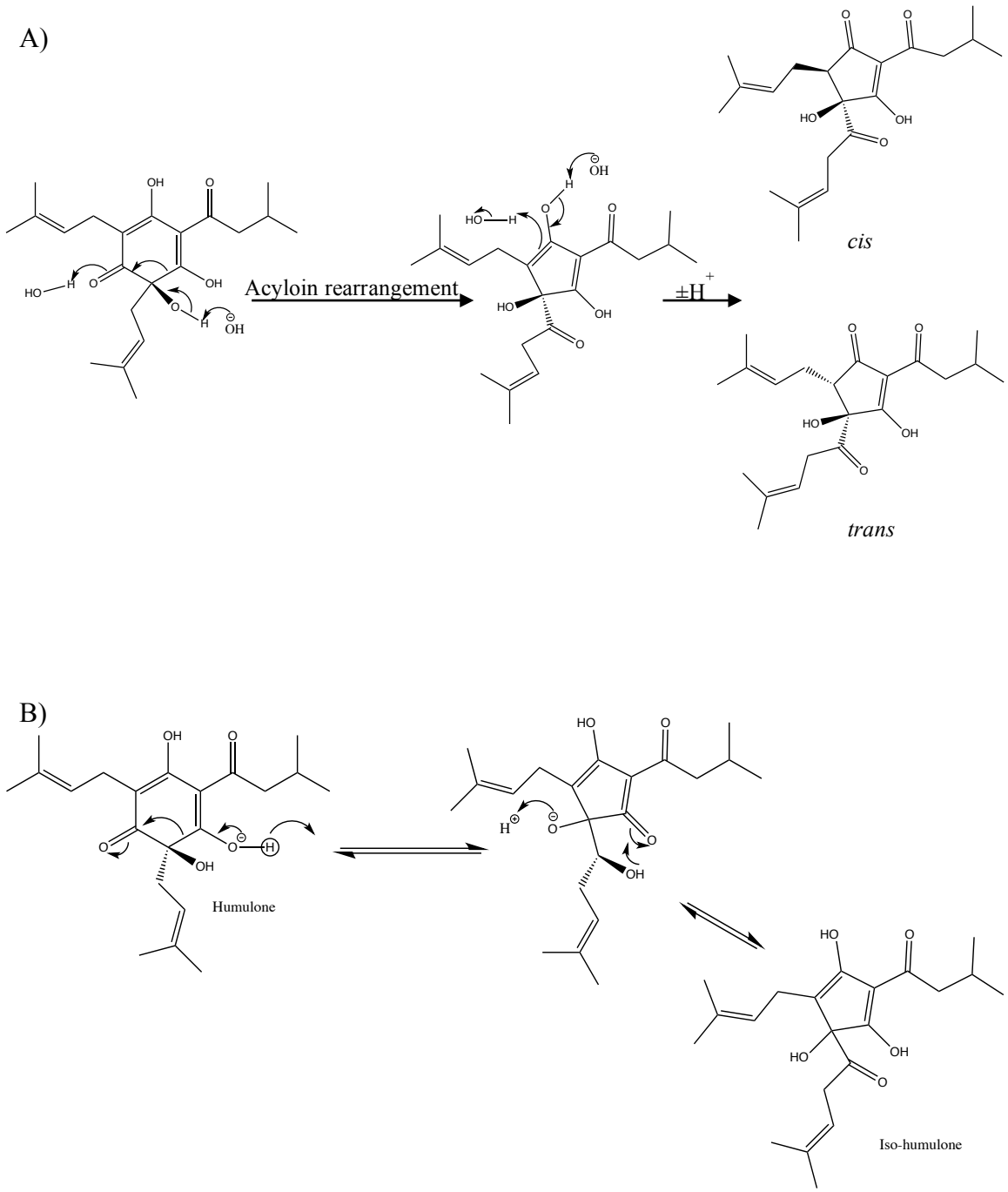

Scheme 1.1. (A) Isomerization reaction from humulone to iso-humulone. (B). Mechanism of acyloin rearrangement.[7]

As they are isomers, both humulone and iso-humulone have a molecular weight of 362 g/mol. Iso-humulone is stable in acidic condition, but it is light sensitive, which is one of the reasons for beer usually being stored in brown or green glass bottles.[2] In addition to the main contributor of bitterness in beer, iso-humulone also plays a role in flavor stabilization, anti-bacteria properties, as well as foam formation;[5] as the concentration of iso-humulone increases, so too does the volume of foam in a typical pour. The bacteriostatic properties of these hop-derived components ensure sterilization conditions during the boiling process.[2,6] The solubility of iso-humulone in beer ranges from 10 to 100 mg/L, much higher than the ~ 6 mg/L solubility in pure water.[5] This solubility increase could be due to the acidity of the beer environment and complexation with other components in the beer matrix.

There are several ways to describe bitterness in brewing. One metric of bitterness level is the alpha acid unit (AAU). The AAU is the weight of hops (in ounces) multiplied by the percentage of humulone in the hops, which indicates the bittering potential of the hop variety.[8] The International bitterness unit (IBU) is another analytical measurement of beer bitterness. IBU utilizes the iso-humulone content (in mg/L) of beer.[8] IBU values can be measured through spectrophotometric techniques, but the results of these measurements contain interferences from other compounds with similar spectral response.[8] As can be seen from their definition, AAU is dependent on the mass and type of the hop used in the brewing process while IBU is independent of those parameters.

1.2 Current Analysis Techniques

Conventionally, the bitterness level of beer is authenticated organoloptically by Cicerones (*i.e.*, Beer Sommeliers).[2] Consequently, the perceived IBU of a particular beer can differ between individuals. Therefore, instrumental characterization is also required to provide a unified bitterness/quality measurement.

Beer is a complex mixture of more than three hundred ingredients.[2] As there is synergistic effect amongst the components with regard to flavour, even a minor change in the concentration of an individual compound can result in significant alternation in the flavour of the final product. Previous studies indicate that iso-humulone contributes almost 80 % of the bitterness flavour.[2] Liquid chromatographic (LC) studies show that iso-humulone can be oxidized by the metal ions, which are from the metal contained in the materials of column, thus suggesting that water quality can dramatically impact the quality of the final product.[2] For LC analysis, special demineralized stationary phases must be utilized to reduce the oxidative degradation, and even then the metal ion contaminants and shelf-life of the column can result in signal loss during characterization.[2,9–11] As a consequence, characterization of iso-humulone *via* LC is not the preferred method. This is further exacerbated by the fact that pure samples of iso-humulone are expensive and difficult to obtain for uses as quantitative standards.[2,11]

Micellar electrokinetic chromatography (MEKC) is another method used to separate humulone and its isomers in beer.[2] This technique combines electrophoretic propulsion

with chromatographic partitioning.[12] Micelles (surfactants) are first added to a buffer solution; then, analyte species can be separated for micellization. Both ionic and neutral species can be analyzed by this method. A working schematic of MEKC is shown in Scheme 1.2.[13] Compared to the LC method, MEKC reduces oxidative degradation of iso-humulone. However, similar to the LC approach, a major problem of MEKC in quantification is the lack of suitable iso-humulone standards for calibration.

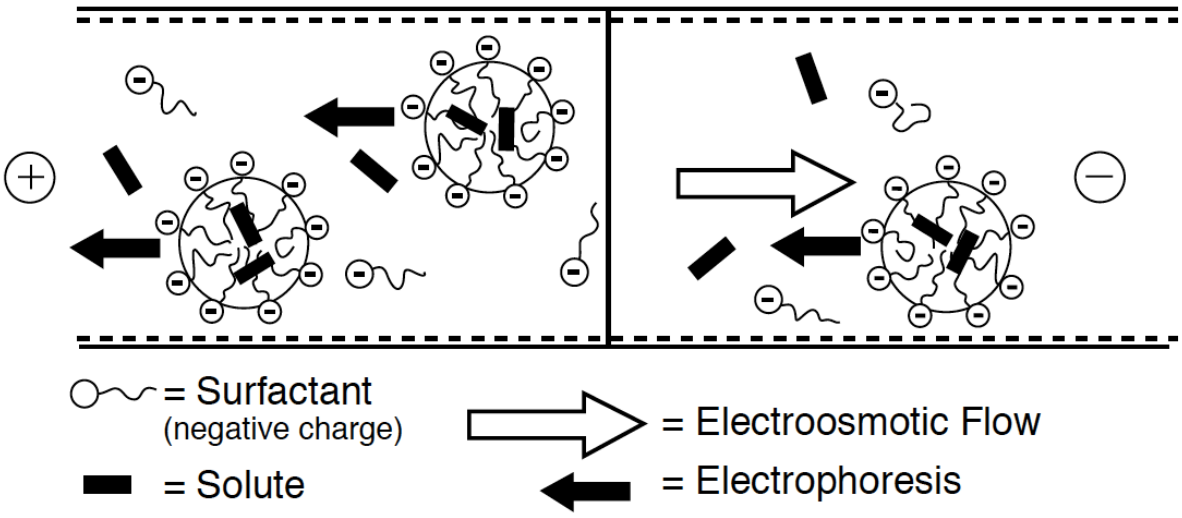

Scheme 1.2. Separation schematic of MEKC. In this case, the detector is assumed to be positioned near the negative electrode.[13]

Mass spectrometry (MS) is a well-established analytical method for chemical analysis.[14] MS analysis measures the mass-to-charge ratio (*m/z*), whereby the mass number (m) of molecular ion, an intrinsic property, is divided by charge number (z), of the chemical species.[14] Commonly, other instruments are coupled to MS for analytical characterization

of separation prior to MS characterization. For instance, LC-MS and MEKC-MS are ordinary "hyphenated" MS analysis techniques. These techniques have also been coupled with ultraviolet-visible spectroscopy (UV-Vis), *e.g.*, LC (LC-UV) and MEKC (MEKC-UV), for use in humulone characterization studies.[15] However, the American Society of Brewing Chemists (ASBC) recommends simple UV-Vis characterization as a stand-alone approach to describe the bitterness level in beer since this methodology is relatively inexpensive, is straightforward to implement and it yields results that are reasonably consistent with organoleptic analysis.[16] Herein, we investigate the efficacy of using differential mobility spectrometry (DMS) to characterize the isomers of humulone and compare this with the results of UV-Vis analysis.

Chapter 2

Introduction to Computational Methods

To elucidate the isomerization process and support experimental findings, quantum chemical calculations on a series of humulone isomers were conducted utilizing the Gaussian 09 software package.[17] Owing to the structural complexity of the molecules and clusters that we propose to study, it is necessary to conduct a systematic search of the potential energy surface (PES) for minimum structures. In this thesis, we employ the basin hopping (BH) search algorithm.[18] The molecular mechanics (MM) level of theory is utilized to screen candidate structures.[19] Then, more accurate electronic structure calculations at the density functional level of theory (DFT) are used to determine the relative energies of the candidate structures generated from the basin hopping simulation.

2.1 Basin Hopping

To find the global minimum structure of humulone and its isomers, the Basin Hopping (BH) algorithm is utilized (see Figure 2.1). The BH algorithm consists of cycles that randomly distort molecular parameters such as dihedral angles, followed by projection of the resulting structure onto the closest local minimum on the PES. By filtering those local minima identified from each cycle against a pre-defined energy barrier (expressed in terms of Boltzmann temperature), the algorithm biases the search towards the global minimum of the model potential energy landscape. An iteration of the search is defined as the

acceptance of new minimum structure.

Figure 2.1. Flow chart of BH search. E_i is the potential energy of the particular MM calculation, E_{GM} is potential energy of current global minimum, and α is random number between 0 and 1. This routine exits when the maximum number of iterations is reached.

In this work, 10,000 iterations, which is commonly used to sample most possible unique structures, are conducted for every BH simulation. The simulation volume (box size) is set to 15 Å cubed. The temperature is set at 2000 K which corresponds to thermally accessible barriers of 2000 K or less. The energy barrier for filtering the minima is adjusted for individual simulations to avoid local kinetic trapping.[20] The average energy barrier used in the simulations is about 175 meV. At each step, each free dihedral angle in the molecule is distorted by a random angle not exceeding 5°. After the BH simulation, those unique structures obtained undergo a hierarchy of optimizations up to the B3LYP/6-311G(d,p) or B3LYP/6-311++G(d,p) level. Frequency calculations are also conducted under the same basis set level as optimization calculations. The subsequent normal mode analyses confirm molecular structures are stable local minima or transition states, and provide thermal dynamic corrections to electronic energies. Computational results may then be compared to experimental data.

2.2 Molecular Mechanics

Molecular mechanics (MM) utilizes classical Newtonian force field models that describe molecules as balls and springs.[21–23] In this project, we use a full periodic table force field for MM, the Universal force field (UFF), which is composed of a set of hybridization dependent atomic bond radii, a set of hybridization angles, a set of effective nuclear charges, torsional and inversion barriers, and van der Waals parameters.[24] Thus, the MM total energy (E_{total}) consists of contributions from bond stretching ($E_{stretch}$), bond angle

bending (E_{bend}), dihedral angle torsion ($E_{torsion}$), and inversion terms ($E_{inversion}$); and non-bonding interactions from van der Waals terms (E_{vdw}) and electrostatic terms (E_{el}).[24] The analytical form of the force field is given in Equation 2.1 and Equation 2.2.[24]

$$E_{total} = \underbrace{E_{stretch} + E_{bend} + E_{torsion} + E_{inversion}}_{\text{bonding interactions}} + \underbrace{E_{vdw} + E_{el}}_{\text{non-bonding interactions}} \qquad \text{Equation 2.1}$$

$$E_{total} = \underbrace{\sum_{Bonds} K_r(r - r_{eq})^2 + \sum_{Angles} K_\theta(\theta - \theta_{eq})^2}_{\text{bonding interactions}} + \underbrace{\sum_{i<j}\left[\frac{A_{ij}}{r_{ij}^{12}} - \frac{B_{ij}}{r_{ij}^{6}} + \frac{q_i q_j}{\varepsilon r_{ij}}\right]}_{\text{non-bonding interactions}}$$

Equation 2.2

For the MM calculations, partial charges for individual atoms are first estimated from a "guess" B3LYP/6-311+G(d,p) optimized structure *via* the CHelpG partition scheme. The subsequent MM calculations are quick, but have limited accuracy. Thus, to improve accuracy, higher level DFT calculations are employed on the unique MM structures.

2.3 Density Functional Theory

Density functional theory (DFT) is an *ab initio* quantum chemical electronic structure method, which deals with the molecular electron density. The electron density is described as the integral over the spin coordinates of all electrons and over all but one of the spatial variables.[25,26]

$$\rho(\vec{r}) = N \int \dots \int |\Psi(\overrightarrow{x_1}, \overrightarrow{x_2}, \dots, \overrightarrow{x_N})|^2 ds_1 d\overrightarrow{x_2} \dots d\overrightarrow{x_N} \qquad \text{Equation 2.3}$$

In Equation 2.2, $\rho(\vec{r})$ determines the probability of discovering any of the *N* electrons

within volume element $d\vec{r}$.[25,26] For DFT, the total energy is expressed in terms of electron density, which itself is a function of the basis orbitals (hence "functional", which is a function of a function). Thus, DFT emphasizes minimizing the spatially-dependent density functional.[27] In early DFT treatments, the exchange correlation energy was not treated explicitly. However, modern developments have yielded functionals which include exact Hartree-Fock (HF) exchange and now there are several different ways of representing this exchange energy.[25,26] It is critical that this quantum mechanical phenomenon be treated accurately in calculations designed to calculate relative thermodynamic energies of, *e.g.*, isomers. With the application of DFT techniques which explicitly treat electron correlation effects, one may achieve excellent accuracy (usually within a few kJ mol^{-1}) at a much more affordable computational cost than common wave function based approaches, especially for large molecular systems.[22,27]

There are three major categories of density functionals: (i) LDA, (ii) GGA, and (iii) hybrid methods. The oldest type, the local-density approximation (LDA) method, assumes energy depends only on the electron density and not, *e.g.*, the Kohn-Sham orbitals or derivatives of the density.[27] The accuracy of DFT is improved using the Generalized Gradient Approximation (GGA), which more realistically depicts molecules with nonhomogeneous electron density due to the incorporation of density gradients.[27] Here we use the B3LYP hybrid method, which combines GGA and exact HF exchange to improve the accuracy of total energy calculations.[28] B3LYP, which stands for the "*Becke, three*

parameter, Lee-Yang-Parr" functional, is a common choice of functional for organic compounds like humulone and its isomers and it has been demonstrated to yield excellent results.[17]

Chapter 3

Introduction to Experimental Methods

The experimental methods utilized in this work and their underlying theories are described in this chapter. Each method is distinct in both its underlying principles and data offered, so that a benefit is conferred when a combination of experimental methods is utilized.

3.1 Differential Mobility Spectrometry

Ion mobility spectrometry (IMS) is extensively used to characterize ions in terms of their unique transportation properties, which are affected by the surrounding environment when these ions pass through the instrument cell driven by an external electric field.[29–32] In the IMS separation region, ions are transported by a gas phase medium, and they are exposed to an electric field (E).[14] Because of the Coulomb force, the ions experience acceleration, which is mitigated by collision with carrier gas molecules.[14] This yields a characteristic equilibrium drift velocity, v_d, which is described by the expression:[14]

$$v_d = K \cdot E \qquad \text{Equation 3.1}$$

Where, K is the ion mobility, and E is the electric field. If the IMS instrumentation is operated at low electric fields, the Mason-Champ equation (Equation 3.2) may be used to describe ion mobility:[14]

$$K = \frac{3}{16}\left(\frac{2\pi}{\mu k_B T}\right)^{\frac{1}{2}} \frac{ze}{N\Omega} \qquad \text{Equation 3.2}$$

Where μ is the reduced mass of the ion / collision gas system:

$$\mu = \frac{mM}{m+M} \qquad \text{Equation 3.3}$$

Where M is the molecular mass of the ion and m is the molecular mass of carrier gas. In equation 3.2, k_B is the Boltzmann constant, T is the gas temperature, z is the molecular charge, *e* is the elementary charge, N is the number density (number of molecules per unit volume), and Ω is the collision cross section.[14]

In differential mobility spectrometry (DMS), ion are subjected to oscillating electric fields which have a low-field and a high-field component.[14] It turns out that ion mobility is field-dependent and can vary dramatically between the low-field and high-field conditions. This differential ion mobility can be expressed as:[14]

$$K\left(\frac{E}{N}\right) = K_0 \times \left[1 + \alpha\left(\frac{E}{N}\right)\right] \qquad \text{Equation 3.4}$$

Which is oftentimes reported in the form:

$$\alpha\left(\frac{E}{N}\right) = \frac{K\left(\frac{E}{N}\right) - K_0}{K_0} \qquad \text{Equation 3.5}$$

Here, N is the number density, $K_0 = K(E)_{|E=0}$ is the mobility of ion under low electrical field, and $\alpha\left(\frac{E}{N}\right)$ is an empirical term that describes the field-dependence of the mobility under the given carrier gas composition, pressure, and temperature conditions.[14,33–35]

IMS is typically used as a pre-filter for mass spectrometry (MS). IMS first separates ions based on size (*viz.*, collision cross section; CCS) prior to MS characterization.[14] Since

isomeric species have different geometric structures, they can potentially be separated and quantified by traditional linear drift tube IMS.[14] However, in practice, it is difficult to resolve species with very similar CCS (like isomers) using traditional IMS techniques. Since DMS takes advantage of mobility differences between high- and low-field conditions, and field oscillations occur at a frequency of *ca*. 3 MHz, slight differences in isomer differential mobilities can be sampled several tens of thousands of times during ion transit of the DMS cell. This oftentimes results in significantly improved separation when compared to IMS.[31,36] However, DMS is not without its drawbacks, the most important of which is the fact that differential mobility is not well understood from a theoretical standpoint. Consequently, a first principles model of DMS separation is not available. Nevertheless, one can confidently interpret DMS data by expanding the analytical method to include additional information from mass spectrometry (*i.e.*, *m/z*, fragmentation spectra, breakdown curves, hydrogen-deuterium exchange profiles)[14] and quantum chemical calculations.

An expanded diagram of the DMS apparatus is shown in Figure 3.1. DMS has four main components: (i) a sample introduction system, (ii) an ionization region, (iii) a differential mobility cell (separation and selection region), and (iv) a detection region (*e.g.*, MS). The differential mobility cell typically adopts one of two geometries; either a cylindrical system (known as FAIMS) or a planar geometry (referred to as DMS).[14] A major advantage of DMS over FAIMS is that one may continuously introduce ions, and hence

monitor all analytes (cations and anions) in real time, by setting the cell voltages to zero since the DMS cell does not impede ion flow to the electrondes.[14] One can thus easily monitor the effect of the applied fields on analyte trajectories.

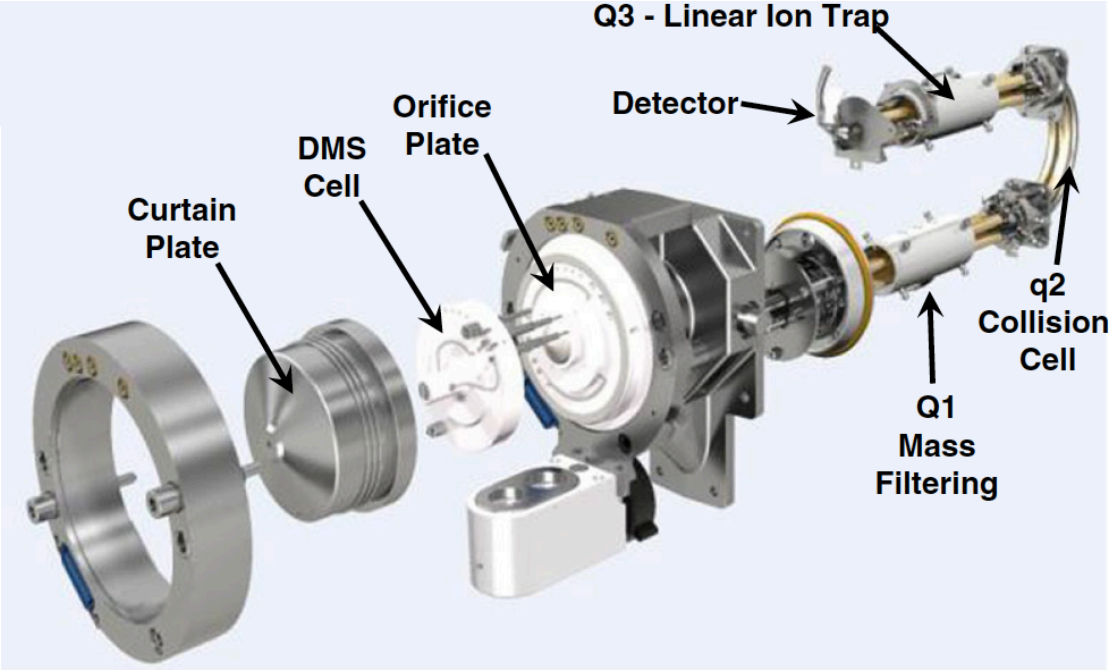

Figure 3.1. DMS apparatus coupled with mass spectrometer.[29]

A schematic diagram of the DMS cell is shown in Figure 3.2.[36] For the experiments described herein, gas phase ions are first generated from an electrospray ionization (ESI) source, then carried through the DMS cell *via* a N_2 gas flow.[33] In the DMS cell, there are two parallel planar electrodes between which a radio frequency alternating electric field of asymmetric sinusoidal waveform, known as the separation voltage (SV).[37] Due to the modulated SV, the trajectory of the ions forms a zigzag-like pattern along the longitudinal axis of the cell.[36] The combination of the asymmetric waveform and the collisions with

carrier gas results in deviation of ion trajectories off of the DMS cell axis and migration of the ions towards one of the planar electrode. Applying an additional DC voltage, referred to as the compensation voltage (CV), redirects the ion's trajectory through the DMS cell.[37] Consequently, the behavior of ions within a DMS cell is encoded by the specific SV/CV settings for optimal transmission. By scanning CV at a fixed SV, one generates an ionogram, as shown in Figure 3.3. By plotting the optimal CV for ion transmission as a function of SV, one generates a dispersion plot, as shown in Figure 3.4.[36]

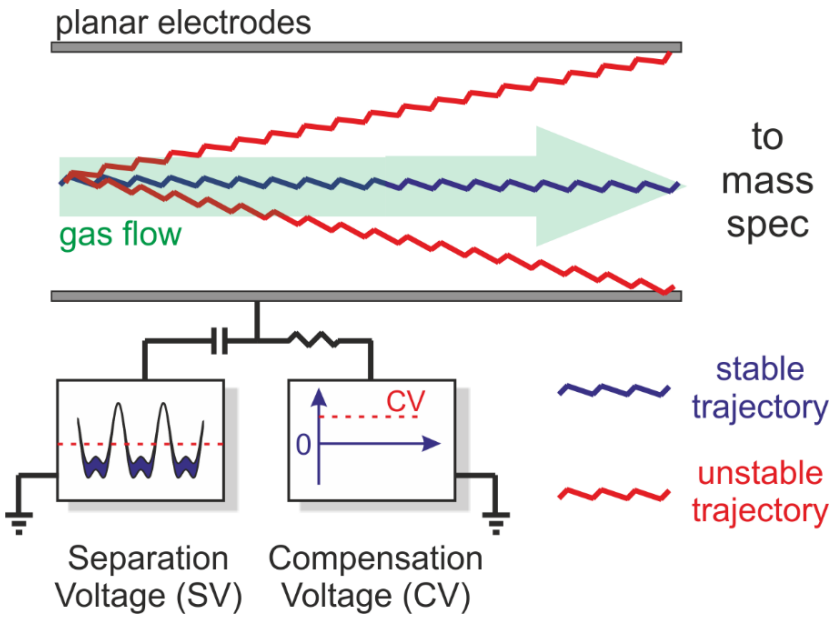

Figure 3.2. Schematic diagram of DMS.[36]

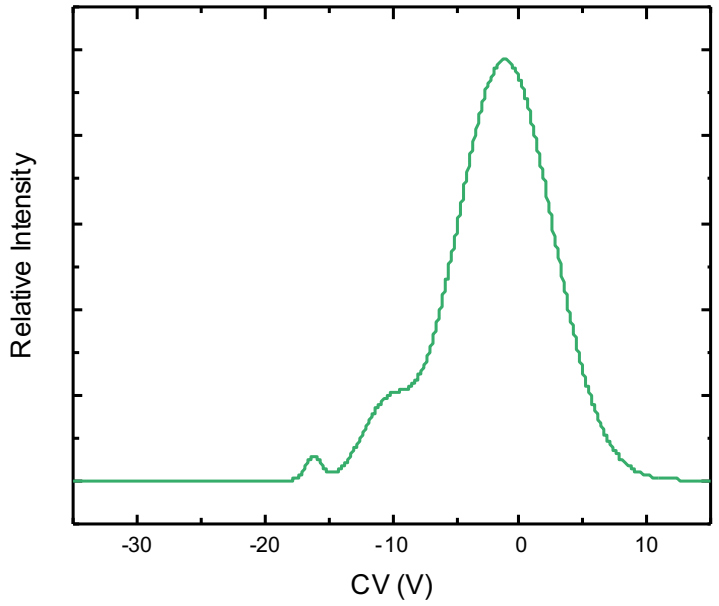

Figure 3.3. Ionogram of an analyte optimal transmission occurs at CV = 0 V.

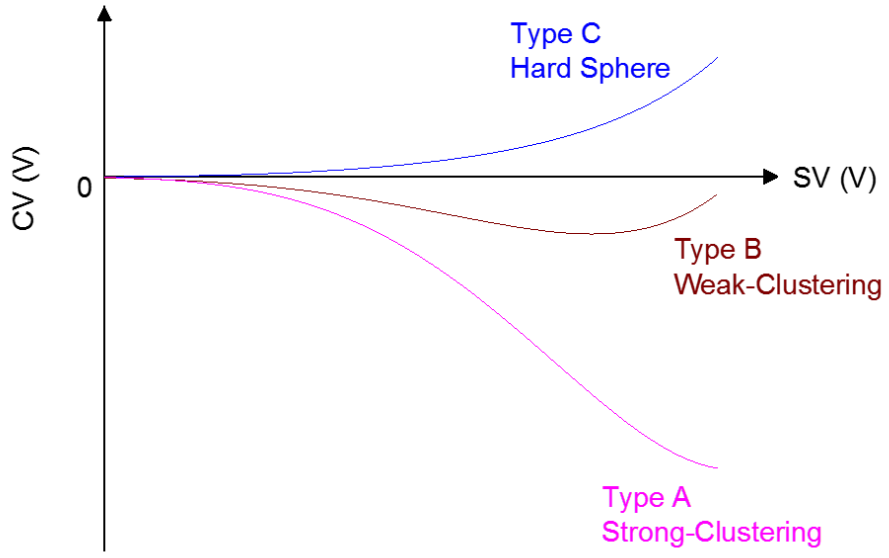

Figure 3.4. Typical ion behavior in DMS as visualized in a dispersion plot.[36]

The dispersion plot can be utilized to intuitively visualize the ions behavior in the DMS cell.[36] As shown in Figure 3.4, there are three general types of ion behavior. Type A behavior, where CV decreases with increasing SV, indicates a strong clustering interaction between analyte and the collision gas in the DMS cell.[36] This behavior is usually observed following the addition of polar solvent vapour to the N_2 carrier gas. Type C behavior, whereby CV increases with increasing SV, indicates that there are negligible ion-solvent interactions, and that the ions behave like "hard spheres" during collisions as they travel through the DMS cell.[36] This behavior is usually observed in pure N_2 or He environments.[36] Type B behavior is an intermediate case to Type A and C. In this case, CV decreases with increasing SV at low SV, and then increases with increasing SV at high SV. This behavior is indicative of weak clustering between analytic ions and carrier gas molecules. In the low-field portion, weak clustering occurs between analytic ions and gas molecules; however, in the high-field portion, de-clustering occurs due to high energy collisions between sample ions and gas molecules, and then ions exhibits "hard sphere" behavior.[29]

In addition to visualizing ion-solvent interaction strengths, inspection of the dispersion plot can provide the SV/CV settings for the most efficient separation of analytes. An example ionogram showing diastereomers separation is shown in Figure 3.5. Under the most efficient separation conditions, the ionogram shows three peaks, indicating that there are three diastereomers present in the probed ensemble. In contrast, the ionogram shown in Figure 3.3, contains only a single peak, which indicates that the analyte exhibits only

one geometric structure, or that the geometries of multiple structures are so similar that those species are not resolved under the experimental conditions utilized.

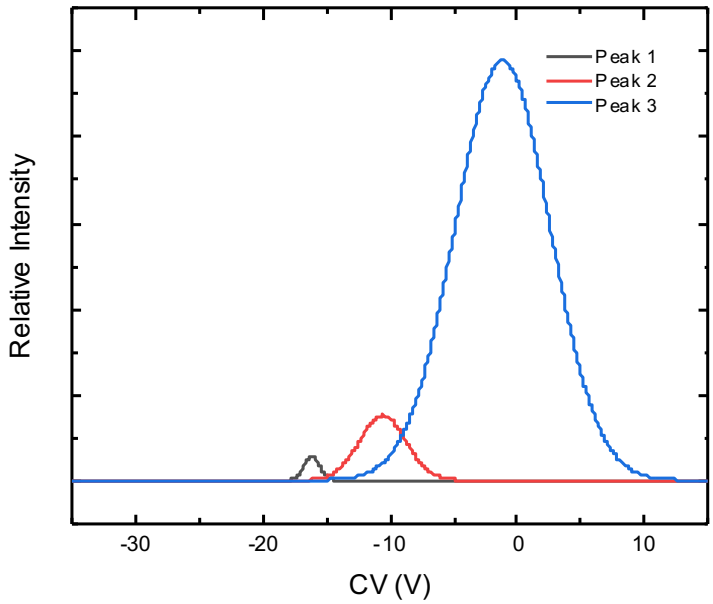

Figure 3.5. Ionogram of separation of analyte optimal transmission occurs at CV = –18 V, CV = –15 V, and CV = 0 V.

To improve analyte separation, the carrier gas of the DMS cell can be modified by introducing a volatile solvent vapour (*e.g.*, isopropanol; IPA).[29] Addition of a modifier can alter the SV/CV conditions required to transmit an analyte ion through the DMS cell owing to dynamic clustering/de-clustering interactions between the modifier molecules and the analyte.[29,32,38] The analyte ions cluster with the modifiers under the low-field portion of the SV, while in the high-field portion, de-clustering of the analyte-modifier complex

spontaneously takes place.[39] Thus, the ions exhibit artificially large CCSs under the low field condition due to microsolvation. Since the ions undergo thousands of clustering/de-clustering cycles during their transit through the DMS cell, the dynamic clustering process can cause substantial deviations of ion trajectories compared to the hard sphere N_2 environment. Moreover, since different isomers/conformers have slightly different ion-solvent interaction potentials, the associated differences in dynamic clustering can lead to significant differences in isomer trajectories through the DMS cell. This results in improved separation of the isomeric species. Since analyte trajectories, and therefore separations, in the DMS cell depend strongly on the analyte-modifier binding energies (*viz*. interaction potentials), selecting an appropriate collision gas composition is important. The choice of modifier is based on the structure of the ions, the properties of the modifier (*i.e.*, vapor pressure), and the binding interactions between the ion and modifier.[29,40] For example, humulone possesses hydroxyl and carbonyl groups (see Scheme 1.1 for structures), which means that the chosen modifier is likely to interact strongly *via* intermolecular hydrogen bonding. Iso-humulone, on the other hand, can exhibit intramolecular hydrogen bonding to partially mask polar functional groups. Thus, the binding energy of the solvent with iso-humulone is likely to be less than that of humulone. By taking advantage of such structural differences and differences in interaction potential, one can isolate each isomeric form.

3.2 Ultraviolet-Visible Spectroscopy

The Ultraviolet-Visible spectroscopy (UV-Vis) technique is widely utilized for

qualitative and quantitative analyses of molecules. The underlying principle of UV-Vis is the absorption of light to excite molecular electronic transitions in the ultraviolet and visible regions of the electromagnetic spectrum (shown in Figure 3.6).[41]

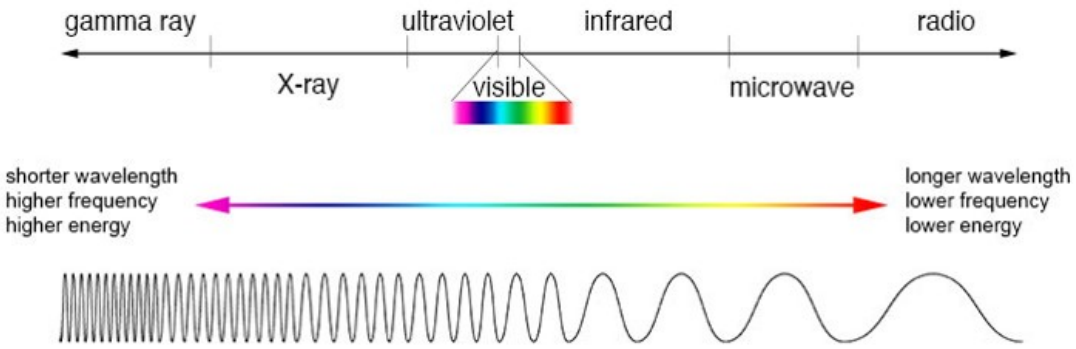

Figure 3.6. The electromagnetic spectrum.[42]

Electronic transitions provide information about the bonding and electronic structure of molecules, and can be used as a tool for molecular identification.[43] The frontier molecular orbitals (MOs) commonly probed with UV-Vis spectroscopy are: σ (bonding orbital), π (bonding orbital), n (non-bonding orbital), σ^* (anti-bonding orbital), and π^* (anti-bonding orbital); electronic transitions may occur between any two of these MOs, but typically absorptions are associated with promotion of electronic population from the ground state. In general, a relatively large amount of energy is required to satisfy $\sigma \rightarrow \sigma^*$ and $n \rightarrow \sigma^*$ transitions. Hence, the light absorption associated with these transitions, typically occurs in the far ultraviolet region (180-240 nm).[43,44] In comparison, $n \rightarrow \pi^*$ and

$\pi \rightarrow \pi^*$ transitions typically occur at lower energy, so the absorbed radiation is of lower frequency and longer wavelength. Conjugated π systems, which consists of alternating single and double bonds, typically absorb in the visible region.[42] A summary of common electronic transitions is provided in Figure 3.7. Humulone, for example, can potentially exhibit $n \rightarrow \sigma^*$, $\pi \rightarrow \pi^*$, and $n \rightarrow \pi^*$ transitions.

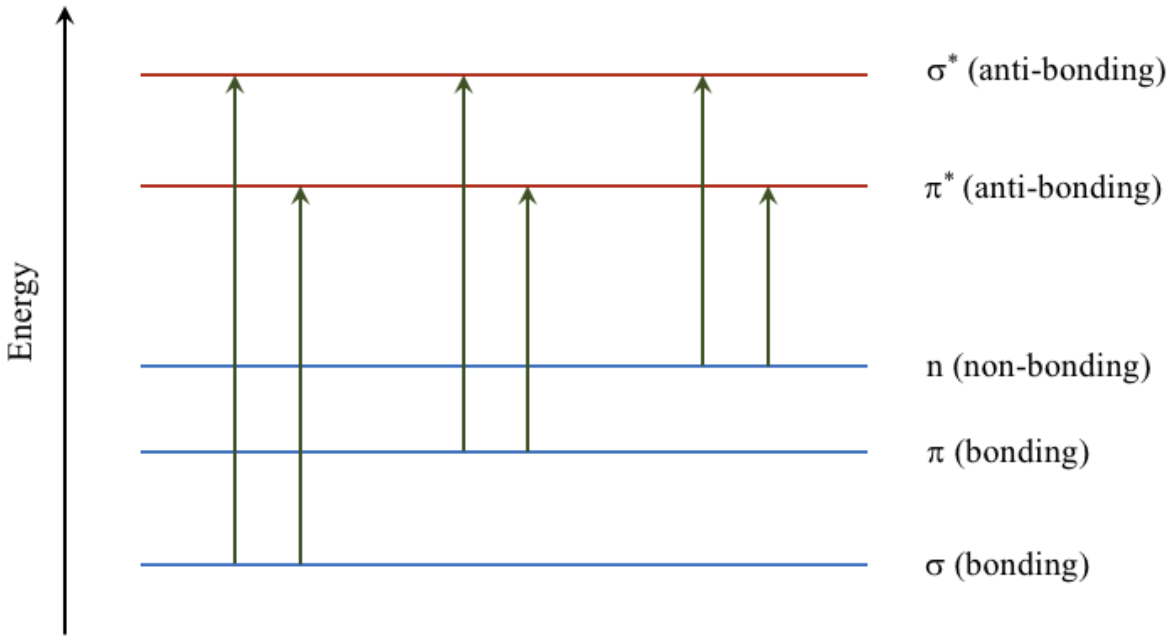

Figure 3.7. Possible electronic transitions in UV-Vis spectroscopy.[43]

The Beer-Lambert Law describes the absorbance of light by matter.[43]

$$A = \log\left(\frac{I_0}{I}\right) = -\log\left(\frac{T(\%)}{100}\right) = \varepsilon bC \qquad \text{Equation 3.6}$$

Here, A is the absorbance, I_0 is the incident light intensity, I is the transmitted light intensity, ε is the molar extinction coefficient (molar absorptivity), *b* is the pathlength (length of the

cuvette), and C is the concentration of the solute. The transmittance (T) is defined as I/I_0, and the percentage form, %T, is often used to express the intensity of absorption.

Experimentally, the electronic transitions of a compound can be measured *via* a bench-top UV-Vis spectrometer.[42] For the UV-Vis spectrometer, the light source should provide output over the range of 200 – 800 nm. This is achieved in this work with a deuterium lamp (190-400 nm) and a tungsten halogen lamp (300-2500 nm).[45] The monochromator, which includes a diffraction grating, separates the incoming light to different wavelengths. The separated light then passes through separate arms containing cuvettes filled with analyte and blank samples, respectively. The intensity of the reference is defined to be 100% Transmission (or zero Absorbance), and sample absorption is calculated as the ratio of two beam intensities. The final light signal is converted to electric current by photodiodes, one for the sample beam and one for the reference beam.[43] A schematic diagram is given for the UV-Vis spectrometer in Figure 3.7.

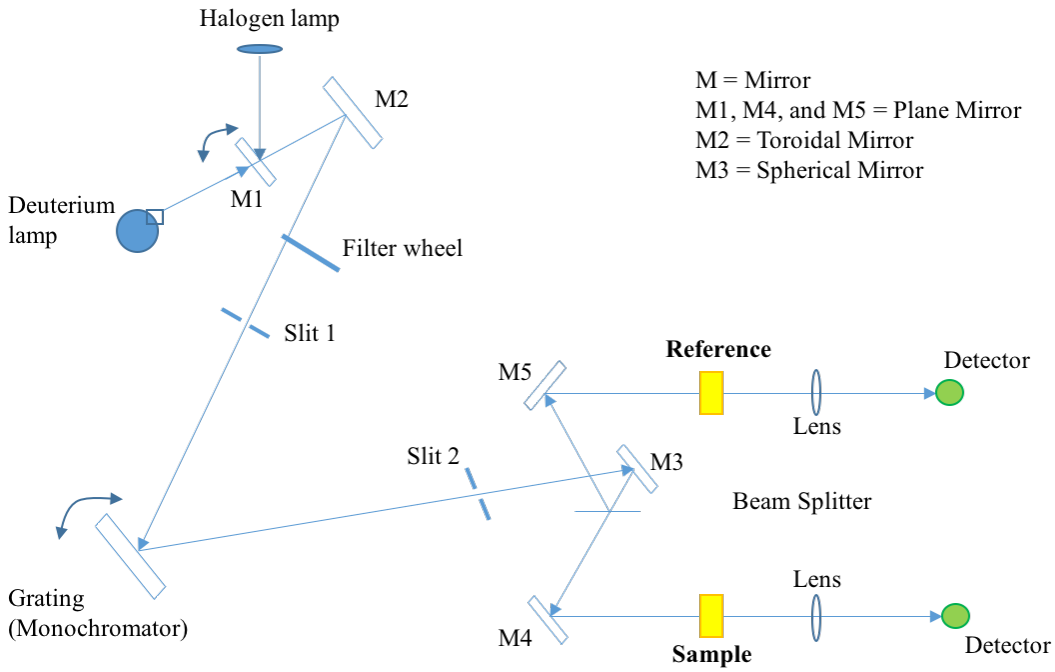

Figure 3.8. Schematic diagram for double-beam UV-Vis spectrophotometer.[42]

Chapter 4

DMS/MS of Humulone

To begin our studies of humulone content in beer, it is necessary to establish protocols for detecting humulone in the DMS-MS apparatus. A first step in this regard is the characterization of a humulone standard.

4.1 Experimental Details

HPLC-grade acetone, acetonitrile, isopropanol (IPA), methanol, ethanol, acetic acid, and formic acid reagents were purchased from Sigma-Aldrich and were utilized without further purification. Analytical grade humulone (2 mg/mL in MeOH/H_2O solvent) was purchased from Carbosynth. Ultra-pure water (18 MΩ) was generated by Z00Q0V0WW Milli-Q Advantage A10 Water Purification System.

The DMS instrument (SelexION, SCIEX, Concord, ON, Canada) is mounted between the vacuum sampling interface of a research-grade QTRAP 5500 system (SCIEX), and a Turbo ESI source.[46] The ESI probe is sustained at a voltage of 5500 V, and the source temperature is 100 °C. The DMS cell temperature is set at 150 °C. In the DMS cell, nitrogen is used as the carrier gas (250 μL/min), and the chemical modifiers, which are entrained in the N_2 carrier using a Perkin Elmer 200 liquid chromatographic pump (Waltham, MA, USA), are gases added at 1.5% (mol ratio). SCIEX Analyst version TF 1.7.1 and SCIEX Peak View version 2.2 were utilized to handle the instrument and record data. The

analytical grade humulone sample is diluted down to a concentration of 100 ng/mL in methanol/water (1:1) for electrospray.

4.2 DMS/MS Results

Under negative-ion ESI conditions, deprotonated humulone and its isomers may be monitored *via* the mass peak at *m/z* 361. The dispersion plots collected for *m/z* 361 under a pure nitrogen (N_2) environment, and in environments seeded with 1.5% methanol (MeOH) and isopropanol (IPA) vapour, are shown in Figure 4.1. A single peak exhibiting Type C behaviour is present under pure N_2 conditions, suggesting the presence of only a single isomer in the sample. However, when MeOH modifier is introduced, one traces exhibiting Type B behaviours are observed.[36] Introducing the stronger clustering IPA modifier results in a single trace with the Type A behaviour. This may result from IPA having a higher gas-phase proton affinity than one isomer, leading to charge scavenging and signal loss for that species.[47] Alternatively, both isomers/tautomers might exhibit very similar interactions with IPA and thus be indistinguishable via DMS with a modified IPA environment.[47,48] Because the protonated cationic signal (*m/z* 363) was weak and masked by noise, analogous positive mode studies not utilize in this research (see supporting information in Appendix III Figure A3.1).[49–51] The separation voltage was set to SV = 3500 V, and the CV range was stepped from –35 V to 5 V in 0.25 V increments. The resulting ionogram of deprotonated humulone (100 ng/mL in MeOH/H_2O solvent) as observed in the N_2 environment seeded with IPA is shown in Figure 4.2.A. By setting the SV = 3500 V and

CV = –18 V, the DMS cell acts as a narrow pass filter to select the deprotonated humulone for subsequent study. The resulting mass spectrum of deprotonated humulone is shown in Figure 4.2.B. Previous work identified the signal at *m/z* 125 ($C_7H_9O_2$) as a common fragment ion of humulone and iso-humulones (see Figure 4.2).[9] Note that the fragmentation spectrum is missing the parent peak at *m/z* 361 ($C_{21}H_{29}O_5$). Attempts were made to create softer ionization conditions, but the parent peak could not be isolated. The absence of parent peak for humulone is attributed to the fact that the collision energy (CE) has a minimum setting of 5 V; thus deprotonated humulone must fragment at a lower CE. The observed fragments are assigned in Table 4.1.

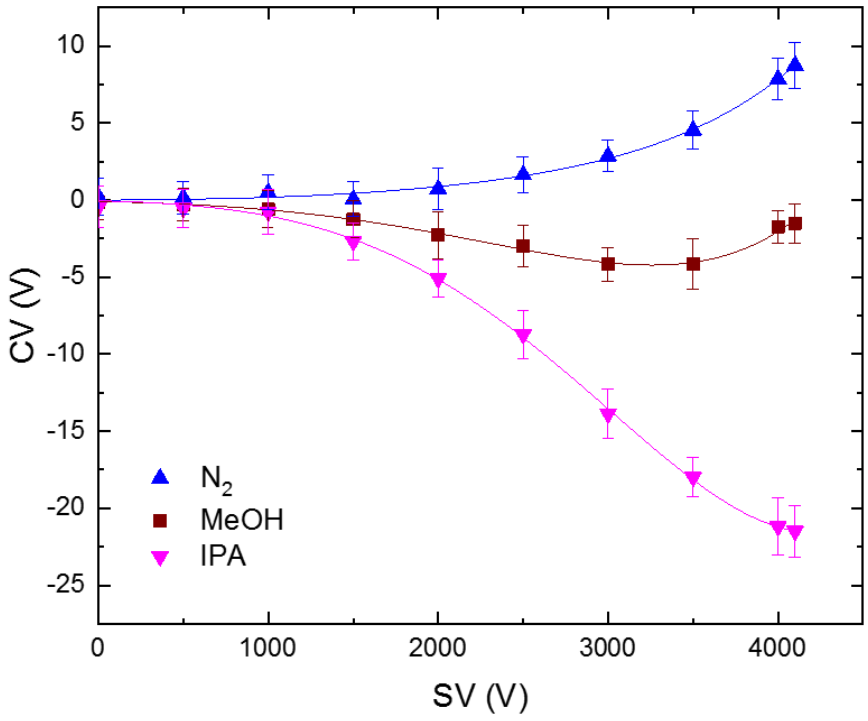

Figure 4.1. The dispersion plot recorded for deprotonated humulone (*m/z* 361) under DMS cell with a pure N_2 environment, and a N_2 environment with 1.5% (mol ratio) methanol vapor and IPA vapor. Error bars are 2σ obtained from Gaussian fits to the ionogram peaks.

Table 4.1. Molecular fragments of deprotonated humulone.

m/z	Molecular formula	Fragmentation
331	$C_{20}H_{27}O_4$	Loss of H_2CO from parent
315	$C_{20}H_{27}O_3$	Loss of HCOOH from parent
297	$C_{20}H_{25}O_2$	Loss of H_2O from *m/z* 315
282	$C_{19}H_{22}O_2$	Loss of $\bullet CH_3$ from *m/z* 297
189	$C_{12}H_{13}O_2$	Loss of C_7H_9 from *m/z* 282
107	C_7H_7O	Loss of H_2O from *m/z* 125

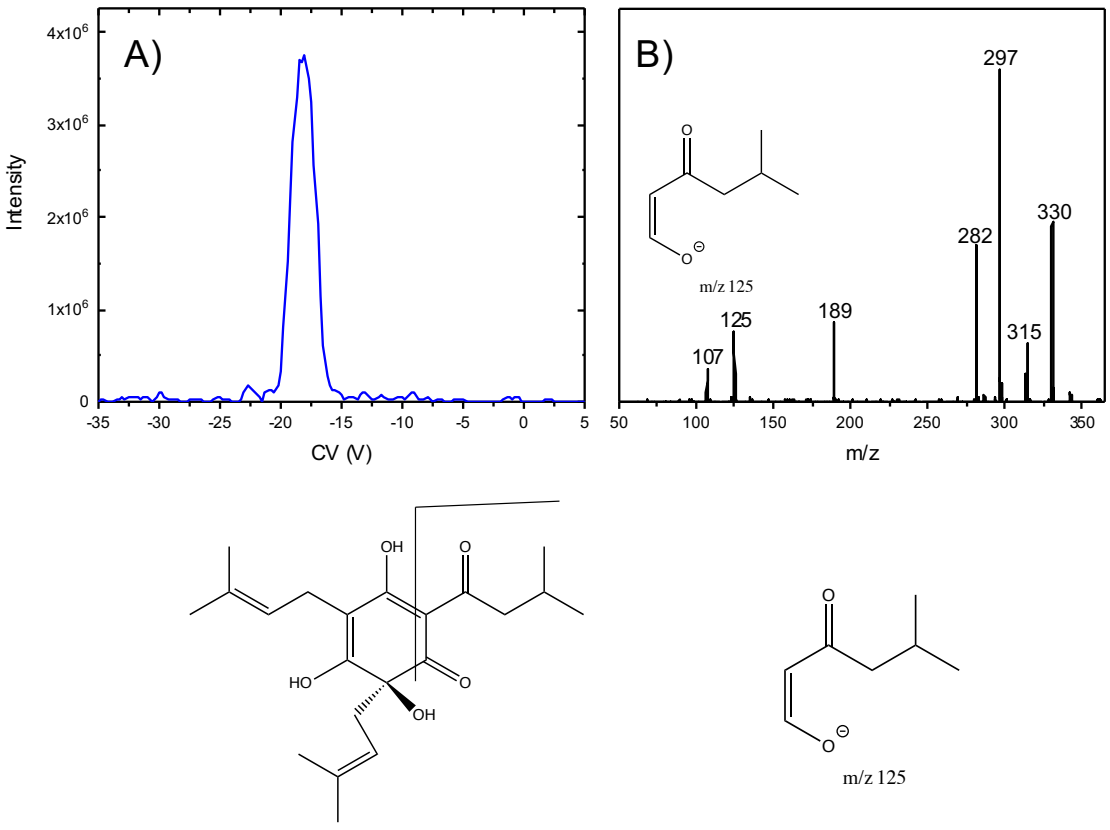

Figure 4.2. (A). The ionogram of deprotonated humulone, (*m/z* 361) recorded in a N_2 environment seeded with 1.5% (mol ratio) IPA at SV = 3500V. (**B**). The mass spectrum observed when setting the DMS to transmit the ions at CV = –18 V.

When the pure humulone sample (2 mg/mL in MeOH/H_2O solvent) is stored in a brown glass bottle in a dark environment at 4 °C for one year, significant changes are observed in the ionogram (see Figure 4.3.A). The ionogram peak at CV = –18 V is nearly depleted, and a new peak is observed at CV = –15 V. There is also some evidence of a weak signal in the CV = –5 to 0 V region of the ionogram. This suggests that isomerization is occurring in the MeOH/H_2O solution, a result which is further supported by the fact that the associated fragmentation spectrum of the CV = –15 V peak differs from that of the CV = –18 V peak. In this case, the diagnostic *m/z* 125 fragment is still observed, and the base peak is *m/z* 360. There are also minor fragments observed at *m/z* 300 and 316. Clearly, one-year storage is well beyond the expected shelf life of beer. However, this result does support the hypothesis that the α-acid chemical composition, and therefore flavour profile, of beer is likely to evolve even when stored in the dark at T = 4 °C. To explore this isomerization process in more detail, a temperature study was conducted.

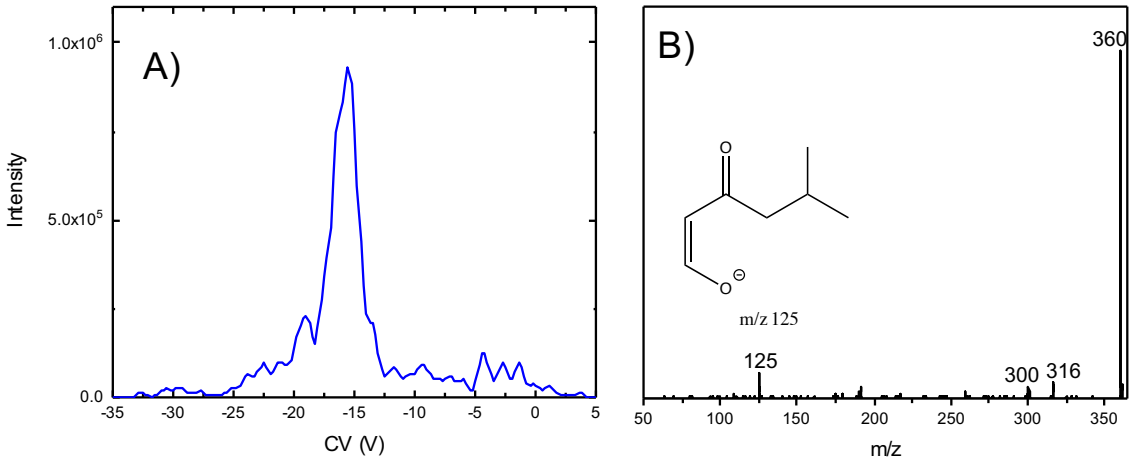

Figure 4.3. (A). The ionogram of the pure humulone standard after storage at 4 °C for one

year, which is diluted to 100 ng/mL by MeOH/H_2O solvent, records for the *m/z* 361 peak under N_2 environment with 1.5% (mol ratio) IPA at SV = 3500 V. **(B).** The associated mass spectrum of **A**.

4.3 Temperature Studies

To further investigate the isomerization of the humulone standard, a series of measurements were conducted at T = 18 °C, 37 °C, 50 °C, 70 °C, and 100 °C. Samples were held at these temperatures and aliquots were extracted for analysis at regular 15 minute intervals for two hours. Figure 4.4 shows the ionograms and associated mass spectra obtained when heating at 37 °C. Negligible changes are observed in either the ionogram or mass spectrum over the two hour sampling period. The same is true for experiments conducted at T = 50 °C (see Figure 4.5).

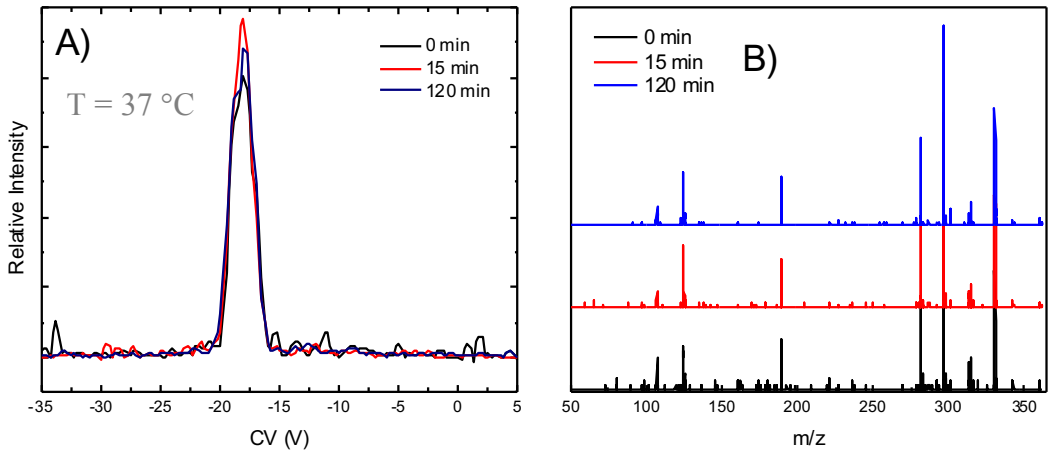

Figure 4.4. (A). The ionogram observed for deprotonated humulone when the ESI solution is heated to 37 °C for (black trace) 0 min, (red trace) 15 min, and (blue trace) 120 min. The humulone standard was diluted to 100 ng/mL in 1:1 MeOH/H_2O solvent. Measurements were acquired in an N_2 environment seeded with 1.5 % (mol ratio) IPA with SV = 3500 V. (**B**). The mass spectra associated with ionograms shown in **A**.

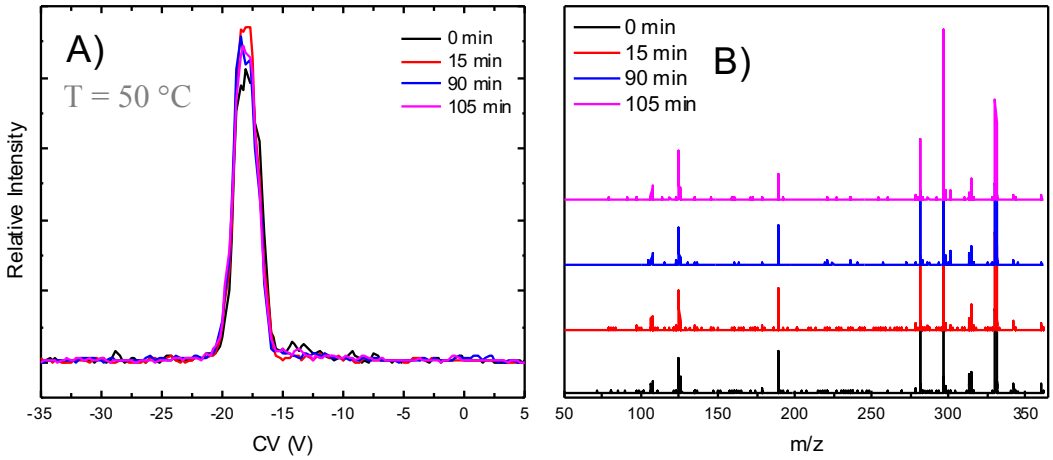

Figure 4.5. (A). The ionogram observed for deprotonated humulone when the ESI solution is heated to 50 °C for (black trace) 0 min, (red trace)15 min, (blue trace) 90 min, and (pink trace) 105 min. The humulone standard was diluted to 100 ng/mL in 1:1 MeOH/H_2O solvent. Measurements were acquired in an N_2 environment seeded with 1.5 % (mol ratio) IPA with SV = 3500 V. (**B**). The mass spectra associated with ionograms shown in **A**.

Interestingly, when the solution temperature is set to 70 °C (see in Figure 4.6), there is some evidence of isomerization; the main feature at CV = –18 V in the ionogram depletes slightly, and there is a concomitant increase in intensity at CV = –15 V. In the associated fragmentation spectra, a slight increase in signal at around *m/z* 300 is also observed. When the solution temperature is increased to 78 °C (the boiling point of the MeOH/H_2O solution), the impact on the ionogram and fragmentation spectrum is much more dramatic. Figure 4.7 shows that when the ESI solution is heated to 78 °C, substantial conversion of the humulone standard into the isomer observed at CV = –15 V occurs. This

change is also observed in the associated mass spectra which evolve from that of the deprotonated humulone standard into that of the nascent isomer (see Figure 4.8).

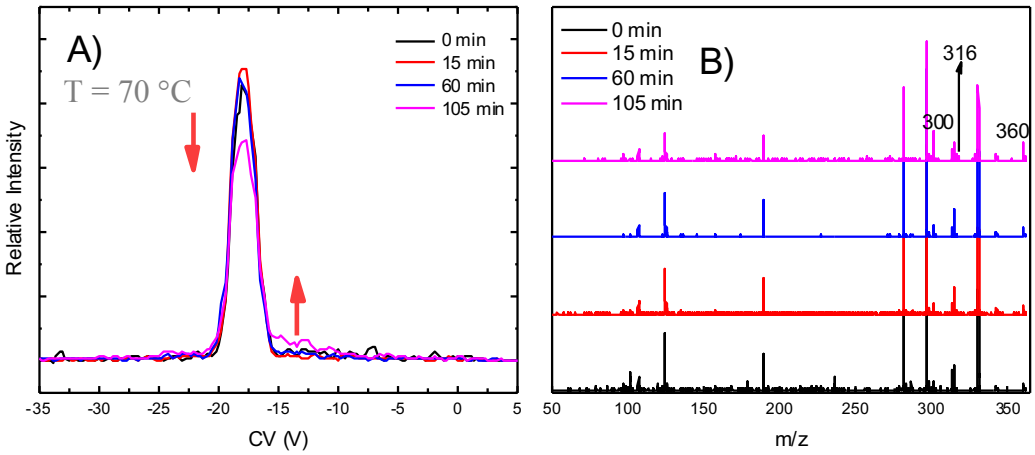

Figure 4.6. (A). The ionogram observed for deprotonated humulone when the ESI solution is heated to 70 °C for (black trace) 0 min, (red trace)15 min, (blue trace) 60 min, and (pink trace) 105 min. The humulone standard was diluted to 100 ng/mL in 1:1 MeOH/H_2O solvent. Measurements were acquired in an N_2 environment seeded with 1.5 % (mol ratio) IPA with SV = 3500 V. **(B).** The mass spectra associated with ionograms shown in **A**.

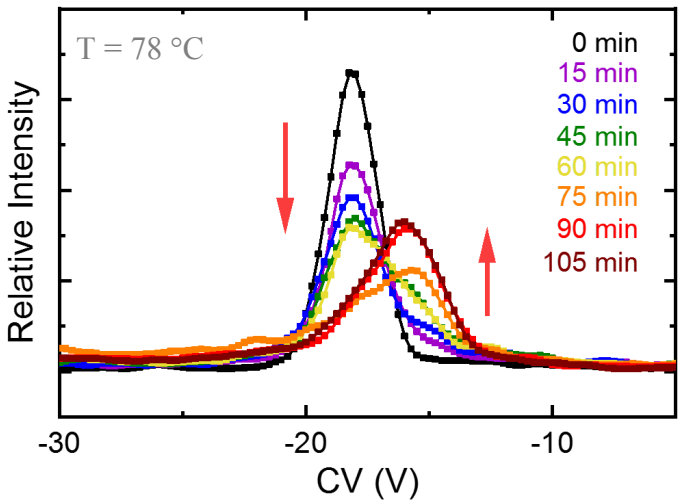

Figure 4.7. The ionogram observed for deprotonated humulone when heated to 78 °C. The

humulone standard was diluted to 100 ng/mL in 1:1 MeOH/H_2O solvent. Measurements were acquired in an N_2 environment seeded with 1.5% (mol ratio) IPA with SV = 3500 V.

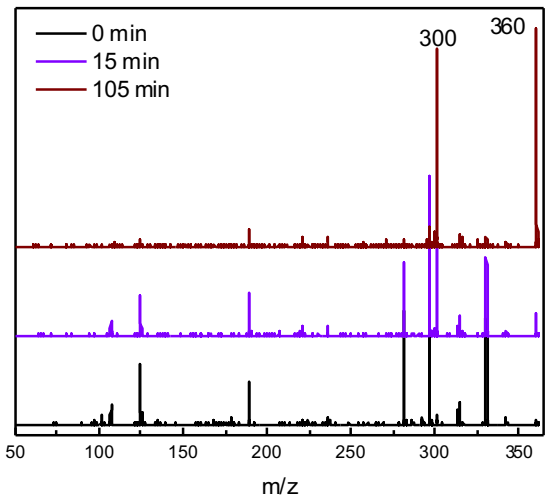

Figure 4.8. The mass spectra observed for deprotonated humulone when heating the ESI solution to 78 °C for (black trace) 0 min, (violet trace)15 min, and (brown trace) 105 min. The humulone standard was diluted to 100 ng/mL in 1:1 MeOH/H_2O solvent. Measurements were acquired in an N_2 environment seeded with 1.5% (mol ratio) IPA with SV = 3500 V.

Based on the results of the T = 78 °C experiments, one can investigate the kinetic behaviour of the humulone isomerization reaction. To extract kinetic data, the ionograms shown in Figure 4.7 were first normalized to the sum of their intensities; then fit to a sum of two Gaussian peaks centered at CV = –18 V and –15 V. The relative area of these peaks is plotted as a function of time in Figure 4.9. Although somewhat noisy, the kinetic data does exhibit a profile that would be expected for a simple pseudo-first-order process described by:

$$\ln A = -kt + \ln A_0 \qquad \text{Equation 4.1}$$

In Equation 4.1, A is the fractional composition of the reactive component, and k is the pseudo-first-order rate constant for the reacting component. A fit of the data yields a value of $k = 0.0131(18)\ min^{-1}$ with $R^2 = 0.927$.

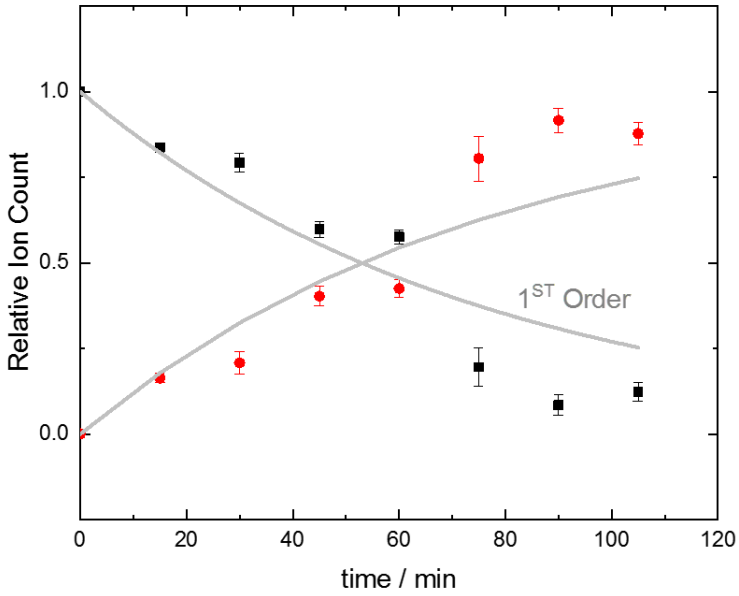

Figure 4.9. The effect of temperature (78 °C) on the isomerization of humulone. Parent peak intensity is plotted in black and nascent isomer intensity is plotted in red. Error bars show 1σ error on the fitted peak area.

To further increase the temperature for kinetics studies, an ethanol/water (1:19) mixture was used in place of the 1:1 MeOH/H_2O solution. The boiling point of the EtOH/H_2O mixture is 96 °C. The dispersion plot of the humulone standard in 1:19 EtOH/H_2O solvent is shown in Figure 4.10. As expected, the analyte ions exhibit nearly identical DMS behaviour regardless of being produced from 1:1 MeOH/H_2O or 1:19 EtOH/H_2O.

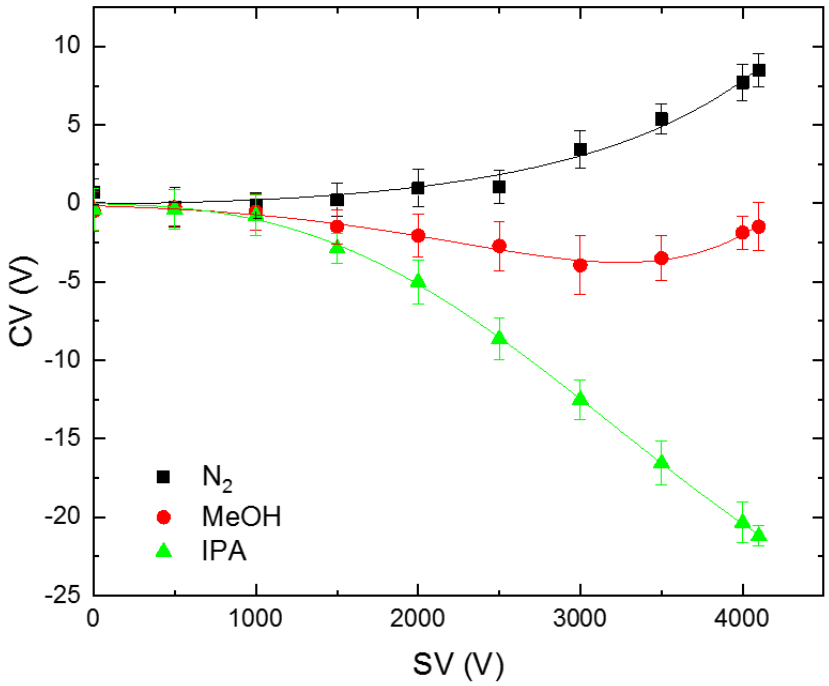

Figure 4.10. The dispersion plot recorded for deprotonated humulone (*m/z* 361) with a pure N_2 environment, and a N_2 environment with 1.5% (mol ratio) methanol vapor and IPA vapor when sprayed from a 1:19 EtOH/H_2O solution. Error bars are 2σ obtained from Gaussian fits to the ionogram peaks.

When the solution temperature is increased to 96 °C, the time evolution of the ionogram and fragmentation spectrum differs significantly from that observed at 78 °C. Figure 4.11 shows that when the EtOH/H_2O ESI solution is heated to 96 °C, substantial conversion of the humulone standard into the isomer observed at CV = –15 V, CV = –5 V, and CV = 0 V occurs.

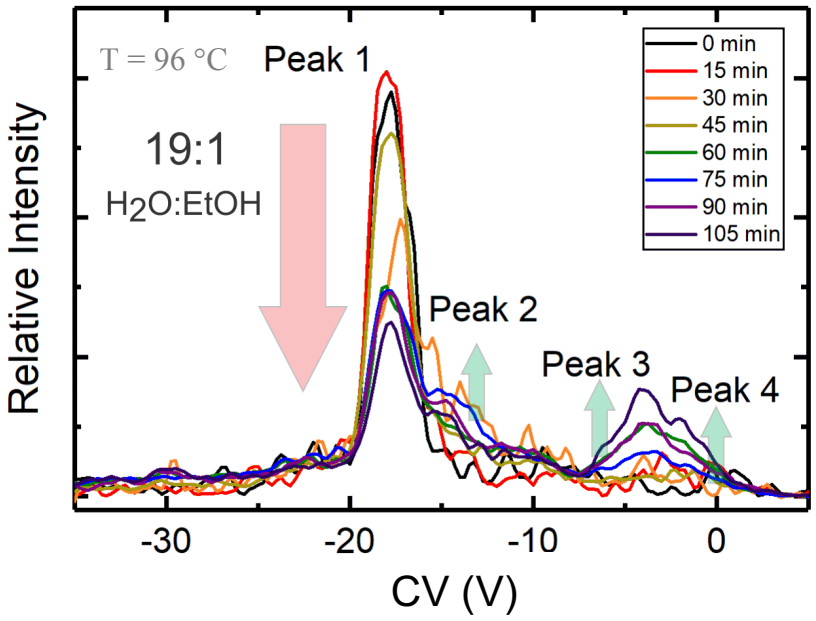

Figure 4.11. The ionogram observed for *m/z* 361 when a humulone solution is heated to 96 °C. The humulone standard was diluted to 100 ng/mL in 1:19 EtOH/H_2O solvent. Measurements were acquired in an N_2 environment seeded with 1.5% (mol ratio) IPA with SV = 3500 V.

Based on the ionogram of the T = 96 °C experiments, one can also investigate the kinetic behaviour of the humulone isomerization reaction. To extract kinetic data, the ionograms shown in Figure 4.11 were first normalized to the sum of their intensities; then fit to a sum of four Gaussian peaks centered at CV = –18 V, –15 V, –5 V, and 0 V. The relative area of these peaks is plotted as a function of time in Figure 4.12. Owing to the noise in these experiments, this study should be repeated. Nevertheless, it is interesting to observed the (apparent) formation of a new isomer in the CV ≈ –2 V region.

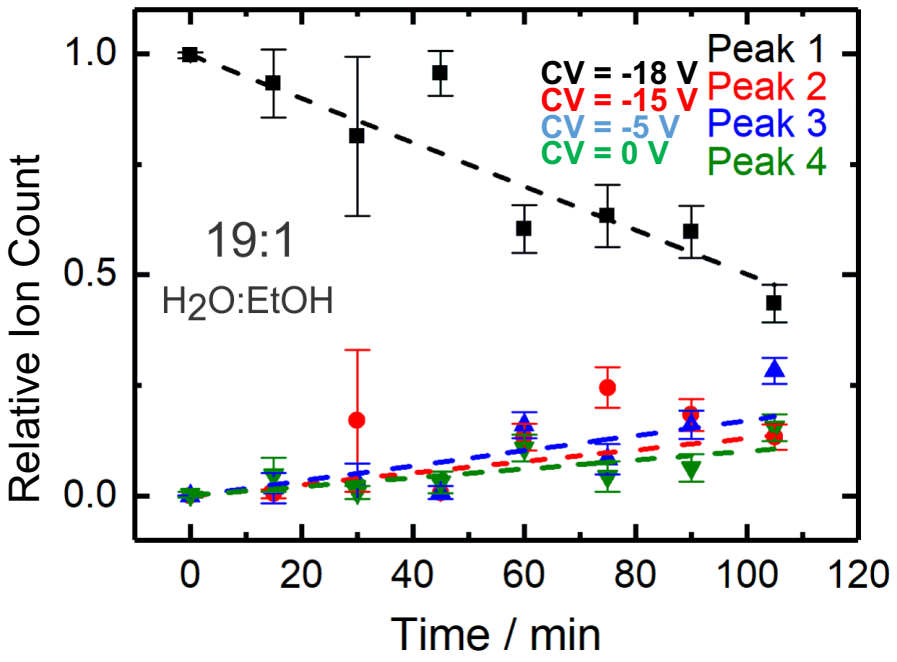

Figure 4.12. The effect of temperature (T = 96 °C) on the isomerization of humulone.

4.4 Computational Results

The calculated global minimum structures of humulone and its isomers as identified by B3LYP/6-311++G (d,p) calculations are shown in Figure 4.13. Neutral humulone has the lowest standard Gibbs energy in the gas phase, and there is a relatively large energy difference between humulone and the *cis*- and *trans*- forms of iso-humulone (*ca.* 35 kJ mol^{-1} and 45 kJ mol^{-1}, respectively). Calculations are ongoing to determine whether the iso-humulone structures are stabilized in protic solution relative to the humulone global minimum. Since humulone isomerizes to the thermodynamically less stable iso-humulone isomers upon boiling, iso-humulone should revert to the more stable humulone structure

when stored at a lower temperature. The rate for this process, of course, depends on the potential energy barriers between the isomeric species.

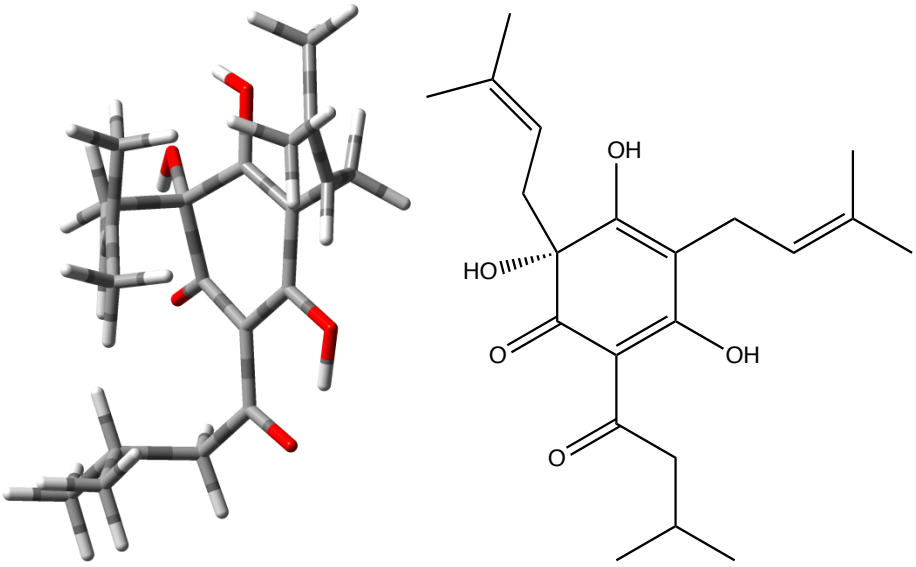

Humulone 0.0 kJ mol^{-1}

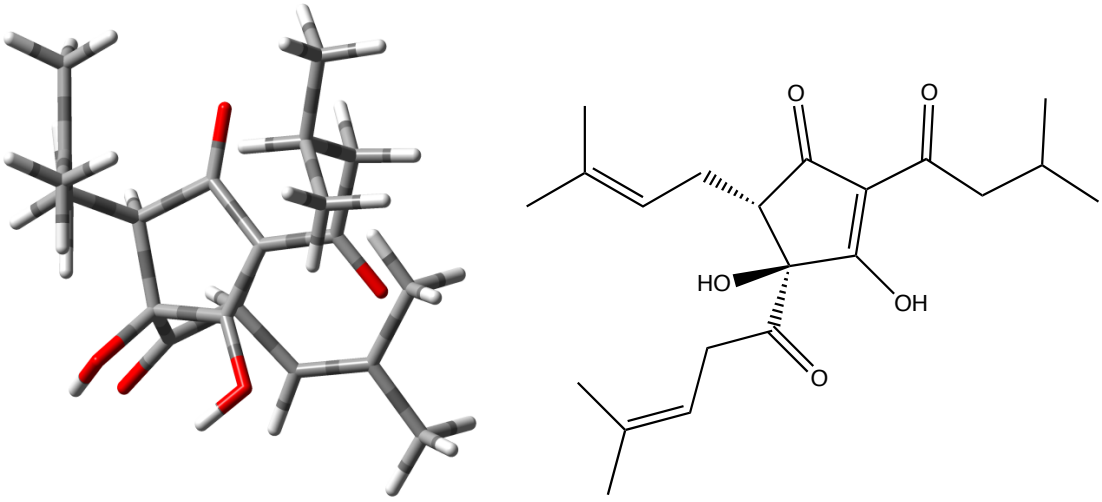

trans Iso-humulone 34.7 kJ mol^{-1}

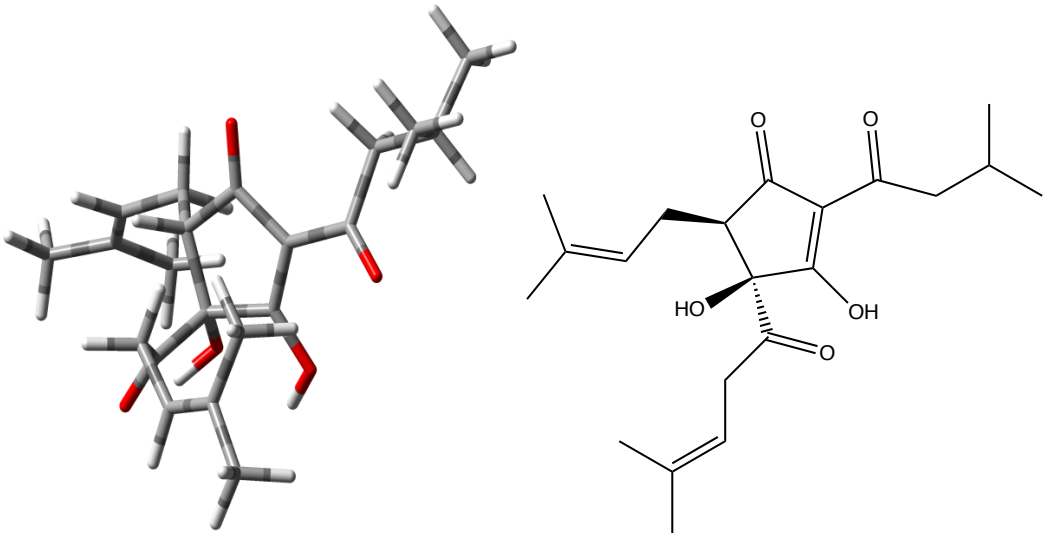

cis Iso-humulone 44.8 kJ mol^{-1}

Figure 4.13. The calculated geometries of neutral humulone and its isomers in the gas phase. Relative Gibbs energies at 298 K are given in kJ mol^{-1}. Calculations used the B3LYP functional and 6-311++G (d, p) basis set.

In DMS experiments, it is the deprotonated (anionic) species which are detected. To investigate the effects of deprotonation, we conducted a similar computational analysis on the anionic species as was undertaken for the neutral species. The calculation results for deprotonated humulone and its isomers are shown in Figure 4.14. For deprotonated humulone, we notice that a single deprotonated prototropic isomer (deprotomer 1) is favoured energetically. The lowest energy iso-humulone structure is a *cis*-isohumulone species, which is 9.2 kJ mol^{-1} above the global minimum. The lowest energy *trans*-isohumulone structure lies 10.1 kJ mol^{-1} above the global minimum isomer. The preferred

site of deprotonation for both the *cis* and *trans* forms is the hydroxy group at position 4 (see Figure 4.14). Note, however, that several low-lying conformers of iso-humulone exist.

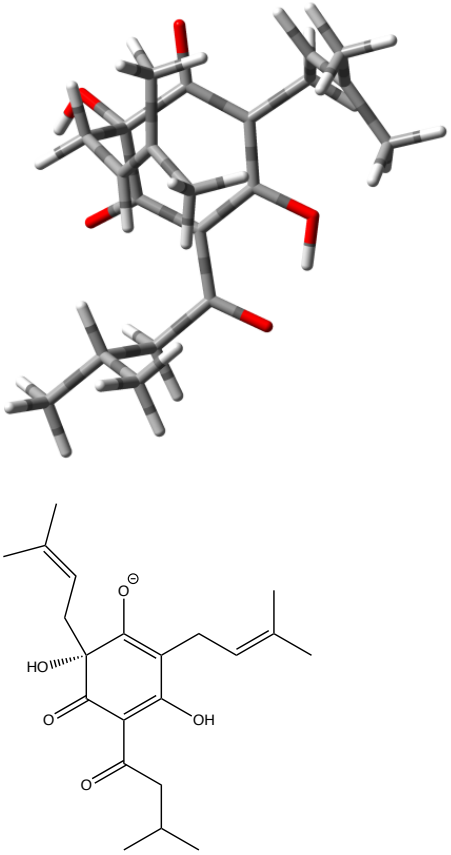

Humulone Isomer 1: 0.0 kJ mol^{-1}

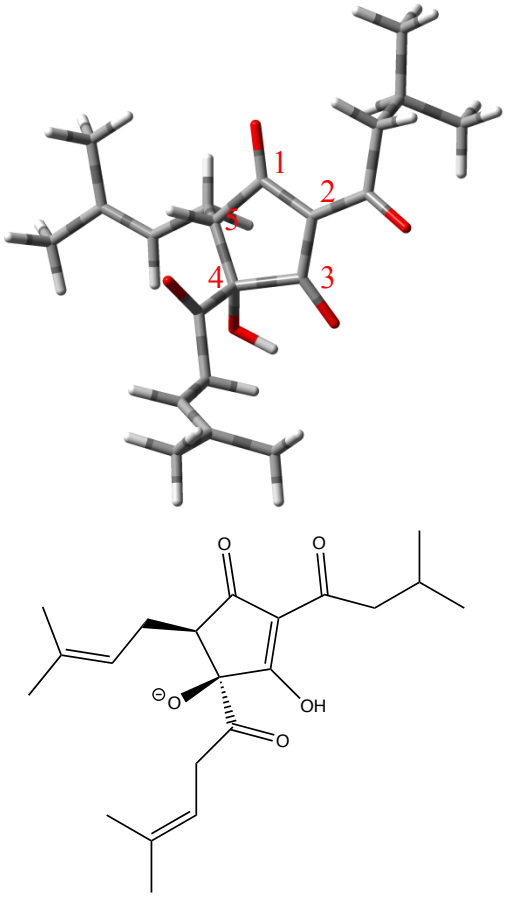

cis Iso-humulone Isomer 2: 9.2 kJ mol^{-1}

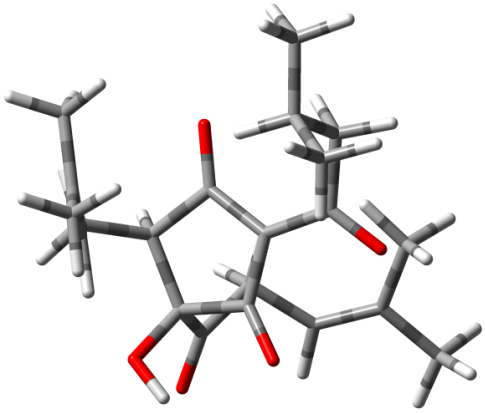

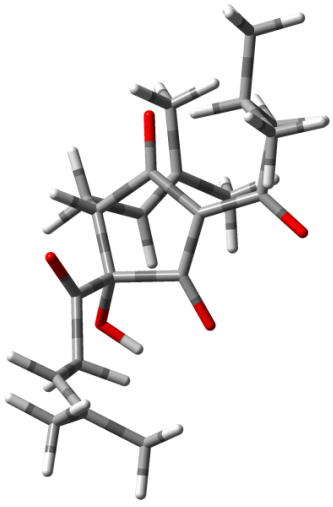

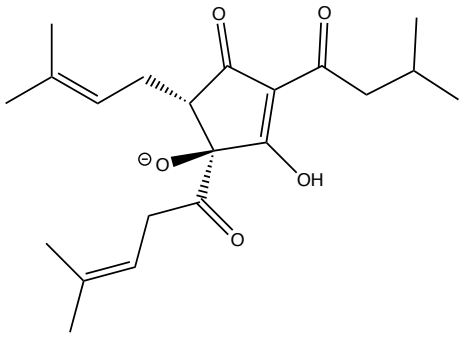

trans Iso-humulone Isomer 3: 10.1 kJ mol^{-1}

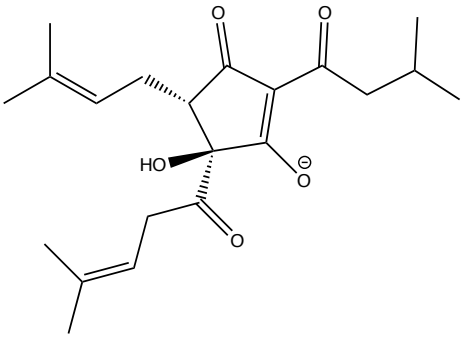

trans Iso-humulone Isomer 4: 12.4 kJ mol^{-1}

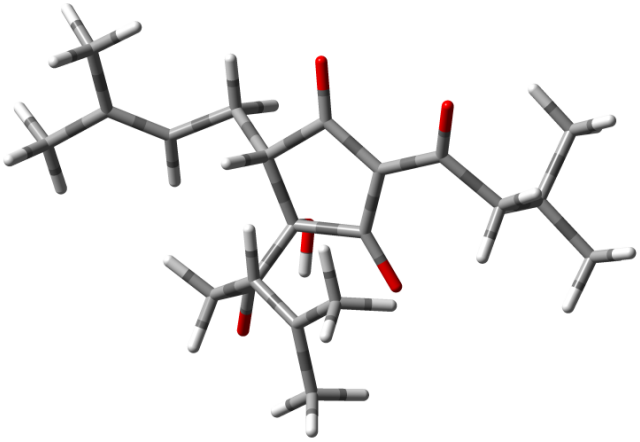

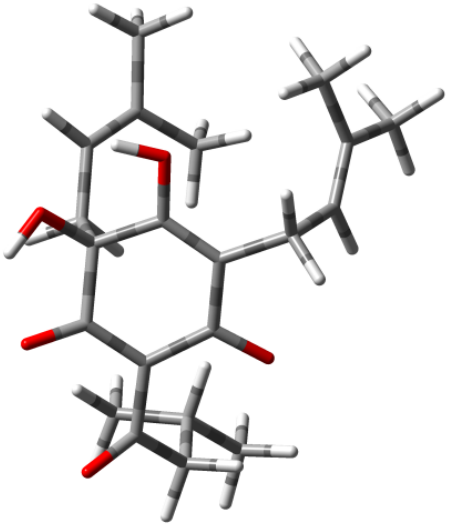

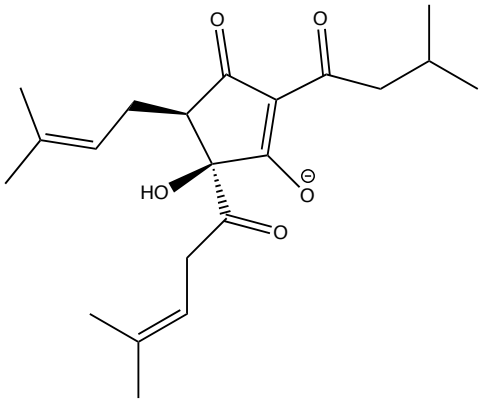

cis Iso-humulone Isomer 5: 19.1 kJ mol^{-1}

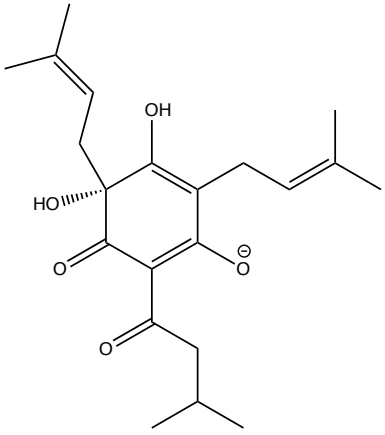

Humulone Isomer 6: 51.2 kJ mol^{-1}

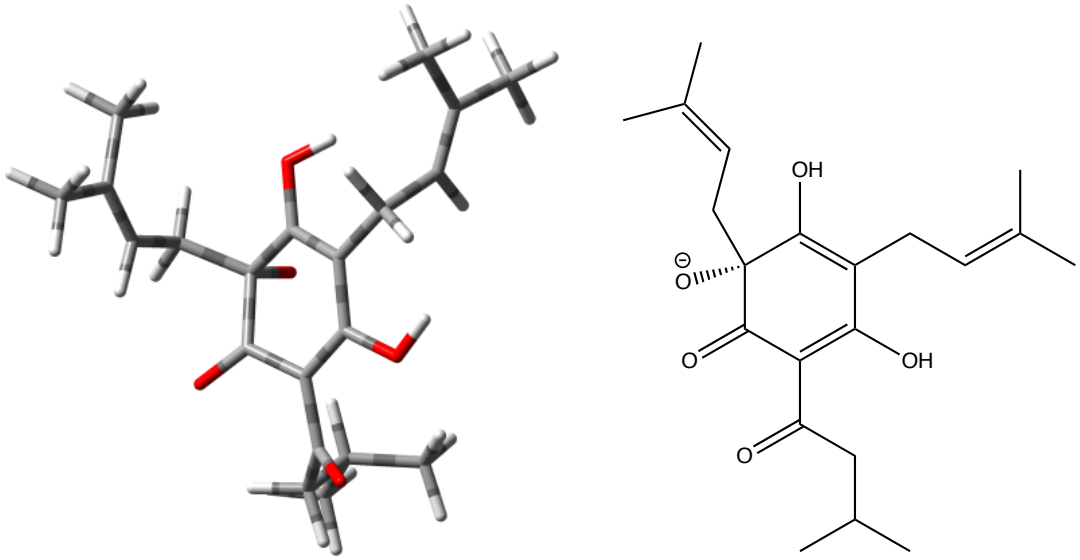

Humulone Isomer 7: 240.7 kJ mol^{-1}

Figure 4.14. The calculated geometries of deprotonated humulone (Isomer 1, 6, and 7) and the deprotonated forms of iso-humulone. Isomer 2 and Isomer 5 are deprotonated forms of *cis* iso-humulone, and Isomer 3 and Isomer 4 are deprotonated forms of *trans* iso-humulone. Relative Gibbs energies at 298 K are given in kJ mol^{-1}. Calculations used the B3LYP functional and 6-311++G (d, p) basis set.

A theoretical investigation on the isomerization mechanism of humulone has been initiated. The assumed pathway involves a large degree of distortion of the six-membered ring in humulone to form bicyclo[3,1,2] intermediates, followed by distortion of the ring to form iso-humulone. The pathway is shown in Figure 4.15. So far, two intermediates are identified along the possible reaction pathways. Preliminary calculations indicate that those intermediates in anionic forms are about 600 kJ mol^{-1} above the global minima of anionic humulone; these deprotonated intermediates are not accessible in gas phase. However, by simply comparing the molecular structures and energetics of humulone/iso-humulone to

the two intermediates, it is apparent that external proton transfer must play a crucial role in completing this isomerization process. This pathway should be further explored and optimized considering different protonation states, experimental solvent conditions, and explicit participation of solvent molecules.

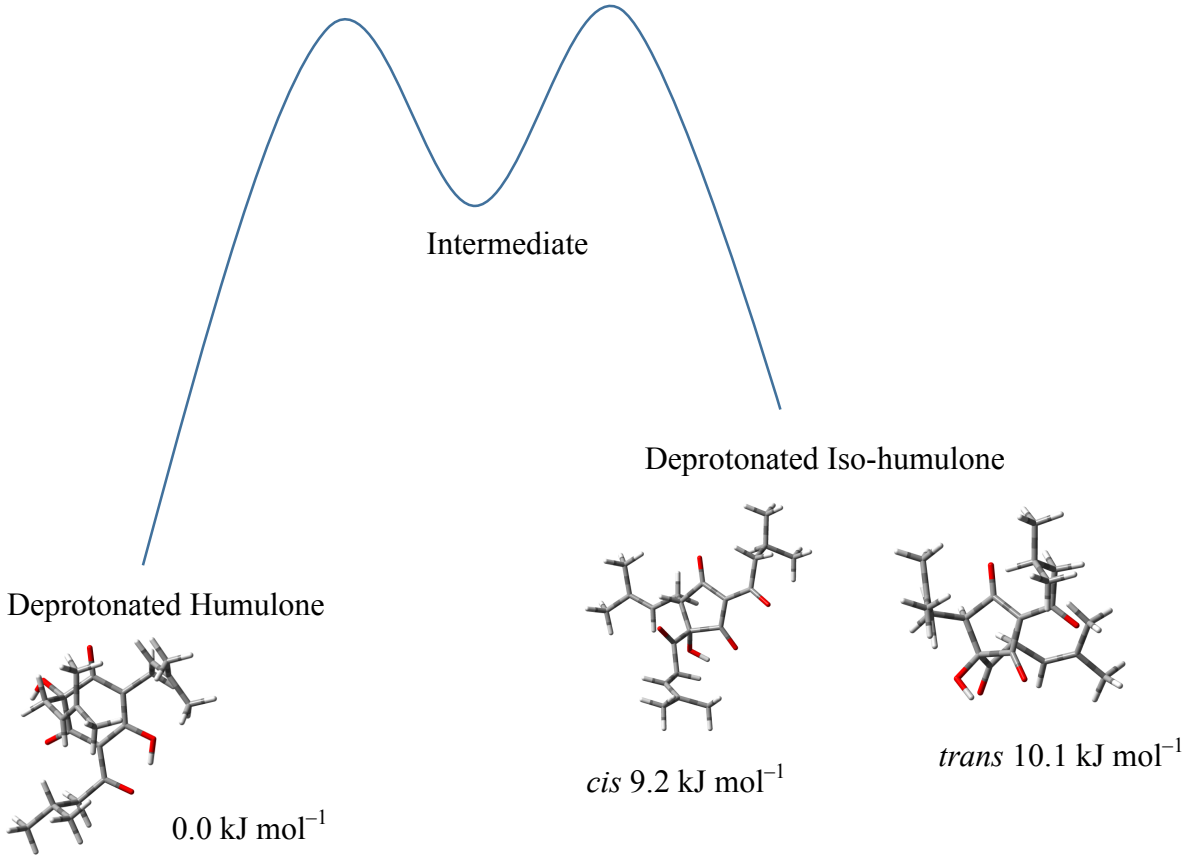

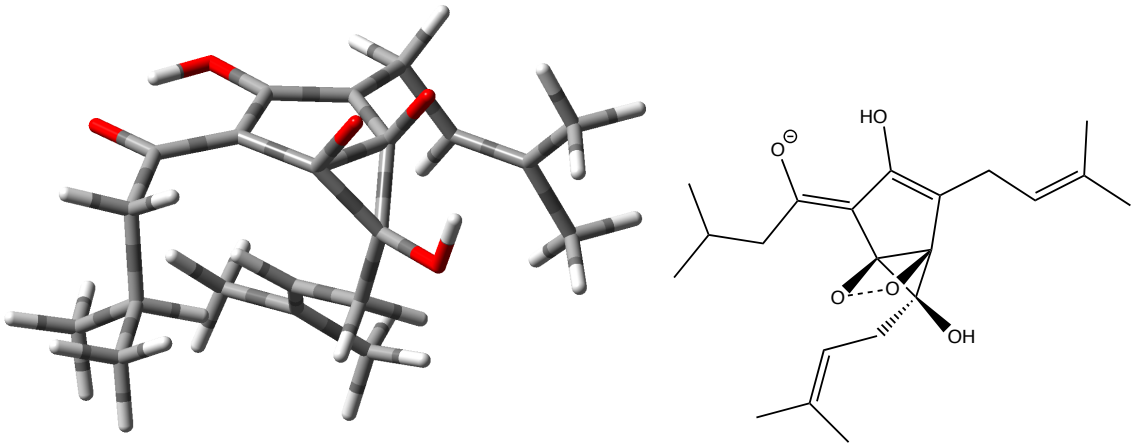

Intermediate 1: 647.4 kJ mol^{-1}

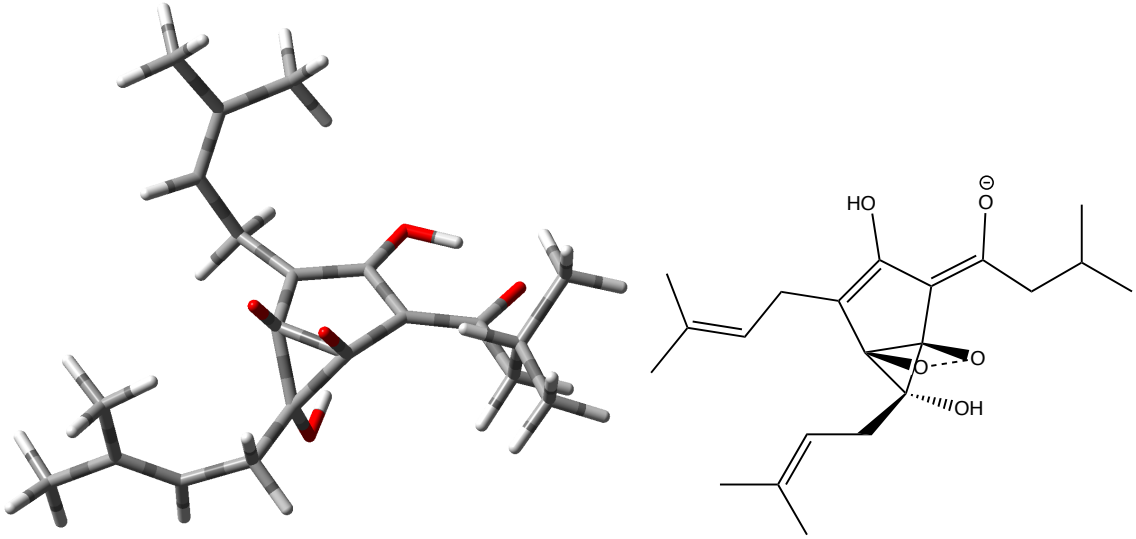

Intermediate 2: 639.7 kJ mol^{-1}

Figure 4.15. The calculated geometries of deprotonated Intermediate 1 and Intermediate 2. Relative Gibbs energies at 298 K are given in kJ mol^{-1}, and they are relative to the global minima deprotonated Humulone Isomer 1, 0.0 kJ mol^{-1}. Calculations used the B3LYP functional and 6-311++G (d, p) basis set.

Chapter 5

Characterization of Humulone Content in Beer

We discussed characterization of humulone standard in Chapter 4. Based on the protocols developed for detecting humulone in the DMS-MS apparatus, studies of humulone content in beer can be conducted. This work was undertaken using beer provided by Innocente brewery. The involved beers are Conscience (CS), Two Night Stand (2NS), Fling (FL), Kolsch (KO), Bystander (BS), Batch-5 Dubbel Vision (Bat), and Inn Oslainte (In).

5.1 Experimental Details

Acetone, isopropanol (IPA), methanol, hydrochloric acid (HCl), iso-octane, and octanol regents are HPLC-grade, and purchased from Sigma-Aldrich company; they are utilized without further purification. Beer samples are provided by Innocente Brewing company. In DMS, beer analytes are measured under the EPI mode using negative-ion ESI. For the measurement, the analyte is continuously infused at SV = 3500 V, and the CV range is scanned from −35 V to 35 V with 0.25 V step sizes. The ionogram of beers is collected for the *m/z* 361 peak. The Lambda 35 UV-Vis spectrometer (PerkinElmer, USA), accompanied with the UV WinLab software package, is utilized to measure the UV-Vis spectra of the beer sample in the region of 250 nm ~ 450 nm.[52] The beer sample and blank, which is iso-octane/octanol solution, are held in quartz cuvettes within the sample chamber.

Samples used in DMS are first centrifuged for 5 minutes to separate yeast cells, then they are sonicated for 10 minutes to degas. Samples are then diluted down to yield a iso-humulone concentration of *ca.* 100 ng/mL, in MeOH/H_2O (1:1).[53]

To prepare beer samples to do the UV-Vis measurements, a procedure based on ASBC is used.[53] Firstly, 3 mL beer samples are degassed and placed into a 15 mL centrifuge tube; then, 0.3 mL 3 M HCl, 6 mL iso-octane and 15 μL octanol are added to the same tube to extract the humulone and iso-humulone. Next, the mixture is centrifuged for 15 minutes, following which the upper organic layer is extracted for measurement.

5.2 DMS/MS Results

Figure 5.1 shows the ionogram recorded for a fresh sample of CS, an India Pale Ale, which exhibits a distinctly bitter hoppy flavour. Although there is one main peak, CV = 0 V, in the ionogram, two shoulders can be observed at CV = –16 V and –10 V. As discussed in Chapter 4, the humulone standard signal appears at CV = –18 V, and the signal of boiled humulone (in MeOH/H_2O at 78 °C) presents at CV = –15 V. The main peak of CS is observed at CV = 0 V and one shoulder at CV = –10 V, which suggests that CS may contain other structural isomers of humulone and iso-humulone.

The fragmentation spectrum of the CV = 0 V peak from the CS sample is shown in Figure 5.1.B. The signal of *m/z* 361 is observed, and both humulone and iso-humulone should have this peak, theoretically. However, we observed previously that the humulone standard did not exhibit the parent peak due to fragmentation post-selection (see Chapter

4). The *m/z* 315 signal indicates that CS contains humulone fragment since this signal was observed in humulone mass spectrum in Figure 4.2.B and Table 4.1. The *m/z* 300 and *m/z* 360 fragments are distinct to iso-humulone. The intensity of *m/z* 300 fragment is much higher than that of *m/z* 315 fragment, which indicates that the majority composition is iso-humulone. The unidentified fragments may belong to another isomer of humulone, perhaps adhumulone (which also has 361 *m/z*).

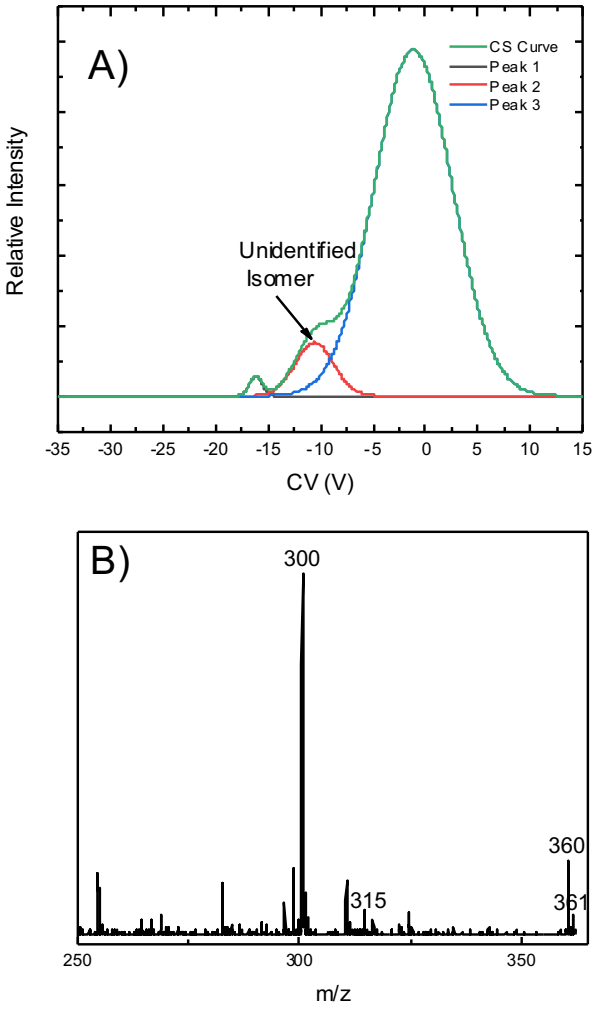

Figure 5.1. (A). The ionogram observed for Conscience beer. The beer sample was diluted

to 100 ng/mL in 1:1 MeOH/H_2O solvent. Measurements were acquired in an N_2 environment seeded with 1.5 % (mol ratio) IPA with SV = 3500 V. (**B**). The mass spectra associated with ionograms shown in **A**.

5.3 Aging Chamber Studies

Environmental Growth Chamber

The study of the humulone to iso-humulone isomerization reaction and the possible reverse reaction in beer was conducted with an environmental growth chamber.[54] The growth chamber used in this project was a double-decker model as shown in Figure 5.2. The growth chamber utilized woodless material with painted aluminum surfaces and polymer foam insulation, and it was equipped with an upward airflow with air uniformly distributed through the aluminum channel floor. Counterweighted light fixtures are used in the chamber to satisfy different light requirements; in our case, aging chamber was operated to create dark environment conditions. The temperature of the chamber can be adjusted from 4 °C to 45 °C with an accuracy of ± 0.5 °C with lights off, and 10 °C – 45 °C with an accuracy of ± 0.5 °C when fully lit.[55]

Figure 5.2. The environmental growth chamber used in this project.[55]

To investigate the effect of temperature on the beer degradation and the reversibility of humulone isomerization, beer samples were stored in aging chamber in which temperature is set at 37 °C. This temperature is chosen to be slightly higher than the normal fermentation temperature, in which the normal brewing temperature is within 20~22 °C and combined with an increment (5.5 ~ 8.3 °C) due to active fermentation.[56] The monitoring results are shown in Figure 5.3.

After being stored in the aging chamber for four weeks, the main peak for the CS sample in the ionogram shifts from CV = 0 V to CV = –15 V, and one small shoulder is at CV = –7 V and the other at CV = –18 V. When CS beer has been stored at 37 °C for six

weeks, compared to fourth week measurement, the main peak appears at more negative position, CV = –18 V, and there is a small peak at CV = –5 V. As mentioned in Figure 4.2.A, the humulone peak appears at CV = –18 V; in addition, Figure 4.7 shows that the peak of boiled humulone at 78 °C appears at CV = –15 V. Moreover, the peak at CV = 0 V can be observed in Figure 4.11 of boiled humulone at 96 °C. Figure 4.14 indicates that *cis* iso-humulone is more stable than the *trans* iso-humulone because the relative Gibbs energy of *cis* form is lower than that of the *trans* form; hence, the CV = –15 V peaks is assigned to *cis* iso-humulone and the CV = 0 V peak is assigned to *trans* iso-humulone. These results demonstrate that one isomer can transition into the other isomer, then reverse back to humulone, when sample is stored at 37 °C.

The fragmentation spectra are shown in Figure 5.3.B (mass spectrum of beer being stored in aging chamber for six weeks). After being stored at 37 °C for six weeks, the mass spectrum is more complex than that of the fresh beer. Although the *m/z* 300 fragment is still observed, the intensity is low, meaning the amount of the same humulone isomer as the fresh beer decreased. Compared to the mass spectrum of fresh beer in Figure 5.1.B, *m/z* 315 and *m/z* 361 fragments appear again, suggesting that humulone may be reproduced. The rest of the observed fragments, for example, m/z 342, may indicate that there is new tautomer/isomer being produced, or more stable fragments of iso-humulone being generated.

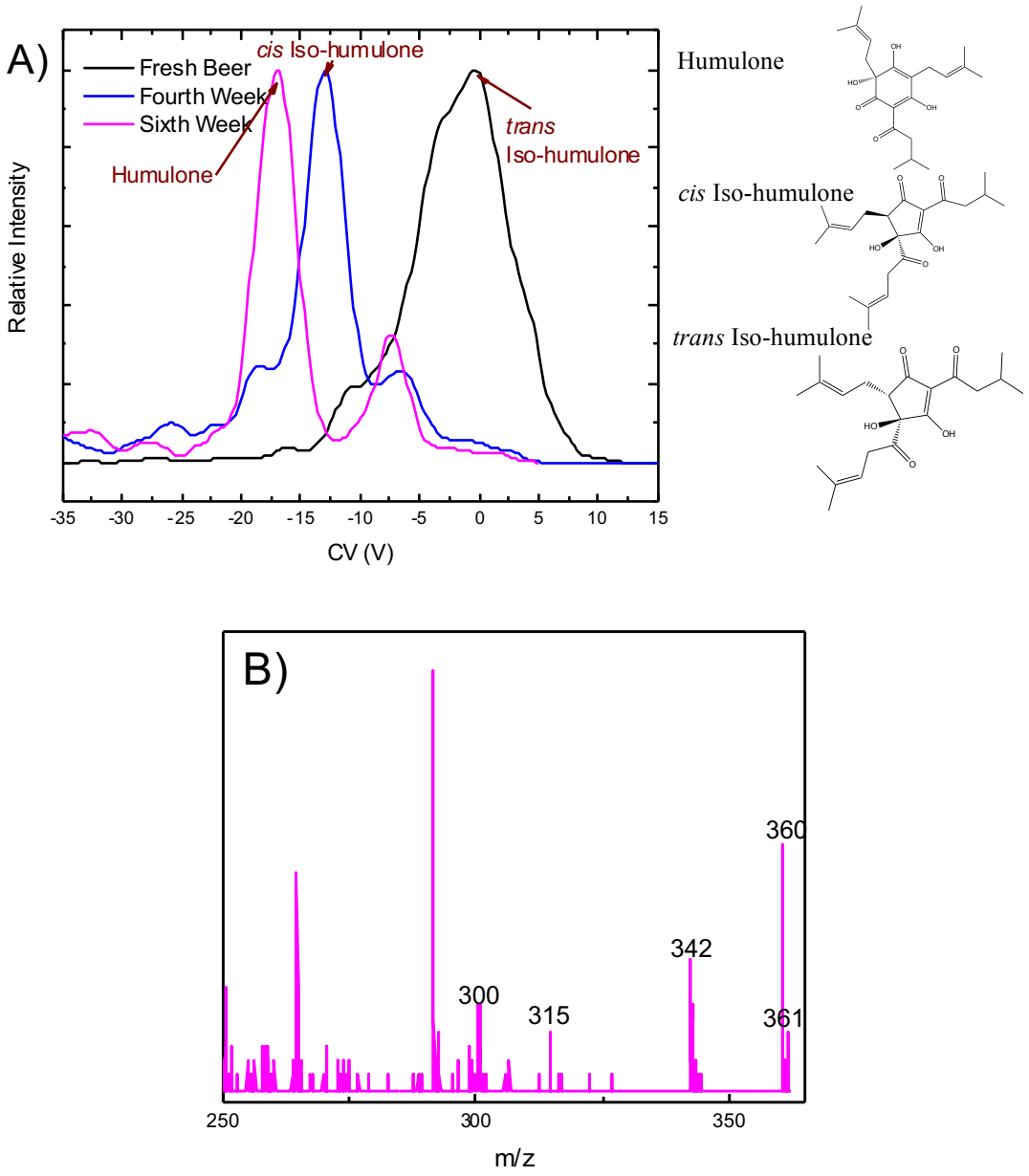

Figure 5.3. (A). The ionogram of Conscience beer at 18 °C (black), heated to 37 °C for four weeks (blue), and six weeks (pink). The beer was diluted to 100 ng/mL in 1:1 MeOH/H_2O solvent. Measurements were acquired in an N_2 environment seeded with 1.5% (mol ratio) IPA with SV = 3500 V. **(B).** The mass spectra associated with the sixth week ionogram in **A**.

The other beers were also utilized in aging chamber studies. Figure 5.4 and Figure 5.5 exhibit ionograms and associated mass spectra of 2NS and FL beers. In Figure 5.4.A, the main peak first appears at CV = 0 V; then this peak shifts to CV = –15 V with two shoulders at CV = –5 V and –18 V when 2NS beer has been stored in aging chamber for four weeks. After six weeks in aging chamber, the main peak changes to CV = –18 V. For fresh 2NS, Figure 5.4.B, there is no *m/z* 300 signal, but the *m/z* 360 is observed, which means less amount of iso-humulone in this beer. After six weeks, Figure 5.4.C, the ratio of *m/z* 300 fragment is increased in beer sample, this spectrum demonstrates that the humulone's isomers become the major component in the sample over time.

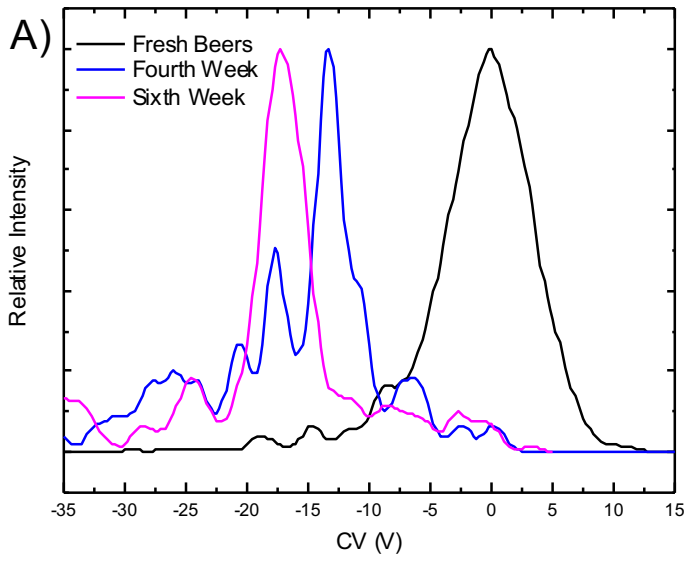

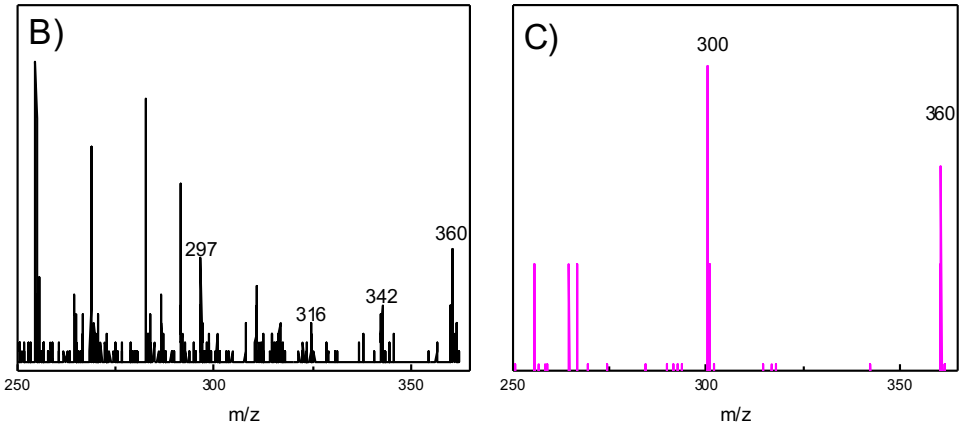

Figure 5.4. (A). The ionogram of Two Night Stand (2NS) at 18 °C (black) when heated to 37 °C for fourth week (blue), and sixth week (pink). The beer was diluted to 100 ng/mL in 1:1 MeOH/H_2O solvent. Measurements were acquired in an N_2 environment seeded with 1.5% (mol ratio) IPA with SV = 3500 V. **(B).** The mass spectra associated with fresh beer. **(C).** The mass spectra associated with sixth week beer.

FL beer exhibits similar trends in DMS ionograms to the CS and 2NS samples. In Figure 5.5.A, fresh FL beer has a peak at CV = 0 V; then, after being stored in aging chamber for four weeks, peak at CV = –15 V and two shoulders at CV = –5 V and –18 V can be observed. After six weeks in the aging chamber, the main peak is observed at CV = –18 V. However, complex mass spectra are observed for fresh FL. Figure 5.5.B shows that *m/z* 300 and *m/z* 360 species are observed, indicating that there is a small amount of iso-humulone in FL beer. Six weeks later, Figure 5.5.C, the signal of *m/z* 300 turns into the base peak.

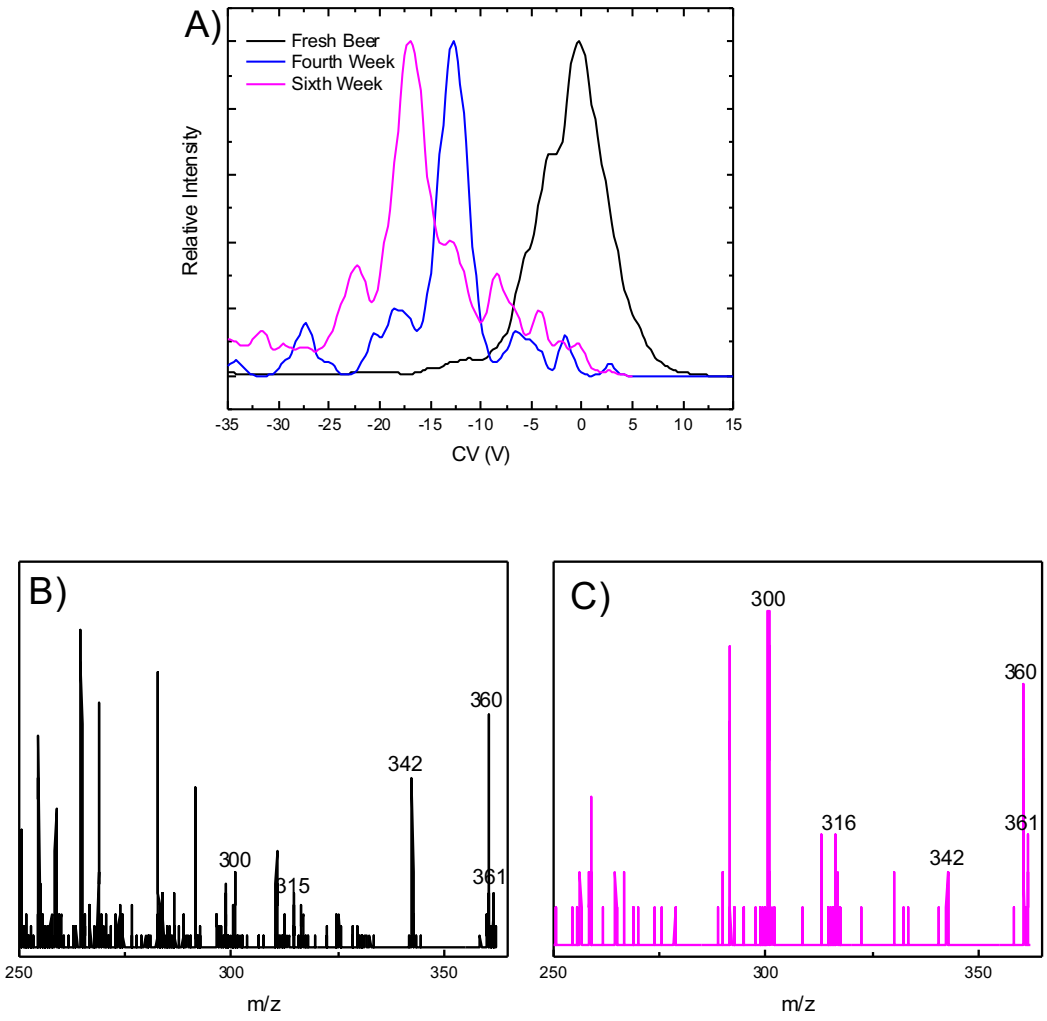

Figure 5.5. (A). The ionogram of Fling (FL) beer at 18 °C (black) when heated to 37 °C for four weeks (blue), and six weeks (pink). The beer was diluted to 100 ng/mL in 1:1 MeOH/H_2O solvent. Measurements were acquired in an N_2 environment seeded with 1.5% (mol ratio) IPA with SV = 3500 V. **(B).** The mass spectra associated with fresh beer. **(C).** The mass spectra associated with sixth week ionogram.

5.4 UV-Vis Results

The general ASBC approach to determine IBU, which is a measurement of bitterness, is to extract beer with iso-octane and detect the peak height at 275 nm *via* UV-Vis spectrometry.[57] The IBU scale is not proportional to the perceived bitterness of beer;

instead, it describes content of iso-humulone in beer.[57] The IBU value can be calculated by Equation 5.1.[57]

$$\text{Bitterness (IBU)} = \text{Abs}_{275} \times 50 \qquad \text{Equation 5.1}$$

Where Abs_{275} is absorbance at 275 nm.

The UV-Vis spectra of beers stored in an aging chamber for six weeks is shown in Figure 5.6. The calculated IBU values are exhibited in Table 5.1. After being stored in aging chamber for six weeks, IBU values of 2NS, FL, KO, BS, Bat, and In are increased, while IBU value of CS is decreased. There is only slightly change between IBU values of 2NS beer. The decreasing IBU value of CS means the lack of iso-humulone content.

It is noticed that changes of IBU values can relate to changes of iso-humulone fragments. In Figure 5.4, for 2NS beer, the *m/z* 300 fragment changes from none to majority composition with time increasing. In the same time, the IBU of 2NS is increased. In Figure 5.5 for FL beer, the intensity of *m/z* 300 is increased; furthermore, the IBU value of FL is increased. Based on Figure 5.3 for CS beer, the *m/z* 300 fragment changes from the majority composition to the minor amount of constituent over time; meanwhile, the IBU values of CS is decreased. Therefore, the increase of *m/z* 300 fragment relates to the increased IBU value. It is likely that the lower IBU values report less content of iso-humulone and more content of humulone or the other humulone's isomers.

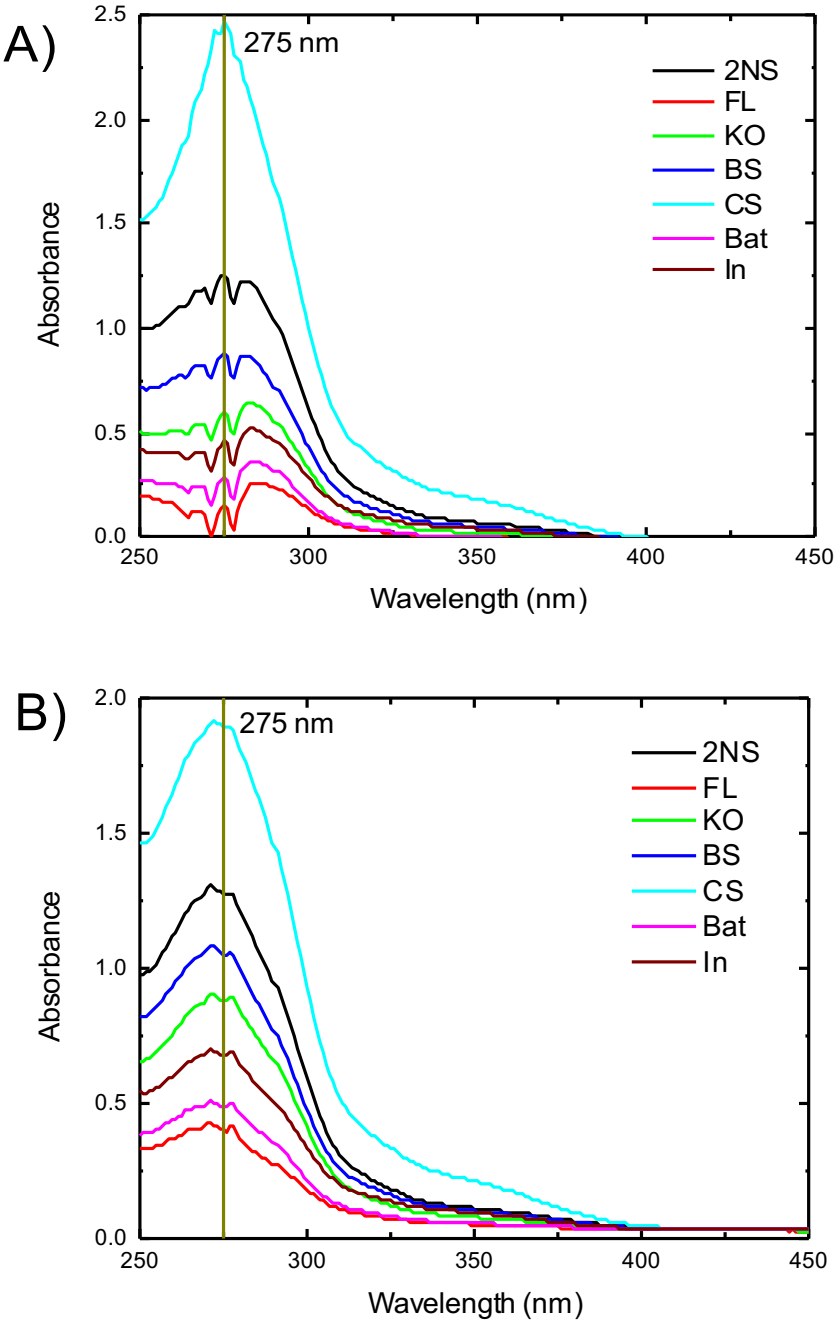

Figure 5.6. (A). The UV-Vis spectra of the extracted humulone and its isomers of Two night stand (2NS), Fling (FL), Kolsch (KO), Bystander (BS), Conscience (CS), Dubbel Vision (Bat), and Inn Oslainte (In) beer fresh samples. **(B).** The UV-Vis spectra of above beers after storing in an aging chamber for six weeks at T = 37 °C. The peak heights are measured at 275 nm which is associated with $\pi \rightarrow \pi^*$ transition in the conjugation system of humulone and its isomers.

Table 5.1. Experimental IBU Values of Different Beers Measured by UV-Vis Spectroscopy

Beer	IBU for fresh beer	IBU for sixth week	Hops
Two Night Stand	63	64	Double IPA*
Fling	8	20	Golden Ale
Kolsch	30	44	Lagered Ale
Bystander	44	53	American Pale Ale
Conscience	124	95	American IPA*
Batch-5 Dubbel Vision	14	24	Belgian Style Dubbel Ale
Inn Oslainte	23	34	Irish Red Ale

*IPA here stands for India Pale Ale.

The calculated UV-Vis spectra of humulone, *cis* iso-humulone, and *trans* iso-humulone using the TD-DFT method at the B3LYP/6-311++G(d,p) level of theory are shown in Figure 5.7. In UV-Vis experiment, iso-octane/octanol solution is used as background, but there is no PCM model for iso-octane/octanol solution in Gaussian; thus, heptane, which has similar chemical properties to this solvent, is chosen as the solvent system for calculation. In Figure 5.7, both *cis* and *trans* iso-humulones show one peak, which appears at $\lambda = 237$ nm, and which has a shoulder at *ca.* 325 nm. Both isomers exhibit similar absorption spectra. In comparison, three peaks, which appear at 220 nm, 255 nm, and 340 nm, are present in the humulone curve.

Based on the theoretical calculation results, iso-humulones have similar peak shape to the experimental UV-Vis spectra in Figure 5.6; however, the curve shape of humulone

differs from those of spectra in Figure 5.6. Furthermore, compared to peak at 275 nm in Figure 5.6, peaks of iso-humulones in Figure 5.7 shift to 237 nm. One reason for this could be that the solvent chosen for analogy calculation is different from the one used in UV-Vis measurement, and the other reason could be the limited accuracy for calculation. However, in Figure 5.7, although these three chemicals exhibit different curve shapes, there are a lot of overlap portions among them. Hence, the UV-Vis measurement cannot easily distinguish humulone and iso-humulone content.

In conclusion, the ASBC approach using UV-Vis spectrophotometer cannot easily distinguish humulone and iso-humulone content in beers. Based on Figure 5.7, *cis* and *trans* iso-humulones exhibit similar peak shape and the same peak positions; thus, signals of isomers affect each other, and then UV-Vis measurement cannot distinguish *cis* and *trans* forms of isomers. Consequently, it is expected UV-Vis measurements provide a convoluted view of humulone content, and therefore flavour profiles, in beer. It is noticed that different beer is brewed by different hop listed in Table 5.1, in which IPA stands for India Pale Ale, 2NS by Double IPA, FL by Golden Ale, KO by Lagered Ale, BS by American Pale Ale, CS by American IPA, Bat by Belgian Style Dubbel Ale, and In by Irish Red Ale.

The integrated iso-humulone signals from DMS ionograms of fresh beers versus associated IBU values, and beers stored in aging chamber for six weeks versus associated IBU values are shown in Figure 5.8. It is clear that the UV-Vis measurements and DMS data shows some correlation, but there is a great deal of scatter owing to the experimental

error associated with both techniques. Moving forward, it is recommended that the DMS methods developed here be utilized to unambiguously characterize humulone content, preferably with the aid of internal standards to better calibrate absolute concentration.

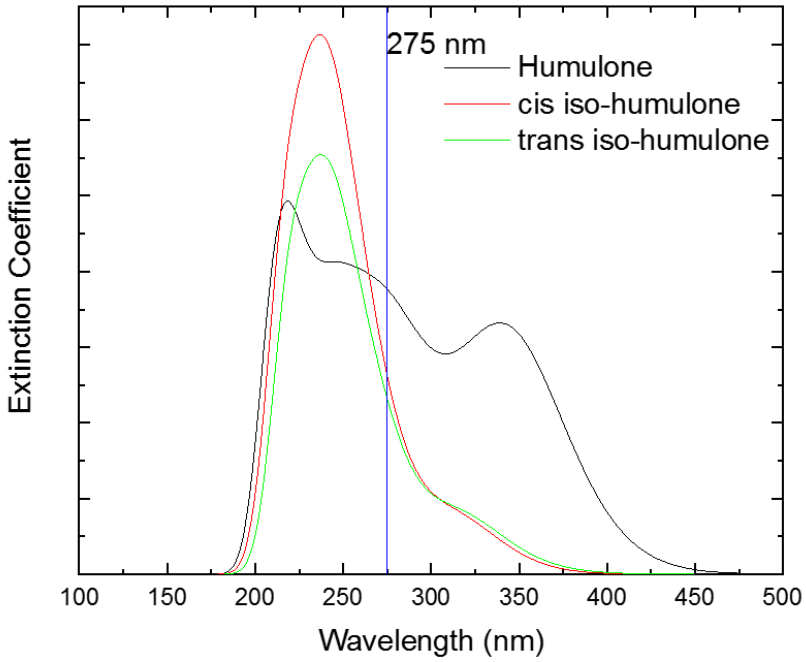

Figure 5.7. The calculated UV-Vis spectra of neutral humulone, *cis* iso-humulone, and *trans* iso-humulone conducted using a heptane PCM using TD-DFT at the B3LYP/6-311++G(d,p) level of theory.

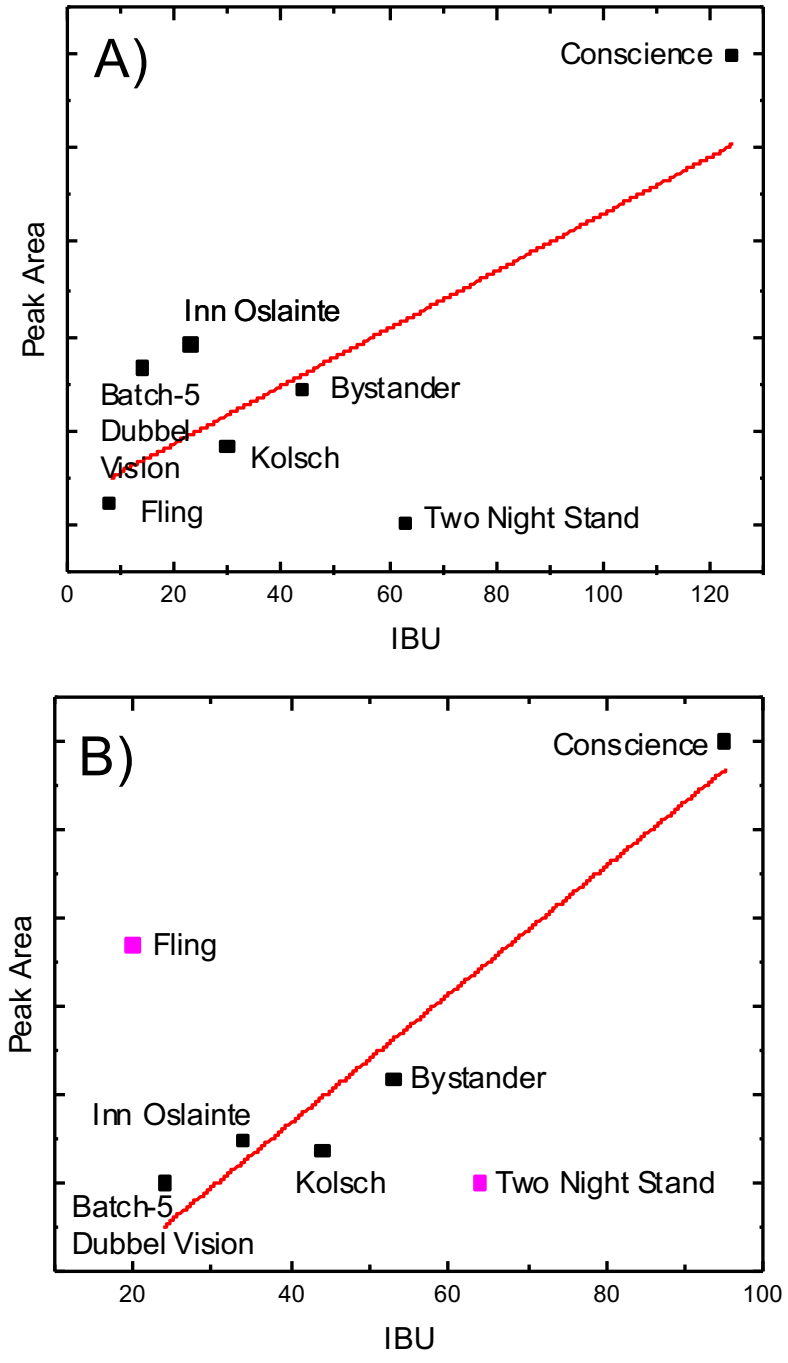

Figure 5.8. (A). The integrate signals of iso-humulone of Two night stand (2NS), Fling (FL), Kolsch (KO), Bystander (BS), Conscience (CS), Batch-5 Dubbel Vision (Bat), and Inn Oslainte (In) fresh beer samples versus their IBU values. **(B).** The integrate signals of iso-humulone of above beers for stored at aging chamber for six weeks versus their IBU values.

Chapter 6

Concluding Remarks

Beer is one of the fermented liquid drinks flavored with hops.[58] While barley provides the sweetness, hop contributes to the bitterness of beer.[58] During the intricate brewing process, humulone, which is one of the vital components of hop, undergoes the isomerization reaction producing iso-humulone. Hence, the humulone concentration profile is of great interest for beer brewing industry. Here, we use differential mobility spectrometry (DMS) to separate and characterize humulone and iso-humulone. In support of the experimental work, computational studies were conducted to investigate thermal kinetic of isomerization reaction. In conjunction, we utilize the conventional UV-Vis spectroscopy method to measure IBU values, and compare them against corresponding DMS measurements. Moreover, theoretical UV-Vis spectra were used to interpret experimental UV-Vis observations.

Chapter 4 discusses characterization of humulone, and these investigations were in a combination of experimental and computational approach. DMS ionogram reports the unique compensation voltage (CV) value of humulone at the specific separation voltage (SV), and characteristic fragments of humulone can be obtained from the mass spectrum mapped in DMS. With the help of the DMS ionogram and mass spectra of humulone and its isomers, the effect of time and temperature on isomerization reaction can be explored.

If temperature is high enough (T ≥ 78 °C), thermally-driven isomeric conversion can be observed with a *ca*. 2 hr period. To investigate the isomerization process, the low-lying isomers of various humulone species were identified using the Basin-hopping (BH) search algorithm, and density functional theory (DFT) was utilized to calculate molecular geometries and properties. Based on theoretical outcomes, it is clear that *cis*- and *trans*-isohumulone is thermally accessible at elevated temperature. However, the barriers to isomerization must still be determined and it is clear that proton-transfer to and from the solvent is an important consideration. Although rough kinetics of reactions were reported, further studies must be performed to determine the more accurate kinetic properties.

Chapter 5 discusses characterization of humulone in beers. Here, this study involved both computational predictions and experimental data to explore the humulone content in beers. DMS ionograms of humulone and its isomers in diverse beers can be obtained. Compared to mass spectra of pure humulone in methanol/water (1:1) solvent, mass spectra of beers were different; moreover, present fragments differed among different beers. An aging chamber was used to provide extra energy for investigating the chemical conversions in beers. Based on ionograms obtained from DMS, temperature affected overall conversions between humulone and its isomers. The distinctive fragments representing changes between humulone and its isomers can be determined. IBU profiles of beers were generated from UV-Vis spectroscopy; changes of IBU values were able to suggest changes of bitterness. Combining DMS and UV-Vis results indicated that there was a linear

correlation between content of iso-humulone and IBU values; moreover, the *m/z* 300 signal can be confirmed from the isomer of humulone. The simulation UV-Vis results calculated from TD-DFT indicated that the UV-Vis measurement cannot easily distinguish humulone and iso-humulone content. However, further investigations should be conducted to determine more accurate relation between DMS results and UV-Vis outcomes.

The various projects explored in this thesis tentatively characterize pure humulone in methanol/water (1:1) solvent and ethanol/water (1:19) solvent, and iso-humulone content in beers. The combined computational and experimental methods allowed for comprehensive analysis and interpretation of data. Results of the combination of DMS results and IBU values have unique implication for the humulone concentration profiles mapping and development. Moving forward, it is recommended that these studies be repeated to provide a statistical assessment of the observed isomerization processes. Furthermore, it is recommended that similar studies be conducted using pre- and post-isomerization hop extract since this should provide an intermediate picture between the pure humulone standard and the post-brewed beer samples.

Overall, we have developed a methodology for detecting humulone in its protonated and deprotonated states. This methodology is easily adopted for studying humulone and its isomers in beer samples. Moreover, we can monitor the temperature dependence of interconversion between the various humulone isomers; based on calculations, we expect that there are two-barriers along humulone to *cis* iso-humulone to *trans* iso-humulone

pathway. This can be probed in more detail with an improved temperature study. Importantly, we found that UV-Vis spectroscopy cannot easily distinguish humulone and iso-humulone content in beer; hence, this measurement cannot be used to determine the age of beer, and it is not useful in estimating the evolution of IBUs over time.

References

1. Urban, J., Dahlberg, C. J., Carroll, B. J. & Kaminsky, W. Absolute configuration of beer's bitter compounds. *Angew. Chemie - Int. Ed.* **52,** 1553–1555 (2013).
2. De Keukeleire, D., Vindevogel, J., Szücs, R. & Sandra, P. The history and analytical chemistry of beer bitter acids. *TrAC - Trends Anal. Chem.* **11,** 275–280 (1992).
3. Malowicki, M. G. & Shellhammer, T. H. Isomerization and degradation kinetics of hop (humulus lupulus) acids in a model wort-boiling system. *J. Agric. Food Chem.* **53,** 4434–4439 (2005).
4. Teghtmeyer, S. Hops. *J. Agric. Food Chem.* **19,** 9–20 (2018).
5. Cortacero-Ramírez, S., Hernáinz-Bermúdez.De Castro, M., Segura-Carretero, A., Cruces-Blanco, C. & Fernández-Gutiérrez, A. Analysis of beer components by capillary electrophoretic methods. *TrAC - Trends Anal. Chem.* **22,** 440–445 (2003).
6. Oladokun, O. *et al.* Modification of perceived beer bitterness intensity, character and temporal profile by hop aroma extract. *Food Res. Int.* **86,** 104–111 (2016).
7. Laws, D. R. J. & Elvidge, J. A. Chemistry of Hop Constituents. Part XXXV1l.l Separation and Characterisation of cis- and trans-lsohumulone and Deduction of Absolute Configurations. *J. Chem. Soc., Faraday Trans.* 2412–2415 (1970).
8. Oladokun, O. *et al.* Perceived bitterness character of beer in relation to hop variety and the impact of hop aroma. *Food Chem.* **230,** 215–224 (2017).

9. Taniguchi, Y., Matsukura, Y., Taniguchi, H., Koizumi, H. & Katayama, M. Development of preparative and analytical methods of the hop bitter acid oxide fraction and chemical properties of its components. *Biosci. Biotechnol. Biochem.* **79,** 1684–1694 (2015).

10. Hofte, A. J. P. *et al.* Characterization of Hop Acids by Liquid Chromatography with Negative Electrospray Ionization Mass Spectrometry. *J. Am. Soc. Brew. Chem.* **56,** 118–122 (1998).

11. Kao, T. H. & Wu, G. Y. Simultaneous determination of prenylflavonoid and hop bitter acid in beer lee by HPLC-DAD-MS. *Food Chem.* **141,** 1218–1226 (2013).

12. Terabe, S. Electrokinetic chromatography: An interface between electrophoresis and chromatography. *TrAC - Trends Anal. Chem.* **8,** 129–134 (1989).

13. Terabe, S. *Micellar Electrokinetic Chromatography. Beckman* (1992).

14. Cumeras, R., Figueras, E., Davis, C. E., Baumbach, J. I. & Chemistry, A. Review on Ion Mobility Spectrometry. Part 1: Current Instrumentation. *HHS Public Access* **140,** 1376–1390 (2016).

15. García-Villalba, R., Cortacero-Ramírez, S., Segura-Carretero, A., Martín-Lagos Contreras, J. A. & Fernández-Gutiérrez, A. Analysis of hop acids and their oxidized derivatives and iso-α-acids in beer by capillary electrophoresis-electrospray ionization mass spectrometry. *J. Agric. Food Chem.* **54,** 5400–5409 (2006).

16. Popescu, V., Soceanu, A., Dobrinas, S. & Stanciu, G. A study of beer bitterness loss

during the various stages of the Romanian beer production process. *J. Inst. Brew.* **119,** 111–115 (2013).

17. Frisch, M. J., Trucks, G. W., Schlegel, H. B., Scuseria, G. E., Robb, M. A., Cheeseman, J.R. et al. *Gaussian 09, Revision D.01. Gaussian, Inc* (2009).

18. Kim, Y., Choi, S. & Kim, W. Y. Efficient basin-hopping sampling of reaction intermediates through molecular fragmentation and graph theory. *J. Chem. Theory Comput.* **10,** 2419–2426 (2014).

19. Hehre, W. J. *A guide to molecular mechanics and quantum chemical calculations*. *Wavefunction, Inc* (2003).

20. Wales, D. J. & Scheraga, H. A. Global optimization of clusters, crystals, and biomolecules. *Science* **285,** 1368–1372 (1999).

21. Allinger, N. L., Li, F. & Yan, L. Molecular mechanics. The MM3 force field for alkenes. *J. Comput. Chem.* **11,** 848–867 (1990).

22. Cramer, C. J. *Essentials of computational chemistry: Theories and models*. **108,** *John Wiley & Sons Ltd* (2002).

23. Box, V. G. S. The Molecular Mechanics of Quantized Valence Bonds. *J. Mol. Model.* **3,** 124–141 (1997).

24. Rappé, A. K., Casewit, C. J., Colwell, K. S., Goddard, W. A. & Skiff, W. M. UFF, a Full Periodic Table Force Field for Molecular Mechanics and Molecular Dynamics Simulations. *J. Am. Chem. Soc.* **114,** 10024–10035 (1992).

25. Rajagopal, A. K. & Callaway, J. Inhomogeneous electron gas. *Phys. Rev. B* **7,** 1912–1919 (1973).

26. Kohn, W. & Sham, L. J. Self-consistent equations including exchange and correlation effects. *Phys. Rev.* **140,** (1965).

27. Orio, M., Pantazis, D. A. & Neese, F. Density functional theory. *Photosynth. Res.* **102,** 443–453 (2009).

28. Zhao, Y. & Truhlar, D. G. Hybrid meta density functional theory methods for thermochemistry, thermochemical kinetics, and noncovalent interactions: The MPW1B95 and MPWB1K models and comparative assessments for hydrogen bonding and van der Waals interactions. *J. Phys. Chem. A* **108,** 6908–6918 (2004).

29. Campbell, J. L., Zhu, M. & Hopkins, W. S. Ion-molecule clustering in differential mobility spectrometry: Lessons learned from tetraalkylammonium cations and their isomers. *J. Am. Soc. Mass Spectrom.* **25,** 1583–1591 (2014).

30. Settanni, G. *et al.* Using differential mobility spectrometry to measure ion solvation: An examination of the roles of solvents and ionic structures in separating quinoline-based drugs. *Analyst* **140,** 6897–6903 (2015).

31. Eiceman, G. A. & Karpas, Z. *Ion mobility spectrometry. Taylor & Francis Group* (2005).

32. Schneider, B. B., Covey, T. R., Coy, S. L., Krylow, E. V. & Nazarov, E. G. Chemical Effects in the Separation Process of a Differential Mobility / Mass Spectrometer

System. *Anal. Chem.* **82,** 1867–1880 (2010).

33. Schneider, B. B., Covey, T. R., Coy, S. L., Krylov, E. V. & Nazarov, E. G. Planar differential mobility spectrometer as a pre-filter for atmospheric pressure ionization mass spectrometry. *Int. J. Mass Spectrom.* **298,** 45–54 (2010).

34. Revercomb, H. E. & Mason, E. A. Theory of plasma chromatography/gaseous electrophoresis- a review. *Anal. Chem.* **47,** 970–983 (1975).

35. Schneider, B. B., Nazarov, E. G., Londry, F., Vouros, P. & Cover, T. R. Differential mobility spectrometry/mass spectrometry: history, theory, design optimization, stimulations, and applications. *Mass Spectrom. Rev.* **35,** 687–737 (2015).

36. Hopkins, W. S. Determining the properties of gas-phase clusters. *Mol. Phys.* **113,** 3151–3158 (2015).

37. Krylov, E. V., Nazarov, E. G. & Miller, R. A. Differential mobility spectrometer: Model of operation. *Int. J. Mass Spectrom.* **266,** 76–85 (2007).

38. Campbell, J. L., Le Blanc, J. Y. & Kibbey, R. G. Differential mobility spectrometry: a valuable technology for analyzing challenging biological samples. *Bioanalysis* **7,** 853–856 (2015).

39. Levin, D. S., Vouros, P., Miller, R. A., Nazarov, E. G. & Morris, J. C. Characterization of gas-phase molecular interactions on differential mobility ion behavior utilizing an electrospray ionization-differential mobility-mass spectrometer system. *Anal. Chem.* **78,** 96–106 (2006).

40. Schneider, B. B., Nazarov, E. G. & Covey, T. R. Peak capacity in differential mobility spectrometry: Effects of transport gas and gas modifiers. *Int. J. Ion Mobil. Spectrom.* **15,** 141–150 (2012).

41. Weckhuysen, B. M. *In-situ Spectroscopy of Catalysts*. *American Scientific Publishers* (2004).

42. Silverstein, R. M., Bassler, G. C. & Morrill, T. C. *Spectrometric identification of organic compounds*. *John Wiley & Sons* (1981).

43. Perkampus, H. H. *UV-Vis spectroscopy and its applications*. *Springer Laboratory* (1992).

44. Moon, J. H. *et al.* Absolute Surface Density of the Amine Group of the Aminosilylated Thin Layers: Ultraviolet−Visible Spectroscopy, Second Harmonic Generation, and Synchrotron-Radiation Photoelectron Spectroscopy Study. *Langmuir* **13,** 4305–4310 (1997).

45. Minas da Piedade, M. E. & Berberan-Santos, M. N. Atomic emission spectra using a UV – Vis spectrophotometer and an optical fiber guided light source. *J. Chem. Educ.* **75,** 1013–1017 (1998).

46. Guevremont, R. & Purves, R. W. High field asymmetric waveform ion mobility spectrometry-mass spectrometry: An investigation of leucine enkephalin ions produced by electrospray ionization. *J. Am. Soc. Mass Spectrom.* **10,** 492–501 (1999).

47. Wu, Z. *et al.* Favorable Effects of Weak Acids on Negative-Ion Electrospray Ionization Mass Spectrometry. *Anal. Chem.* **76,** 839–847 (2004).

48. Schneider, B. B., Covey, T. R. & Nazarov, E. G. DMS-MS separations with different transport gas modifiers. *Int. J. Ion Mobil. Spectrom.* **16,** 207–216 (2013).

49. Hua, Y. *et al.* Comparison of negative and positive ion electrospray tandem mass spectrometry for the liquid chromatography tandem mass spectrometry analysis of oxidized deoxynucleosides. *J. Am. Soc. Mass Spectrom.* **12,** 80–7 (2001).

50. Lentz, N. B. & Houk, R. S. Negative Ion Mode Electrospray Ionization Mass Spectrometry Study of Ammonium-Counter Ion Clusters. *J. Am. Soc. Mass Spectrom.* **18,** 285–293 (2007).

51. Kruve, A., Kaupmees, K., Liigand, J. & Leito, I. Negative electrospray ionization via deprotonation: Predicting the ionization efficiency. *Anal. Chem.* **86,** 4822–4830 (2014).

52. Muthén, L. K. & Muthén, B. O. *UV-Vis Spectrometer User's Guide*. *Perkin Elmer* (2000).

53. Andrés-Iglesias, C., Blanco, C. A., Blanco, J. & Montero, O. Mass spectrometry-based metabolomics approach to determine differential metabolites between regular and non-alcohol beers. *Food Chem.* **157,** 205–212 (2014).

54. Mottillo, C. & Friščić, T. Advances in solid-state transformations of coordination bonds: From the ball mill to the aging chamber. *Molecules* **22,** 144 (2017).

55. http://www.egc.com/index_2.php (accessed Jun 14, 2018).

56. Plamer, J. J. *How to brew: Everything you need to know to brew great beer every time. Brewers Publications* (2017).

57. Mcgivney. Determination of International Bitterness Units in Wort Using the Spectrophotometric Method. *J. Am. Soc. Brew. Chem.* **69,** 294 (2011).

58. De Keukeleirc, D. Fundamentals of beer and hop chemistry. *Quim. Nova* **23,** 108–112 (2000).

Appendix I: Energy Summary

Neutral humulone and its isomers: summary of Gibbs' energies and relative energies at 298 K are given in kJ mol^{-1}. Calculations used the B3LYP functional and 6-311++G(d,p) basis set.

Table A1.1. The Gibbs' Energies and Relative Energies of Neutral Humulone and Its Isomers

Chemicals	Gibbs (hartree)	Relative energy (kJ mol^{-1})
Humulone	-1194.4102	0.00
trans iso-humulone	-1194.3970	34.67
cis iso-humulone	-1194.3932	44.78

Deprotonated humulone and deprotonated humulone derivatives: summary of Gibbs' energies and relative energies at 298 K are given in kJ mol^{-1}. Calculations used the B3LYP functional and 6-311++G(d,p) basis set. These are associated to Figure 4.11. The calculated geometries of deprotonated humulone are Isomer 1, 2, and 3. Isomer 4 and Isomer 7 are deprotonated forms of *cis* iso-humulone, and Isomer 5 and Isomer 6 are deprotonated forms of *trans* iso-humulone.

Table A1.2. The Gibbs' Energies and Relative Energies of Deprotonated Humulone and Deprotonated Iso-humulone

Chemicals	Gibbs (hartree)	Relative energy (kJ mol^{-1})
Isomer 1	-1193.9050	0.00
Isomer 2	-1193.9015	9.21
Isomer 3	-1193.9011	10.13
Isomer 4	-1193.9002	12.44
Isomer 5	-1193.8977	19.14
Isomer 6	-1193.8855	51.22
Isomer 7	-1193.8133	240.70
Intermediate 1	-1193.6584	647.42
Intermediate 2	-1193.6613	639.67

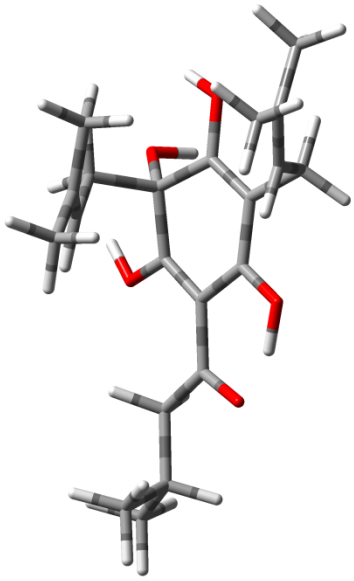

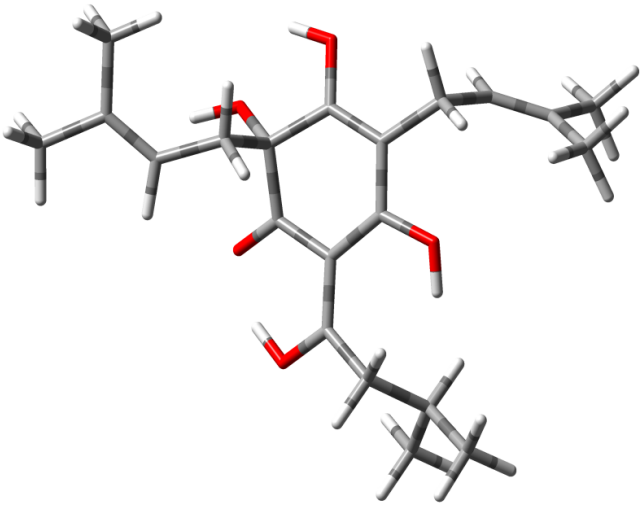

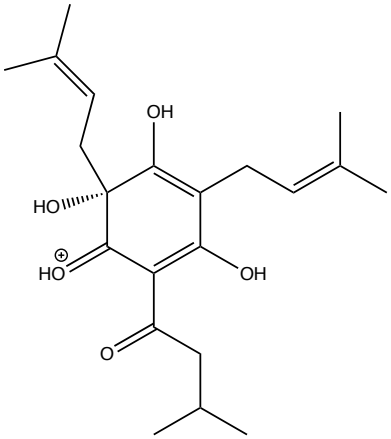

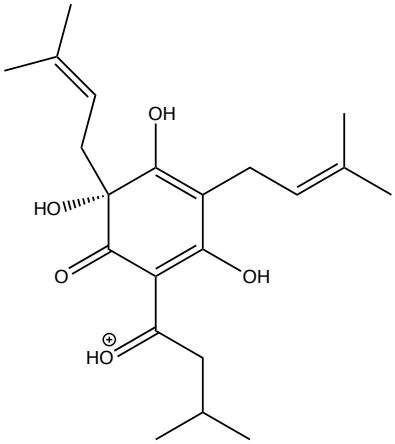

Isomer 1: 0.0 kJ mol^{-1}

Isomer 2: 1.0 kJ mol^{-1}

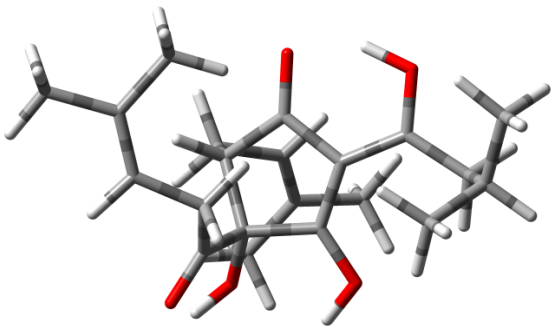

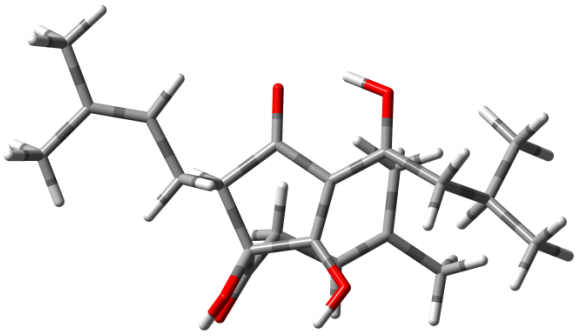

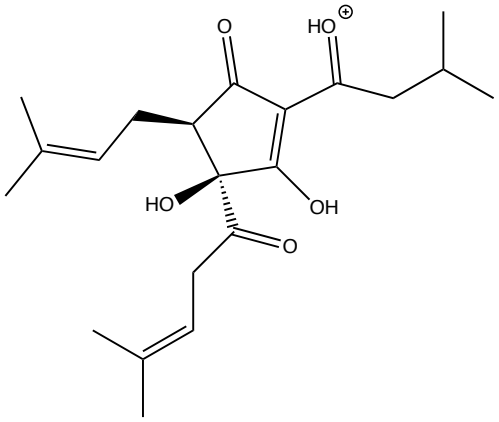

Isomer 3: 9.7 kJ mol^{-1}

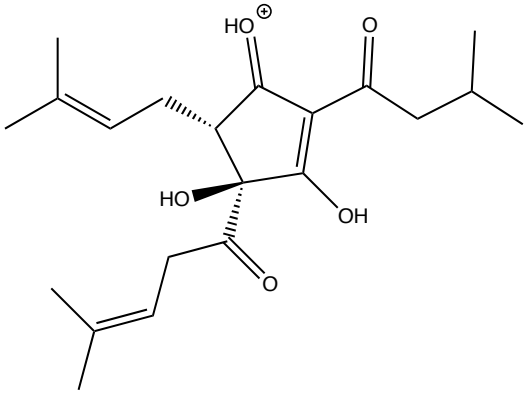

Isomer 4: 14.7 kJ mol^{-1}

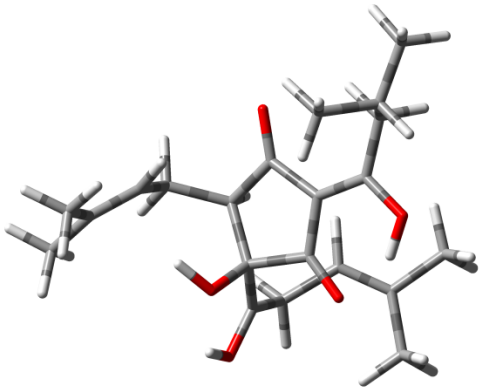

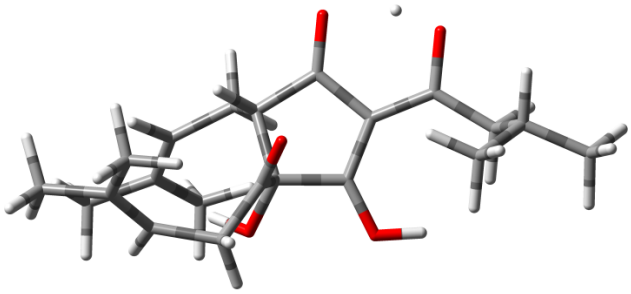

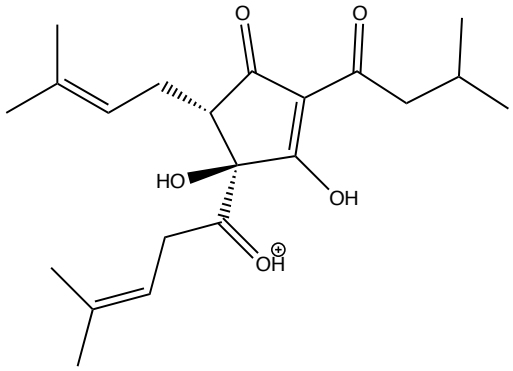

Isomer 5: 26.4 kJ mol^{-1}

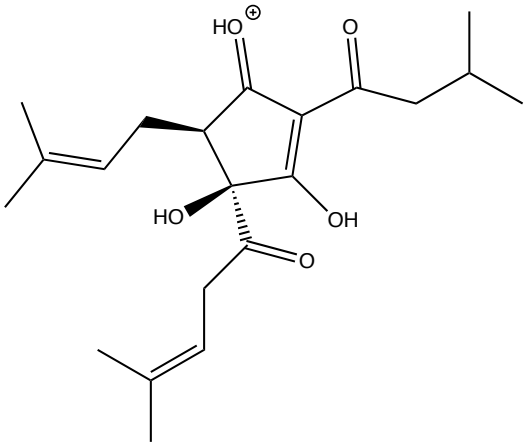

Isomer 6: 27.0 kJ mol^{-1}

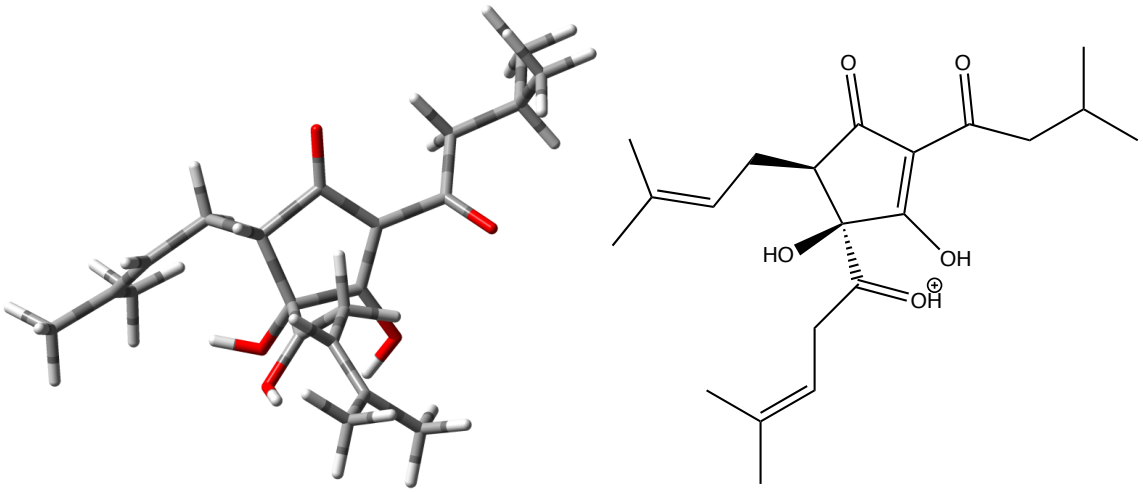

Isomer 7: 113.7 kJ mol^{-1}

Figure A1. The calculated geometries of protonated humulone (Isomer 1 and 2) and its isomers. Isomer 3, Isomer 6 and Isomer 7 are protonated forms of *cis* iso-humulone, and Isomer 4 and Isomer 5 are protonated forms of *trans* iso-humulone. Relative Gibbs energies at 298 K are given in kJ mol^{-1}. Calculations used the B3LYP fuctional and 6-311++G (d, p) basis set.

Protonated humulone and protonated isomeric humulone: summary of Gibbs' energies and relative energies at 298 K are given in kJ mol^{-1}. Calculations used the B3LYP functional and 6-311++G(d,p) basis set. These are associated to Figure A1. The calculated geometries of protonated humulone are Isomer 1 and 2. Isomer 3, Isomer 6, and Isomer 7 are protonated forms of *cis* iso-humulone, and Isomer 4 and Isomer 5 are protonated forms of *trans* iso-humulone.

Table A1.3. The Gibbs' Energies and Relative Energies of Protonated Humulone and Protonated Iso-humulone

Chemicals	Gibbs (hartree)	Relative energy (kJ mol^{-1})
Isomer 1	-1194.7555	0.00
Isomer 2	-1194.7551	1.00
Isomer 3	-1194.7518	9.71
Isomer 4	-1194.7499	14.74
Isomer 5	-1194.7454	26.40
Isomer 6	-1194.7452	26.98
Isomer 7	-1194.7121	113.68

Appendix II: Structures

Neutral Humulone and Iso-humulone

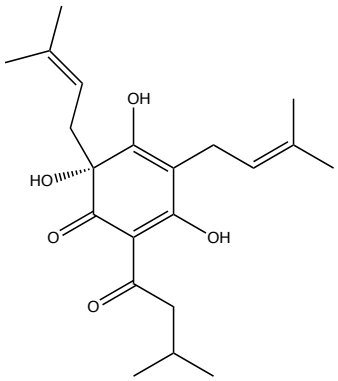

Humulone

C	1.127848	0.579592	-1.200812
C	0.958972	1.696000	-0.455730
C	-1.559163	1.395768	-0.445490
C	-1.365979	0.115432	-1.081879
C	-0.035043	-0.246313	-1.428952
O	1.964302	2.559284	-0.234149
H	1.573646	3.380323	0.107549
O	0.191290	-1.366617	-2.070892
H	-0.729801	-1.808573	-2.197832
C	2.453463	0.199541	-1.830252
H	2.263705	-0.100495	-2.866061
H	3.085093	1.085615	-1.863020
C	3.139481	-0.943734	-1.121689
H	2.610231	-1.890407	-1.188297
C	4.294738	-0.907998	-0.447407
C	5.135736	0.325483	-0.237364
H	5.323329	0.474660	0.832493
H	6.116762	0.207246	-0.712077
H	4.675912	1.235559	-0.620581
C	4.853980	-2.156227	0.190924
H	4.957647	-2.026986	1.275359
H	4.221997	-3.027985	0.009442
H	5.856842	-2.374641	-0.194180
C	-2.450184	-0.788751	-1.426274
C	-3.867441	-0.525401	-0.985665
H	-4.156426	0.489637	-1.259777
H	-4.500598	-1.240624	-1.517059
C	-4.055316	-0.704077	0.542816

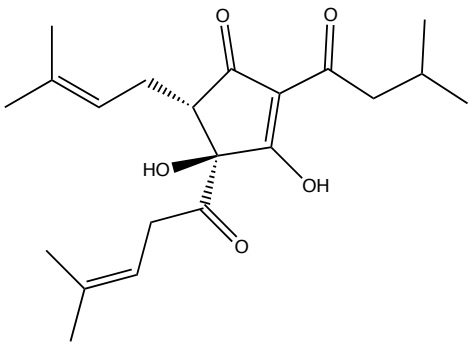

trans Iso-humulone

C	0.869506	-1.683992	0.338348
C	0.069923	0.570912	-0.007148
C	-0.061261	-1.714452	-0.910901
H	0.471846	-2.083687	-1.792720
C	-0.390560	-0.228758	-1.156633
O	-0.954093	0.160203	-2.161720
C	-0.120580	2.035349	0.211580
O	0.629916	2.636573	0.961264
C	-1.255309	2.729888	-0.509107
H	-1.078834	3.805837	-0.425618
H	-1.231099	2.438597	-1.562533
C	-2.651846	2.380987	0.065704
H	-2.763380	1.290805	0.036314
C	-2.800962	2.842316	1.521600
H	-3.784761	2.568693	1.914326
H	-2.044317	2.398239	2.173288
H	-2.701697	3.930259	1.597980
C	-3.744645	2.989387	-0.823010
H	-4.740360	2.746805	-0.439525
H	-3.659811	4.081064	-0.854628
H	-3.676295	2.616394	-1.848491
C	0.690690	-0.273192	0.865916
O	1.102184	-0.004877	2.091854
H	1.273597	-0.854532	2.533716
O	0.577276	-2.588876	1.381139
H	1.290430	-3.254830	1.359345
C	2.335649	-1.975557	-0.123586
C	3.063434	-1.059300	-1.085419

H	-3.394397	0.007750	1.046760
C	-3.687316	-2.121265	0.999167
H	-4.326541	-2.865124	0.512892
H	-2.651489	-2.373473	0.756325
H	-3.813474	-2.222615	2.080956
C	-5.496452	-0.351840	0.927882
H	-6.206905	-1.019775	0.429000
H	-5.646628	-0.451292	2.006895
H	-5.739471	0.675714	0.644506
O	-2.207904	-1.857169	-2.034979
O	-2.608110	2.029289	-0.342537
C	-0.332279	2.004089	0.245991
O	-0.462053	3.415004	0.328491
H	-1.405876	3.601258	0.185316
C	-0.300201	1.448630	1.728292
H	0.495979	2.003038	2.227272
H	-1.246097	1.790270	2.159924
C	-0.149783	-0.032234	1.894143
H	-1.049654	-0.615928	1.723968
C	0.975243	-0.693364	2.196392
C	2.309785	-0.046656	2.452895
H	2.287401	1.041579	2.409597
H	2.691484	-0.343925	3.436200
H	3.031012	-0.390605	1.707276
C	0.988500	-2.197868	2.281440
H	0.003508	-2.629495	2.093130
H	1.691152	-2.609970	1.548040
H	1.329918	-2.531914	3.267937
H	3.561709	-1.708998	-1.814119
H	2.371751	-0.409864	-1.618354
C	4.097314	-0.266092	-0.310939
H	4.755207	-0.878251	0.300442
C	4.275354	1.061206	-0.310473
C	3.470979	2.052597	-1.107713
H	2.742395	1.591823	-1.774382
H	2.933407	2.728601	-0.435324
H	4.139098	2.670064	-1.718188
C	5.358346	1.677180	0.539947
H	6.065818	2.240973	-0.078451
H	4.924446	2.387805	1.252059
H	5.915774	0.925290	1.101431
O	2.855339	-2.978150	0.321122
C	-1.336843	-2.584241	-0.766095
H	-1.809504	-2.592977	-1.749066
H	-1.007460	-3.609630	-0.564507
C	-2.311057	-2.164102	0.301923
H	-1.941621	-2.258000	1.319264
C	-3.572839	-1.743617	0.134526
C	-4.435140	-1.420728	1.330726
H	-4.785940	-0.382846	1.292730
H	-5.331628	-2.052005	1.346138
H	-3.899522	-1.566974	2.270596
C	-4.263144	-1.565408	-1.193936
H	-5.111319	-2.255373	-1.278527
H	-4.676014	-0.553845	-1.273865
H	-3.608946	-1.720726	-2.050472

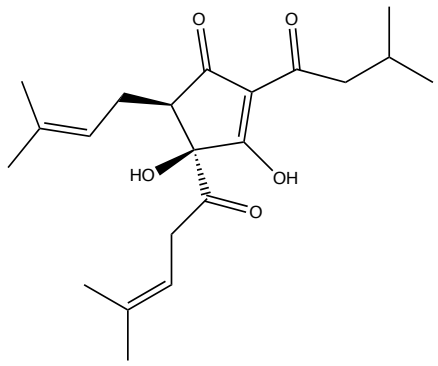

cis Iso-humulone

C	0.082208	0.249034	0.957830
C	-1.310797	0.434190	0.383076
C	-1.353820	-0.596013	-0.788230

C	0.104938	-1.081645	-0.910350
C	0.899878	-0.538630	0.204863
H	-1.611167	-0.115366	-1.737790
O	0.478221	-1.810783	-1.808575
C	2.326884	-0.841303	0.529177
C	2.871716	-2.182862	0.078675
H	2.606271	-2.325729	-0.974884
H	2.282955	-2.942773	0.613444
C	4.371987	-2.399116	0.319547
H	4.595009	-2.088113	1.345690
C	4.720477	-3.887325	0.176448
H	4.493487	-4.250313	-0.831913
H	5.785468	-4.058224	0.358282
H	4.157669	-4.501642	0.886071
C	5.225084	-1.543982	-0.628457
H	5.016280	-0.480208	-0.501079
H	6.290981	-1.700386	-0.437943
H	5.031901	-1.811381	-1.673549
O	2.989246	-0.036610	1.158569
O	0.354291	0.794692	2.130598
H	-0.491026	1.060564	2.531385
C	-1.558906	1.865251	-0.187713
C	-0.596525	2.495240	-1.174920
H	0.053527	1.748262	-1.627515
H	-1.209931	2.945240	-1.963818
C	0.194011	3.573400	-0.461454
H	-0.424719	4.316761	0.034580
C	1.525495	3.693898	-0.382151
C	2.134912	4.835779	0.392757
H	2.764826	5.454318	-0.256487
H	1.374899	5.475491	0.844809
H	2.782722	4.453026	1.189275
C	2.527652	2.764241	-1.012538
H	3.094054	2.237271	-0.237697
H	2.080234	2.015800	-1.666219
H	3.248323	3.337424	-1.605789
O	-2.558546	2.439656	0.189103
O	-2.219318	0.235651	1.444425
H	-2.917047	0.906151	1.327832
C	-2.332078	-1.773916	-0.578173
H	-2.219514	-2.168179	0.432041
H	-2.004925	-2.557980	-1.271279
C	-3.760182	-1.414138	-0.887356
H	-3.911020	-1.017308	-1.891521
C	-4.844980	-1.552310	-0.114101
C	-6.210819	-1.170601	-0.630555

H	-6.169785	-0.796667	-1.655490
H	-6.891211	-2.030037	-0.608210
H	-6.664860	-0.396378	-0.000903
C	-4.837168	-2.093762	1.292300
H	-3.835683	-2.270500	1.680571
H	-5.341886	-1.397148	1.971453
H	-5.396809	-3.035415	1.341621

Deprotonated Humulone and Deprotonated Iso-humulone (Associated to Figure 4.11 and Table A.2)

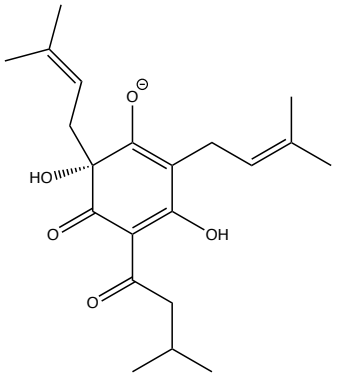

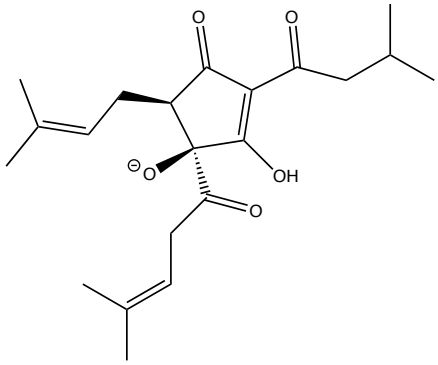

Isomer 1				Isomer 2			
C	1.141700	0.435796	-1.423888	C	0.113800	-0.902897	0.849767
C	0.929414	1.768503	-0.953349	C	0.669547	0.535714	0.534701
C	-1.608788	1.168011	-0.801154	C	-0.471648	1.213172	-0.236805
C	-1.282232	-0.196325	-1.097961	C	-1.400317	0.046855	-0.656471
C	0.110945	-0.487865	-1.431651	C	-0.997108	-1.173187	0.001897
O	1.824870	2.618820	-0.883639	H	-0.097119	1.668624	-1.155972
O	0.402571	-1.743739	-1.805520	O	-2.349419	0.251904	-1.418126
H	-0.466282	-2.259827	-1.761493	C	-1.632160	-2.486079	-0.113414
C	2.537421	0.056980	-1.882498	C	-2.946804	-2.593254	-0.886386
H	2.486052	-0.850600	-2.483423	H	-3.073721	-3.650227	-1.144884
H	2.900994	0.863434	-2.529158	H	-2.883363	-1.996182	-1.798488
C	3.531308	-0.096704	-0.754473	C	-4.173586	-2.107282	-0.080594
H	3.911001	0.846503	-0.369782	H	-3.970477	-1.078043	0.232442
C	3.956215	-1.231241	-0.185016	C	-5.418183	-2.078837	-0.977917
C	3.467380	-2.608984	-0.557506	H	-5.649382	-3.081541	-1.358111
H	3.104551	-3.132359	0.336739	H	-6.296176	-1.721758	-0.427447
H	2.647647	-2.587298	-1.273332	H	-5.263028	-1.417687	-1.834857
H	4.285898	-3.218798	-0.963925	C	-4.416680	-2.961156	1.171701
C	4.978908	-1.213067	0.926763	H	-4.647294	-3.997505	0.897919
H	5.327440	-0.200904	1.145847	H	-3.538175	-2.984717	1.820448
H	4.567814	-1.639555	1.851508	H	-5.260947	-2.570805	1.751518
H	5.853134	-1.823786	0.664137	O	-1.150062	-3.502004	0.385561
C	-2.258175	-1.244495	-1.136818	O	0.637631	-1.519756	1.781640
C	-3.688566	-1.018232	-0.677729	C	1.939271	0.368565	-0.328957
H	-4.110014	-0.151859	-1.187720	C	3.207726	-0.001305	0.440458
H	-4.246685	-1.916660	-0.960786	H	2.934768	-0.766807	1.170278
C	-3.808982	-0.801698	0.847670	H	3.466853	0.884494	1.035693
H	-3.227462	0.088490	1.101128	C	4.353598	-0.400666	-0.439105

C	-3.250453	-1.991850	1.637789
H	-2.203036	-2.180058	1.389767
H	-3.316948	-1.809074	2.715646
H	-3.809950	-2.906690	1.411793
C	-5.269134	-0.524061	1.224351
H	-5.645455	0.358249	0.698694
H	-5.908324	-1.375587	0.961140
H	-5.372983	-0.348725	2.300684
O	-1.963125	-2.426511	-1.480302
O	-2.746152	1.671171	-0.781593
C	-0.464760	2.120397	-0.404102
O	-0.818646	3.436724	-0.800565
H	-1.788817	3.400160	-0.852532
C	-0.375664	2.103799	1.166489
H	0.347115	2.883300	1.409821
H	-1.358373	2.440636	1.515007
C	-0.031027	0.785071	1.794291
H	-0.823034	0.040553	1.771767
C	1.146337	0.415517	2.311114
C	2.363741	1.300379	2.393269
H	3.232369	0.770106	1.994953
H	2.260762	2.224392	1.826348
H	2.588547	1.545649	3.440224
C	1.356227	-0.984094	2.832555
H	2.092751	-1.505943	2.210083
H	1.752137	-0.973759	3.856499
H	0.432110	-1.566741	2.824424
H	4.617754	0.327912	-1.201810
C	5.056675	-1.539299	-0.398838
C	6.190730	-1.778233	-1.367365
H	6.000364	-2.667543	-1.981150
H	6.335438	-0.927889	-2.037394
H	7.133920	-1.960953	-0.835996
C	4.806966	-2.676362	0.560367
H	5.685567	-2.845886	1.196367
H	3.945195	-2.516277	1.206804
H	4.635972	-3.608422	0.008718
O	1.927519	0.501413	-1.534253
O	1.026363	1.134637	1.780006
C	-1.274690	2.273245	0.551740
H	-1.520969	1.867165	1.538946
H	-2.215330	2.411665	0.015965
C	-0.547954	3.578631	0.730482
H	0.269358	3.544849	1.446697
C	-0.775695	4.738838	0.099059
C	0.065571	5.958347	0.394761
H	-0.555281	6.794224	0.743982
H	0.818360	5.751540	1.158701
H	0.582945	6.310082	-0.507455
C	-1.839236	4.956084	-0.949023
H	-1.386369	5.304580	-1.885880
H	-2.407912	4.054370	-1.172847
H	-2.543457	5.737643	-0.634424
H	1.087302	0.380183	2.393258

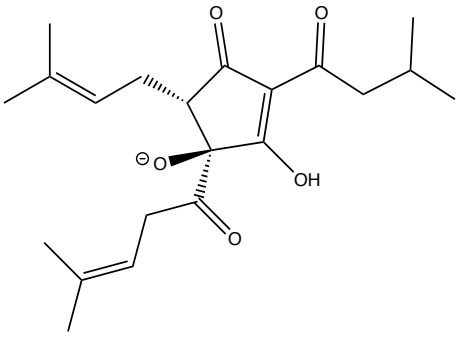

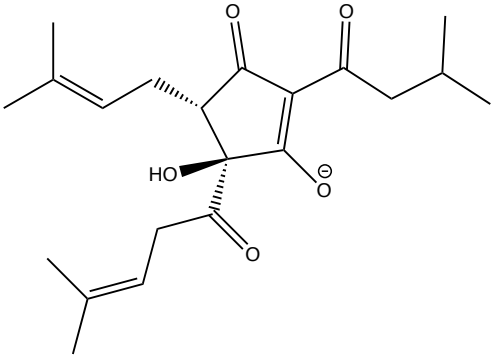

Isomer 3

C	0.852659	-1.764786	0.311177
C	0.014609	0.538602	0.185532
C	-0.084946	-1.647678	-0.908994
H	0.446185	-1.880518	-1.838896

Isomer 4

C	-0.482644	-1.446027	-0.310165
C	0.731373	0.533781	0.439861
C	0.697032	-1.229258	-1.263202
H	0.335674	-1.106750	-2.287019

C	-0.472797	-0.152636	-0.977580	C	1.289194	0.131549	-0.831236
O	-1.113523	0.270612	-1.948284	O	2.144660	0.686444	-1.526741
C	-0.136941	1.964383	0.473611	C	1.104456	1.706950	1.228411
O	0.502226	2.535833	1.357042	O	0.664629	1.919421	2.358023
C	-1.122982	2.775543	-0.367581	C	2.056708	2.727682	0.602400
H	-0.882898	3.831762	-0.203032	H	2.452287	3.332409	1.425920
H	-0.984944	2.526351	-1.422243	H	2.875813	2.204981	0.104091
C	-2.602753	2.517439	-0.005341	C	1.375390	3.649843	-0.435290
H	-2.777750	1.440758	-0.096548	H	0.902144	3.005729	-1.182889
C	-2.924184	2.941850	1.434483	C	0.295856	4.534836	0.202907
H	-2.773158	4.019830	1.565792	H	0.736631	5.220050	0.936795
H	-3.967082	2.716158	1.684448	H	-0.212882	5.138074	-0.557605
H	-2.282974	2.431934	2.157024	H	-0.455812	3.938424	0.724653
C	-3.525426	3.225690	-1.006705	C	2.427777	4.500198	-1.159506
H	-3.337551	2.874068	-2.024977	H	1.963007	5.154153	-1.906169
H	-4.580477	3.042226	-0.772938	H	2.971909	5.137548	-0.451341
H	-3.365534	4.310750	-0.986777	H	3.154030	3.863008	-1.671538
C	0.694086	-0.384417	1.049452	C	-0.188193	-0.461413	0.881032
O	1.092610	-0.302129	2.207013	O	-0.722851	-0.709772	1.964880
O	0.495740	-2.807702	1.192996	O	-0.628306	-2.759733	0.224988
C	2.327086	-1.930429	-0.112960	H	-0.778469	-2.607716	1.175913
C	2.927946	-0.938637	-1.123754	C	-1.825362	-1.022131	-0.946934
H	3.202177	-1.540753	-2.001059	C	-3.075327	-1.460723	-0.182917
H	2.191407	-0.204592	-1.441741	H	-3.133684	-2.550420	-0.309321
C	4.161818	-0.287815	-0.552556	H	-2.881600	-1.305500	0.880741
H	4.906616	-0.992853	-0.192101	C	-4.335474	-0.805506	-0.661659
C	4.397243	1.020576	-0.395549	H	-4.483761	-0.840220	-1.738115
C	3.455481	2.128575	-0.791683	C	-5.265179	-0.183584	0.074161
H	3.998321	2.918590	-1.324875	C	-5.207890	-0.006872	1.571017
H	2.638910	1.791095	-1.428655	H	-5.286763	1.055048	1.832901
H	3.003902	2.583744	0.096982	H	-6.055543	-0.511574	2.052689
C	5.669481	1.489756	0.268902	H	-4.289842	-0.387538	2.016658
H	6.308850	0.652674	0.558414	C	-6.485807	0.421083	-0.578288
H	6.242868	2.149942	-0.394524	H	-6.538954	1.500091	-0.386343
H	5.439684	2.071264	1.170032	H	-6.483182	0.268519	-1.659789
O	3.017148	-2.811731	0.351394	H	-7.408374	-0.014484	-0.172662
C	-1.335350	-2.565712	-0.897353	O	-1.887585	-0.378883	-1.973499
H	-0.983664	-3.599493	-0.806854	C	1.777638	-2.339650	-1.283835
H	-1.797158	-2.466793	-1.881458	H	1.287732	-3.271843	-1.587893
C	-2.343988	-2.310162	0.190929	H	2.477831	-2.071340	-2.077517
H	-1.998111	-2.557159	1.190096	C	2.506362	-2.586363	0.010108
C	-3.590222	-1.836847	0.056854	H	1.903079	-3.048041	0.787373
C	-4.221447	-1.414149	-1.246863	C	3.783502	-2.308837	0.304511
H	-3.505549	-1.356233	-2.065112	C	4.348281	-2.641836	1.665292
H	-5.031705	-2.100136	-1.529921	H	5.220884	-3.303560	1.581233
H	-4.673903	-0.421191	-1.142614	H	4.690151	-1.734925	2.179352

C	-4.485934	-1.680065	1.263099
H	-3.992918	-2.015091	2.178127
H	-5.414701	-2.254123	1.143379
H	-4.781123	-0.632150	1.399397
H	0.878042	-2.553636	2.046634
H	3.607270	-3.130929	2.301202
C	4.764831	-1.645970	-0.629642
H	5.601566	-2.320960	-0.856104
H	4.312112	-1.320638	-1.564683
H	5.197220	-0.757936	-0.153909

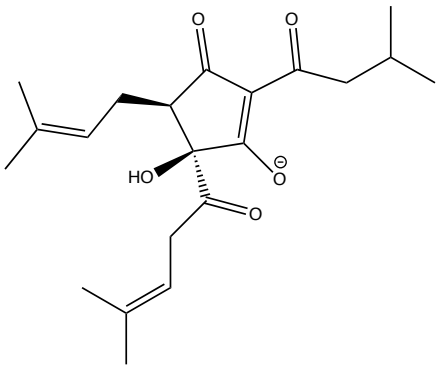

Isomer 5

C	-0.859882	0.117183	-0.568533
C	0.691391	0.091199	-0.905590
C	1.323635	-0.682812	0.265353
C	0.126735	-1.294108	1.047534
C	-1.108863	-0.740271	0.543428
H	1.788435	0.020579	0.964782
O	0.327111	-2.102324	1.947359
C	-2.424393	-1.007338	1.126654
C	-3.666777	-0.604510	0.326838
H	-3.547444	0.418979	-0.035765
H	-4.513796	-0.651841	1.020207
C	-3.940907	-1.512694	-0.893025
H	-3.042786	-1.499713	-1.518609
C	-4.223130	-2.962865	-0.476700
H	-3.401369	-3.379195	0.110428
H	-5.129018	-3.023654	0.138177
H	-4.370600	-3.599265	-1.356691
C	-5.095829	-0.945069	-1.729372
H	-4.863007	0.064974	-2.078113
H	-5.293656	-1.569613	-2.608094
H	-6.020390	-0.897406	-1.140607
O	-2.576436	-1.547517	2.221119
O	-1.615946	0.779975	-1.284414
C	1.196373	1.518025	-1.113949
C	1.427553	2.469255	0.065207
H	2.373851	2.162575	0.526387

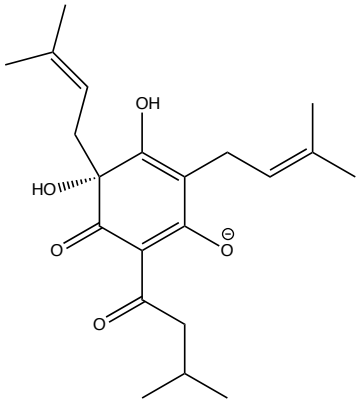

Isomer 6

C	0.479403	0.073232	-1.482063
C	0.839060	-1.164476	-1.119217
C	-1.577312	-1.774280	-0.699474
C	-1.945337	-0.405885	-0.868602
C	-0.907373	0.560963	-1.197725
O	2.066196	-1.695940	-1.392101
H	1.984528	-2.646050	-1.216297
O	-1.110528	1.780657	-1.362374
C	1.426069	1.011355	-2.198496
H	2.198073	0.424285	-2.698320
H	0.854537	1.541976	-2.966439
C	2.035365	2.046423	-1.283989
H	1.342436	2.830720	-0.990270
C	3.282842	2.074388	-0.799177
C	4.325323	1.013471	-1.054035
H	5.172664	1.421793	-1.621094
H	4.732944	0.654332	-0.100439
H	3.930161	0.146761	-1.581805
C	3.747698	3.202571	0.091425
H	4.081135	2.826335	1.067653
H	4.607859	3.722346	-0.351404
H	2.957140	3.936875	0.262478
C	-3.358891	-0.022457	-0.730241
C	-3.688056	1.380354	-0.204585
H	-4.779492	1.423366	-0.117601
H	-3.353880	2.118860	-0.935460

H	1.603332	3.447573	-0.386503	C	-3.042779	1.706290	1.157023
C	0.352533	2.525841	1.124878	H	-1.958692	1.637224	1.031077
H	0.503259	1.897397	1.997816	C	-3.472892	0.705407	2.237795
C	-0.774058	3.246445	1.061521	H	-4.557831	0.741911	2.391369
C	-1.791805	3.183552	2.171003	H	-3.215402	-0.318294	1.954142
H	-1.985969	4.180766	2.586348	H	-2.987781	0.926245	3.195400
H	-2.748101	2.806108	1.790341	C	-3.372658	3.144778	1.574295
H	-1.470731	2.525402	2.980188	H	-4.455752	3.280336	1.683521
C	-1.167095	4.096179	-0.118016	H	-2.906715	3.398108	2.533676
H	-1.545908	5.071194	0.211375	H	-3.016625	3.857631	0.824623
H	-0.348277	4.260137	-0.819289	O	-4.289749	-0.798797	-0.932862
H	-1.970503	3.598623	-0.673186	O	-2.277763	-2.797430	-0.693005
O	1.415699	1.905697	-2.248790	C	-0.089471	-2.033356	-0.323124
O	0.845278	-0.618955	-2.129297	O	0.216212	-3.404329	-0.570917
H	0.834880	0.061798	-2.819616	H	-0.677229	-3.788634	-0.708451
C	2.384908	-1.738226	-0.098204	C	0.045725	-1.756841	1.209507
H	1.968667	-2.391802	-0.870012	H	-0.643407	-2.458777	1.692759
H	2.532549	-2.346319	0.795128	H	-0.321639	-0.749701	1.402703
C	3.671925	-1.147444	-0.602477	C	1.438560	-1.959166	1.722050
H	3.605864	-0.700130	-1.593037	H	1.799787	-2.984227	1.666656
C	4.860486	-1.096858	0.016218	C	2.279593	-1.018552	2.169694
C	6.054883	-0.453044	-0.648226	C	3.689782	-1.367780	2.577977
H	6.879440	-1.169512	-0.761205	H	4.413851	-0.824135	1.957933
H	5.804231	-0.064685	-1.637858	H	3.885652	-1.076660	3.618072
H	6.445336	0.376920	-0.044800	H	3.891810	-2.436863	2.476548
C	5.137924	-1.654172	1.390903	C	1.953979	0.449674	2.266570
H	5.528771	-0.870499	2.052495	H	2.514968	1.010167	1.512736
H	4.253992	-2.080163	1.863994	H	0.899893	0.669785	2.103354
H	5.909657	-2.433837	1.345230	H	2.240294	0.844328	3.249301

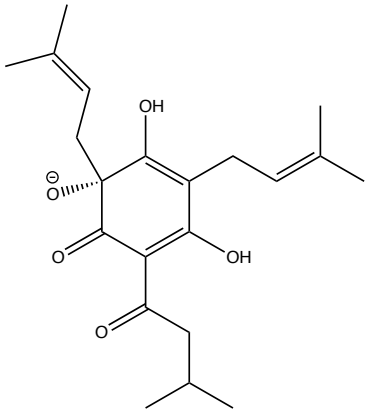

Isomer 7

C	0.773474	-0.764506	0.714473

C	1.010755	0.150541	-0.276979
C	-1.296667	1.129200	0.024126
C	-1.603146	-0.014814	0.900423
C	-0.567828	-0.859675	1.249139
O	2.219389	0.228623	-0.889440
O	-0.838669	-1.890052	2.100562
H	-0.067168	-2.461072	2.154509
C	1.893390	-1.698950	1.154732
H	2.771205	-1.098082	1.414333
H	1.641818	-2.202220	2.098956
C	2.252204	-2.742191	0.115976
H	1.392915	-3.189484	-0.380353
C	3.471941	-3.131263	-0.286894
C	4.772015	-2.618308	0.283284
H	4.637873	-1.827226	1.020908
H	5.322631	-3.434540	0.767310
H	5.421164	-2.235251	-0.513205
C	3.631832	-4.164106	-1.376445
H	4.202764	-3.758660	-2.220607
H	4.187754	-5.037015	-1.011604
H	2.666138	-4.505187	-1.753646
C	-2.990935	-0.244998	1.376633
C	-4.122864	0.054923	0.393759
H	-5.053776	-0.235521	0.893631
H	-4.134755	1.134594	0.226635
C	-3.995595	-0.659662	-0.969685
H	-3.019520	-0.409208	-1.399969
C	-5.077437	-0.156295	-1.934717
H	-6.083394	-0.359856	-1.545108
H	-4.987648	0.922352	-2.092332
H	-4.991433	-0.645639	-2.910990
C	-4.069841	-2.185104	-0.811979
H	-3.945585	-2.683999	-1.779148
H	-3.288427	-2.555229	-0.142811
H	-5.037456	-2.491263	-0.394206
O	-3.257174	-0.693857	2.485810
O	-2.056896	2.093264	-0.076761
C	-0.053473	1.035663	-0.888031
O	-0.462544	0.315056	-1.975054
C	0.487109	2.453624	-1.249029
H	1.260393	2.307283	-2.003115
H	-0.361889	2.946931	-1.730202
C	0.951188	3.285331	-0.089099
H	0.162168	3.543703	0.615761
C	2.184409	3.733242	0.191504
C	3.404269	3.482616	-0.659736

H	4.194603	3.000551	-0.069243
H	3.193663	2.841881	-1.514259
H	3.823637	4.429354	-1.028086
C	2.448299	4.560382	1.428279
H	1.535612	4.719577	2.007148
H	3.185074	4.074445	2.082732
H	2.864696	5.544063	1.170051
H	2.655505	-0.633448	-0.862435

Protonated Humulone and Protonated Iso-humulone (Associated to Figure A.1 and Table A.3)

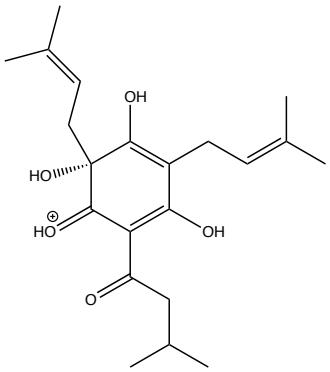

Isomer 1

C	1.142057	-0.080111	-1.275057
C	1.204478	1.263054	-1.066687
C	-1.255555	1.344601	-0.522863
C	-1.352016	-0.014935	-0.673510
C	-0.111671	-0.718025	-1.011159
O	2.318155	1.944029	-1.331791
H	2.174796	2.896325	-1.214498
O	-0.144358	-2.000224	-1.162860
H	-1.117609	-2.304427	-1.009000
C	2.313367	-0.888797	-1.803082
H	1.922406	-1.608538	-2.529480
H	2.973803	-0.215818	-2.346769
C	3.063367	-1.637298	-0.723114
H	2.460077	-2.340537	-0.154653
C	4.374876	-1.571792	-0.454848
C	5.365527	-0.686730	-1.166409
H	4.909944	0.011931	-1.867310
H	6.086361	-1.297306	-1.721185
H	5.946248	-0.106575	-0.441473
C	4.980036	-2.454655	0.608858
H	5.485187	-1.856542	1.375680
H	4.232724	-3.083595	1.095967
H	5.743704	-3.109634	0.175637
C	-2.615704	-0.811260	-0.565920
C	-3.942886	-0.165053	-0.272695
H	-4.160140	0.495777	-1.123193
H	-3.827887	0.515802	0.578238
C	-5.108588	-1.140383	-0.033006

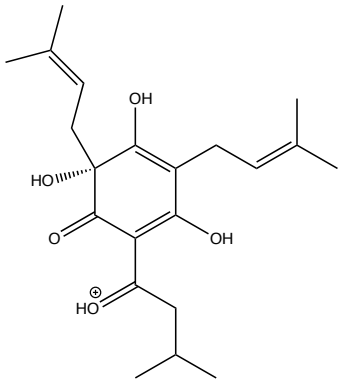

Isomer 2

C	0.425865	-1.451470	-0.447728
C	-0.813658	-1.681612	0.103626
C	-1.093581	0.722627	0.749672
C	0.177893	1.007543	0.078704
C	0.892380	-0.114933	-0.474437
O	-1.228176	-2.911199	0.325855
H	-2.050384	-2.865874	0.852712
O	2.107062	0.008234	-0.989309
H	2.500570	0.877245	-0.835186
C	1.329984	-2.602079	-0.860340
H	0.689352	-3.442450	-1.141714
H	1.885476	-2.316395	-1.752064
C	2.256258	-3.028012	0.257799
H	1.748867	-3.319157	1.175041
C	3.592290	-3.120694	0.224972
C	4.456313	-2.792774	-0.965001
H	5.236491	-2.077318	-0.683033
H	3.906190	-2.377645	-1.808968
H	4.975843	-3.692115	-1.313302
C	4.351676	-3.613006	1.431961
H	5.080209	-2.865897	1.766252
H	3.688897	-3.844437	2.267347
H	4.921550	-4.516210	1.188158
C	0.592327	2.359364	0.030107
C	1.704220	2.944993	-0.791966
H	1.396238	3.965263	-1.033857
H	1.793704	2.413745	-1.744110
C	3.095289	3.028533	-0.077031

H	-5.081514	-1.898033	-0.821976
C	-6.439779	-0.382667	-0.136676
H	-7.280442	-1.062431	0.018958
H	-6.509929	0.405923	0.620135
H	-6.565980	0.080793	-1.119516
C	-4.982416	-1.850463	1.322591
H	-5.009940	-1.127413	2.145424
H	-5.813641	-2.543949	1.469050
H	-4.058373	-2.427241	1.399321
O	-2.540745	-2.033209	-0.732490
O	-2.305186	2.128033	-0.348888
C	0.079214	2.043363	-0.447078
O	-0.018603	3.353954	-1.019783
H	-0.159270	3.295802	-1.976541
C	0.399381	2.319281	1.089267
H	1.366166	2.823491	1.098087
H	-0.345727	3.063774	1.389885
C	0.363748	1.144462	2.014466
H	-0.628040	0.775497	2.263332
C	1.412178	0.561177	2.619223
C	2.851721	0.954519	2.431100
H	2.997145	1.837028	1.808489
H	3.316731	1.147908	3.402759
H	3.405118	0.128660	1.972652
C	1.194998	-0.575297	3.583304
H	1.566153	-0.307806	4.578236
H	0.142162	-0.846805	3.673099
H	1.757758	-1.460516	3.268976
H	-2.020091	3.059833	-0.342078
H	3.402544	2.022574	0.251485
C	3.047391	3.910483	1.176254
H	2.748437	4.930941	0.920606
H	2.350130	3.535865	1.928071
H	4.037272	3.956649	1.635161
C	4.136842	3.534193	-1.084630
H	4.206411	2.890132	-1.966012
H	3.888228	4.543703	-1.424331
H	5.124683	3.573338	-0.621021
O	-0.055046	3.260075	0.711457
O	-1.674124	1.537467	1.466439
C	-1.792717	-0.591373	0.424560
O	-2.587441	-1.063562	1.482238
H	-3.404219	-0.539633	1.511495
C	-2.691981	-0.336843	-0.875266
H	-2.068051	0.144133	-1.633659
H	-2.964428	-1.320825	-1.258074
C	-3.898862	0.492049	-0.557773
H	-3.714115	1.549080	-0.389621
C	-5.175113	0.066563	-0.487398
C	-5.636821	-1.348680	-0.715082
H	-6.331167	-1.380043	-1.561190
H	-4.833105	-2.056388	-0.915389
H	-6.196862	-1.709297	0.153891
C	-6.283363	1.046695	-0.203171
H	-6.862405	0.735220	0.672527
H	-5.907644	2.055599	-0.028943
H	-6.985132	1.079934	-1.043361
H	-0.797578	2.812748	1.230652

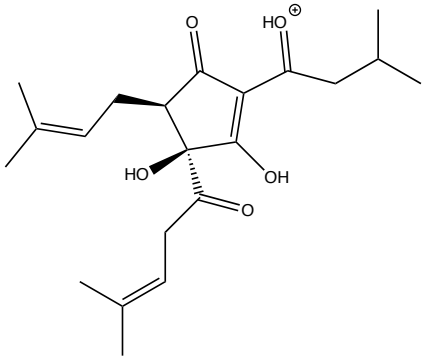

Isomer 3

C	0.729256	0.370736	0.924959
C	0.372224	-1.095132	0.928165
C	0.250043	-1.438573	-0.595848
C	0.022804	-0.072887	-1.220194

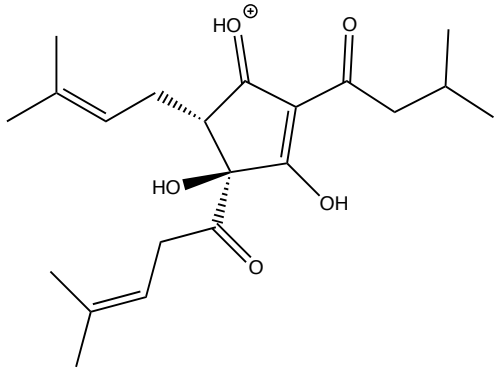

Isomer 4

C	0.893925	1.024095	1.043730
C	-0.301473	-0.920281	0.290757
C	1.828647	0.262003	0.035519
H	2.225293	0.912899	-0.745955

C	0.381847	0.990771	-0.265579	C	0.887689	-0.766503	-0.565986
H	-0.609078	-2.080283	-0.803679	O	1.075956	-1.445814	-1.570330
O	-0.336808	0.150630	-2.371258	C	-1.194122	-2.017040	0.110056
C	0.448292	2.350544	-0.679161	O	-0.981725	-2.793125	-0.898540
C	0.851696	3.500249	0.164864	C	-2.344547	-2.339622	0.982468
H	1.468714	4.154009	-0.458179	H	-2.481578	-3.424080	0.974990
H	1.449356	3.142281	1.002748	H	-2.123025	-2.011858	1.998701
C	-0.347142	4.355758	0.724353	C	-3.684096	-1.659183	0.517874
H	0.157150	5.111039	1.335686	H	-3.485116	-0.589274	0.386026
C	-1.125354	5.083094	-0.375819	C	-4.192653	-2.243357	-0.803735
H	-0.465416	5.673428	-1.015891	H	-3.479677	-2.128494	-1.623258
H	-1.683978	4.393648	-1.014515	H	-4.410166	-3.310416	-0.700473
H	-1.847652	5.766212	0.077489	H	-5.119630	-1.745573	-1.098461
C	-1.267005	3.544914	1.643258	C	-4.719463	-1.821199	1.638303
H	-0.710391	3.046523	2.441568	H	-4.922902	-2.877928	1.835394
H	-1.997575	4.205249	2.115541	H	-4.385492	-1.358153	2.570032
H	-1.833078	2.789405	1.087409	H	-5.662197	-1.351252	1.348633
O	0.119199	2.615116	-1.900125	C	-0.242145	0.054734	1.269484
O	1.326613	0.890544	1.953633	O	-0.979578	0.149732	2.335746
H	1.603195	0.157415	2.544473	H	-0.571455	0.807780	2.936451
C	-1.035748	-1.352703	1.642242	O	1.413965	1.333730	2.303135
C	-2.333328	-0.793074	1.107005	H	1.523903	2.306090	2.327507
H	-2.820021	-0.309021	1.964152	C	0.430313	2.393719	0.376818
H	-2.161862	-0.028834	0.351129	C	-0.303802	2.441576	-0.940508
C	-3.207756	-1.921879	0.590946	H	0.119079	3.290083	-1.490818
H	-3.278308	-2.768659	1.267056	H	-0.131403	1.541917	-1.530455
C	-3.905691	-1.946124	-0.552481	C	-1.782384	2.674078	-0.687251
C	-4.756531	-3.144840	-0.889358	H	-1.997638	3.404758	0.087587
H	-5.807617	-2.854047	-0.988608	C	-2.805645	2.158044	-1.383432
H	-4.457450	-3.572281	-1.852417	C	-2.670883	1.209811	-2.545410
H	-4.687663	-3.924309	-0.129535	H	-1.659173	0.833058	-2.699553
C	-3.955062	-0.838376	-1.571428	H	-3.344609	0.355548	-2.427226
H	-3.352262	0.032548	-1.313392	H	-2.975313	1.712127	-3.470247
H	-3.624517	-1.201498	-2.550013	C	-4.220066	2.576997	-1.071425
H	-4.988045	-0.498437	-1.699798	H	-4.674643	3.063342	-1.941075
O	-0.986356	-2.085125	2.598466	H	-4.844482	1.706820	-0.841046
O	1.337992	-1.764664	1.680471	H	-4.268484	3.270156	-0.230690
H	0.850554	-2.320834	2.322271	O	0.731955	3.382649	0.996871
C	1.524830	-2.123864	-1.181774	C	3.036263	-0.426496	0.753966
H	1.256153	-2.411364	-2.204194	H	3.522642	0.342926	1.351234
H	1.681025	-3.044997	-0.621728	H	2.645660	-1.161195	1.468367
C	2.761713	-1.268226	-1.211494	C	3.989776	-1.080991	-0.204762
H	2.702142	-0.395826	-1.861365	H	3.603843	-1.950827	-0.728938
C	3.943774	-1.502043	-0.618976	C	5.253881	-0.712300	-0.462978
C	5.104183	-0.564228	-0.837717	C	6.090080	-1.499146	-1.439857
H	4.842064	0.273622	-1.486349	H	6.987890	-1.892155	-0.950611

H	5.469322	-0.166118	0.115556
H	5.946690	-1.095611	-1.293157
C	4.255074	-2.686137	0.256014
H	5.038307	-3.295565	-0.207815
H	4.653699	-2.352310	1.219751
H	3.396598	-3.325409	0.451655
H	-0.147879	1.760137	-2.377199
H	5.539205	-2.337117	-1.869379
H	6.436258	-0.857987	-2.257895
C	5.965944	0.458438	0.162869
H	6.852889	0.113705	0.705073
H	6.326057	1.141129	-0.614233
H	5.354047	1.033608	0.857756
H	-0.175807	-2.461269	-1.421480

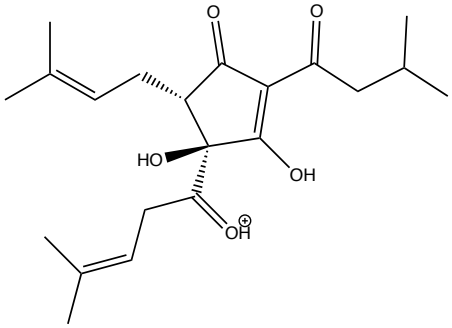

Isomer 5

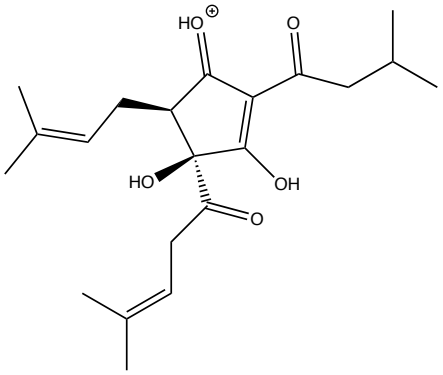

Isomer 6

C	1.151643	-0.725245	-0.264911
C	-1.062622	0.289453	0.017977
C	1.109063	-0.012411	1.114023
H	0.975659	-0.776584	1.886368
C	-0.232000	0.774579	1.118942
O	-0.476743	1.613279	1.956268
C	-2.380078	0.639637	-0.305635
O	-2.956373	0.091766	-1.346893
C	-3.226987	1.603054	0.444284
H	-4.142359	1.065618	0.719212
H	-2.713156	1.909611	1.354841
C	-3.632349	2.854052	-0.395547
H	-4.123106	2.491595	-1.304474
C	-4.642242	3.686031	0.402596
H	-4.963114	4.553839	-0.178731
H	-5.533752	3.105436	0.654357
H	-4.202727	4.054131	1.334918
C	-2.410200	3.690092	-0.794764
H	-1.704603	3.123472	-1.410612
H	-2.720958	4.560896	-1.376723
H	-1.876703	4.051859	0.089625
C	-0.349681	-0.649961	-0.786123
O	-0.724169	-1.245972	-1.786956
H	-2.326618	-0.522757	-1.803816
O	1.928602	-0.090239	-1.273857
H	2.355969	0.726402	-0.921560
C	-1.019496	-0.429025	-0.773692
C	0.420929	-0.085284	-0.471138
C	0.643932	-0.661062	0.966354
C	-0.765948	-0.768561	1.496895
C	-1.733490	-0.706765	0.387363
H	1.208181	0.033433	1.590752
O	-1.092101	-0.947622	2.666530
C	-3.119906	-0.877496	0.659738
C	-4.251862	-0.829184	-0.305364
H	-4.897363	-1.682347	-0.075130
H	-3.916028	-0.957702	-1.338852
C	-5.100861	0.481083	-0.186985
H	-5.406985	0.555819	0.861203
C	-4.292636	1.729703	-0.557245
H	-3.409710	1.867241	0.073389
H	-3.969924	1.698709	-1.604407
H	-4.911076	2.622242	-0.442313
C	-6.357671	0.339495	-1.052458
H	-6.103421	0.234787	-2.112302
H	-6.957569	-0.525311	-0.758646
H	-6.983346	1.228939	-0.951149
O	-3.463242	-1.072450	1.884859
O	-1.387810	-0.360913	-2.021234
H	-2.328146	-0.551113	-2.155035
C	0.418116	1.518272	-0.344474
C	1.336290	2.284486	-1.270044

C	1.626738	-2.150460	-0.241545	H	1.270565	1.870627	-2.277412
C	1.226447	-3.219899	0.708457	H	0.980534	3.315243	-1.278897
H	1.568884	-4.168910	0.292060	C	2.771786	2.181364	-0.778660
H	1.841999	-3.050241	1.606183	H	3.371869	1.415988	-1.259790
C	-0.239207	-3.237592	1.100593	C	3.344665	2.961079	0.151134
H	-0.497881	-2.695048	2.003689	C	4.801561	2.790104	0.497306
C	-1.197928	-3.927525	0.464155	H	5.267779	1.982144	-0.068973
C	-0.988322	-4.735486	-0.786092	H	5.354175	3.713196	0.292064
H	0.046702	-4.773313	-1.125676	H	4.926827	2.584998	1.566248
H	-1.334922	-5.762360	-0.633882	C	2.639752	4.062651	0.896508
H	-1.588714	-4.320442	-1.602307	H	2.698222	3.886598	1.976215
C	-2.604903	-3.934839	0.999602	H	3.139331	5.020229	0.713720
H	-3.307815	-3.578345	0.239191	H	1.587646	4.165722	0.635375
H	-2.910020	-4.956084	1.249942	O	-0.274633	2.015484	0.506901
H	-2.712597	-3.317772	1.892667	O	1.260276	-0.521631	-1.493534
O	2.459697	-2.451807	-1.152118	H	2.031456	-0.977512	-1.110541
C	2.334719	0.837826	1.512859	C	1.336055	-2.053715	1.010676
H	2.095935	1.244996	2.501180	H	0.773669	-2.771362	0.409234
H	3.200573	0.186444	1.648364	H	1.268109	-2.391986	2.050824
C	2.638459	1.986684	0.578515	C	2.785445	-1.991723	0.597017
H	1.811754	2.677906	0.426279	H	3.372678	-1.239242	1.120810
C	3.819020	2.303125	0.011045	C	3.433206	-2.796041	-0.265561
C	3.951829	3.547609	-0.829056	C	4.914387	-2.631846	-0.493294
H	4.686380	4.226728	-0.383259	H	5.445127	-3.547360	-0.211294
H	4.320293	3.306963	-1.831801	H	5.129859	-2.461973	-1.553549
H	3.006854	4.083955	-0.924655	H	5.331182	-1.805330	0.083984
C	5.094564	1.517599	0.173287	C	2.801422	-3.923243	-1.039959
H	5.831120	2.121805	0.713635	H	3.229828	-4.878003	-0.716595
H	4.975022	0.581606	0.718579	H	1.719843	-3.989663	-0.925906
H	5.537693	1.296567	-0.803156	H	3.027566	-3.828468	-2.106755
H	2.640311	-1.602126	-1.657953	H	-2.624855	-1.057238	2.480833

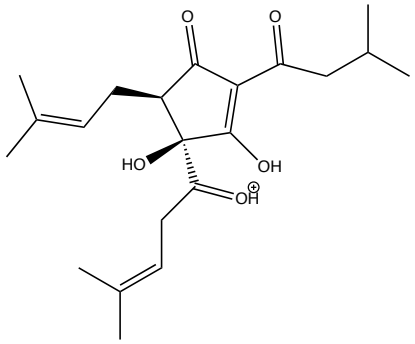

Isomer 7

C	0.354100	-0.072273	1.040594
C	-1.016251	-0.362398	0.418721
C	-0.639099	-1.044912	-0.949069

C	0.866786	-0.714869	-1.103336
C	1.378431	-0.166763	0.165817
H	-1.176504	-0.606863	-1.795777
O	1.472880	-0.923181	-2.127123
C	2.795442	0.282471	0.443140
C	3.910394	-0.648975	0.043584
H	3.716986	-0.989555	-0.981634
H	3.784788	-1.546221	0.669264
C	5.332323	-0.084695	0.187338
H	5.405648	0.383293	1.174701
C	6.357674	-1.224638	0.114098
H	7.373139	-0.838583	0.232020
H	6.191943	-1.968211	0.899512
H	6.310191	-1.739021	-0.851631
C	5.621364	0.987475	-0.872804
H	4.922758	1.823909	-0.803233
H	6.630081	1.388760	-0.746743
H	5.556862	0.565659	-1.881676
O	2.943924	1.359521	0.978788
O	0.404426	0.276884	2.319625
H	-0.391309	-0.040296	2.777182
C	-1.687080	0.953881	0.096452
C	-1.026116	2.119395	-0.572218
H	-0.271305	2.483533	0.140030
H	-0.434524	1.755876	-1.419367
C	-2.020476	3.176728	-0.984172
H	-2.461514	3.038234	-1.967974
C	-2.351187	4.282338	-0.283283
C	-3.327260	5.274767	-0.853624
H	-4.151978	5.453748	-0.157087
H	-2.829850	6.239221	-0.999927
H	-3.737957	4.952113	-1.810719
C	-1.774897	4.651707	1.056306
H	-1.248942	5.608267	0.973778
H	-2.575834	4.806167	1.786073
H	-1.075801	3.922436	1.466049
O	-2.902512	1.075913	0.444175
O	-1.773496	-1.083739	1.345617
H	-2.328891	-1.749163	0.893387
C	-0.894962	-2.570420	-0.956600
H	-0.325649	-3.041484	-0.153722
H	-0.465593	-2.929553	-1.898928
C	-2.360692	-2.921332	-0.892631
H	-2.986448	-2.399139	-1.615942
C	-2.955598	-3.850224	-0.120072
C	-4.433218	-4.118200	-0.251259

H	-4.941384	-3.993365	0.710683
H	-4.908468	-3.464520	-0.984214
H	-4.602793	-5.155471	-0.558814
C	-2.244387	-4.724927	0.879716
H	-1.194652	-4.472382	1.025245
H	-2.746318	-4.685570	1.851698
H	-2.291939	-5.768737	0.551211
H	-3.218271	1.978914	0.147710

Appendix III: DMS Ionograms Summary of Beers

Using the EPI mode to monitor the *m/z* signal, the separation voltage was set to SV = 3500 V, and the CV range was stepped from -35 V to 5 V in 0.25 V increments, the resulting ionogram of protonated humulone (100 ng/mL in MeOH/H_2O solvent) are observed in the N_2 environment seeded with IPA (see Figure A3.1).

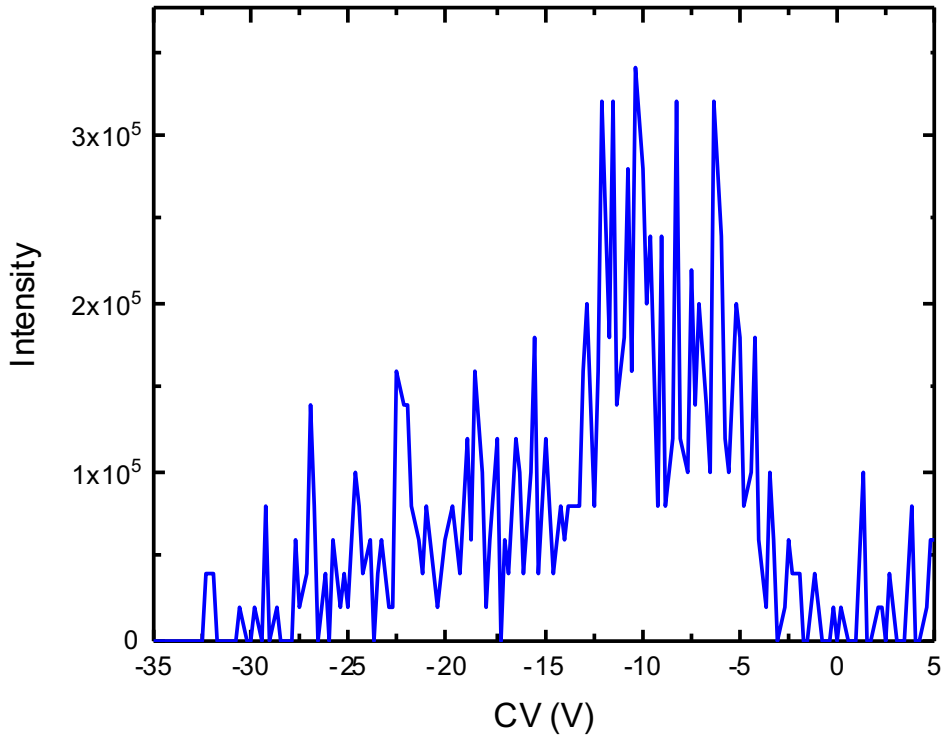

Figure A3.1. The ionogram of protonated humulone (*m/z* 363) recorded in a N_2 environment seeded with 1.5% (mol ratio) IPA at SV = 3500 V.

Table A3.1 shows beer samples' properties, including alcohol percentages, IBU provided by Innocente brewery, and hops styles.

Table A3.1. Beer Properties

Beer	Alcohol Percentage	IBU from Brewery	Hops
Two Night Stand	8.5 %	100	Double IPA*
Fling	5.0 %	25	Golden Ale
Kolsch	4.2 %	20	Lagered Ale
Bystander	4.7 %	53	American Pale Ale
Conscience	5.7 %	80	American IPA*
Batch-5 Dubbel Vision	7.9 %	18	Belgian Style Dubbel Ale
Inn Oslainte	5.2 %	18	Irish Red Ale

*IPA here stands for India Ale Pale

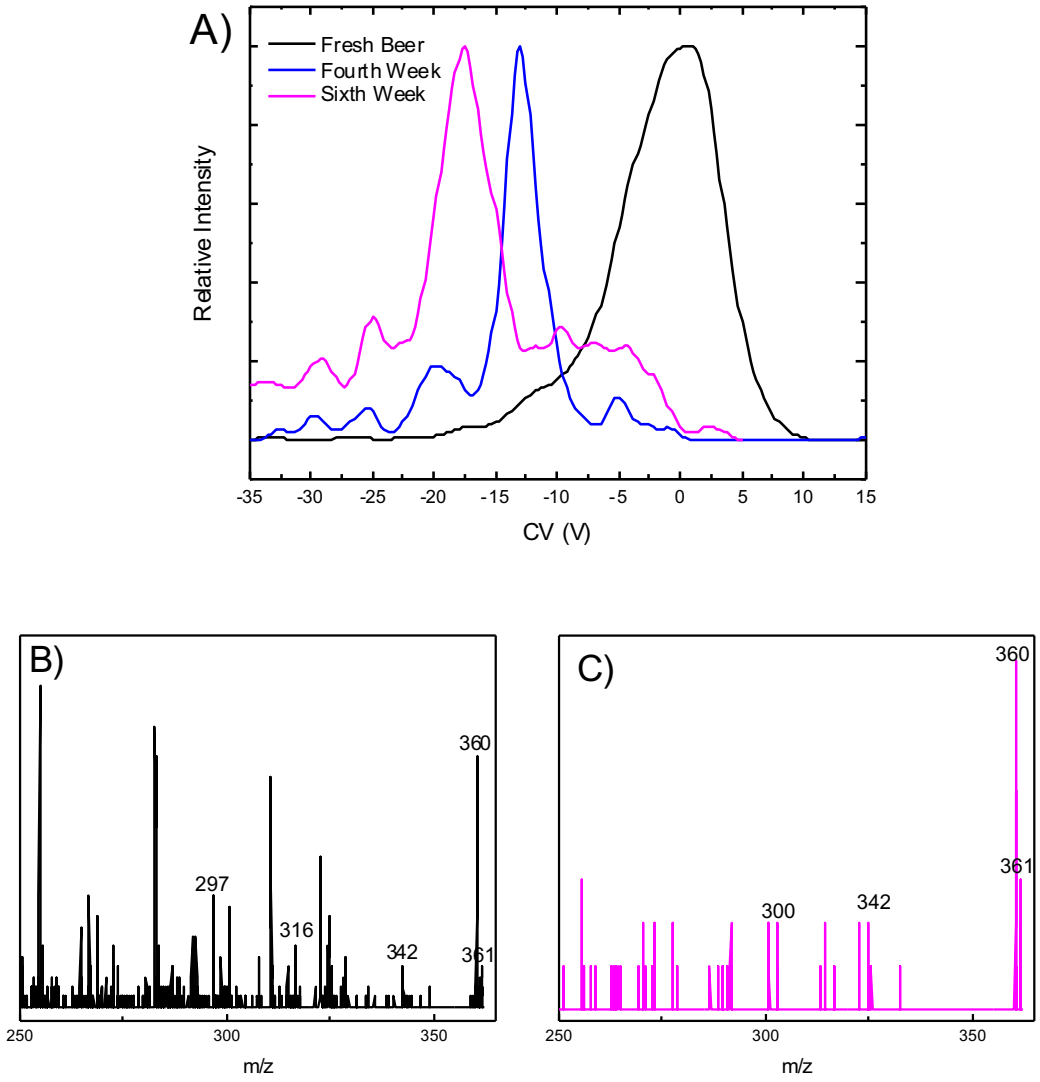

Figure A3.2. (A). The ionogram of Kolsch (KO) at 18 °C (black) when heated to 37 °C for four weeks (blue), and six weeks (pink). The beer was diluted to 100 ng/mL in 1:1 MeOH/H_2O solvent. Measurements were acquired in an N_2 environment seeded with 1.5% (mol ratio) IPA with SV = 3500 V. **(B).** The mass spectra associated with fresh beer. **(C).** The mass spectra associated with sixth week beer.

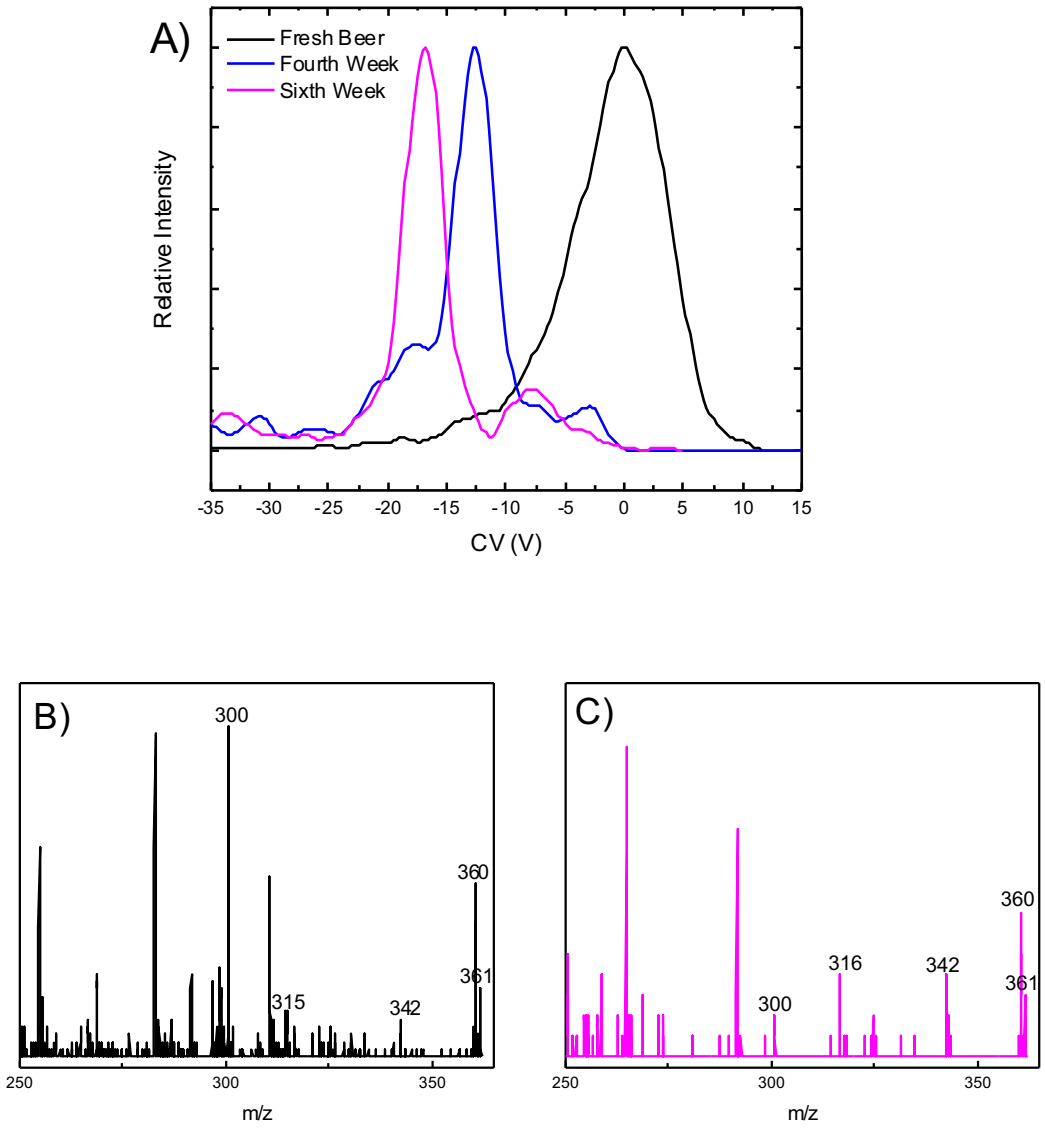

Figure A3.3. (A). The ionogram of Bystander (BS) at 18 °C (black) when heated to 37 °C for four weeks (blue), and six weeks (pink). The beer was diluted to 100 ng/mL in 1:1 MeOH/H_2O solvent. Measurements were acquired in an N_2 environment seeded with 1.5% (mol ratio) IPA with SV = 3500 V. **(B).** The mass spectra associated with fresh beer. **(C).** The mass spectra associated with sixth week beer.

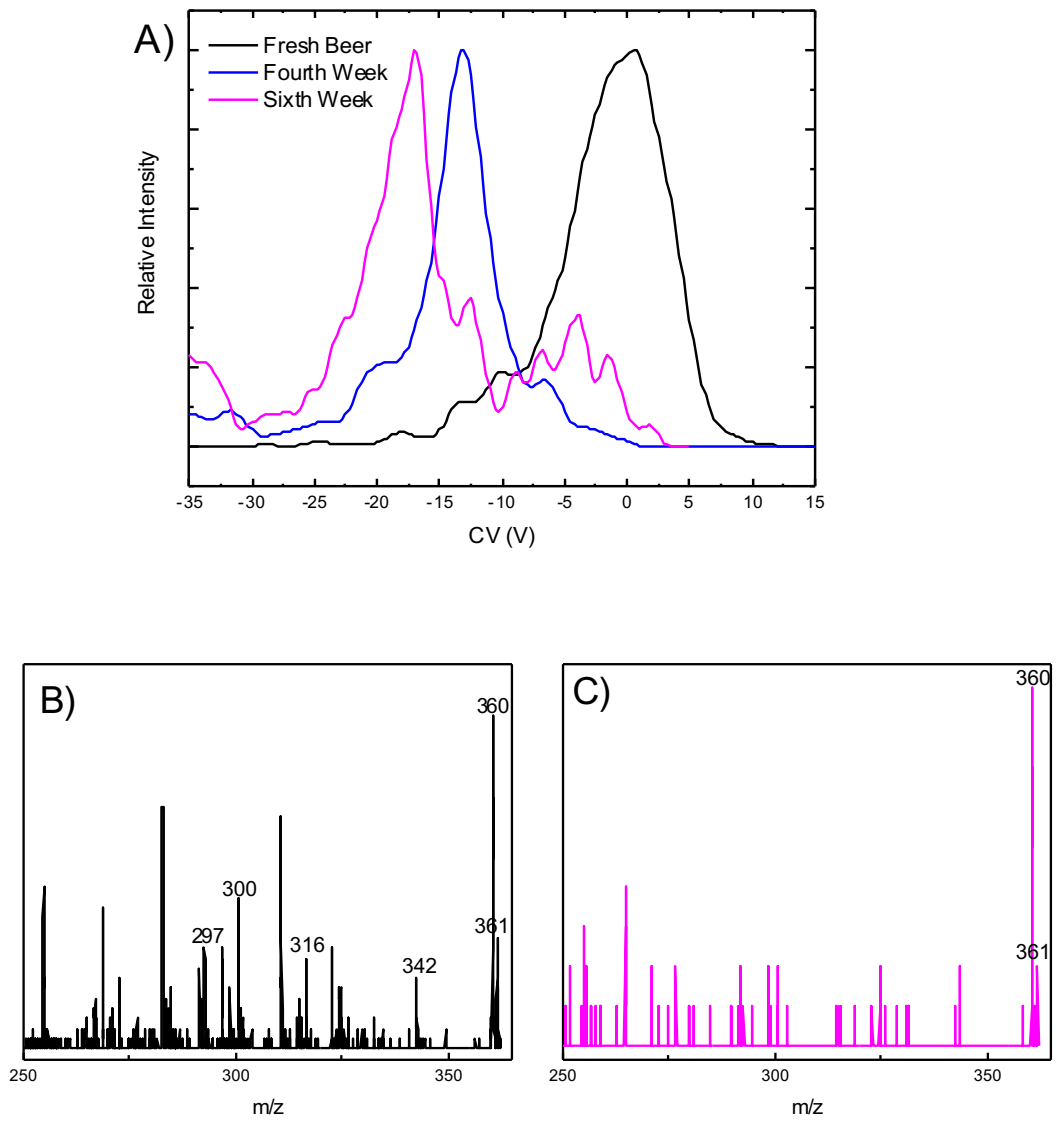

Figure A3.4. (A). The ionogram of Batch-5 Dubbel Vision (Bat) at 18 °C (black) when heated to 37 °C for four weeks (blue), and six weeks (pink). The beer was diluted to 100 ng/mL in 1:1 MeOH/H_2O solvent. Measurements were acquired in an N_2 environment seeded with 1.5% (mol ratio) IPA with SV = 3500 V. **(B).** The mass spectra associated with fresh beer. **(C).** The mass spectra associated with sixth week beer.

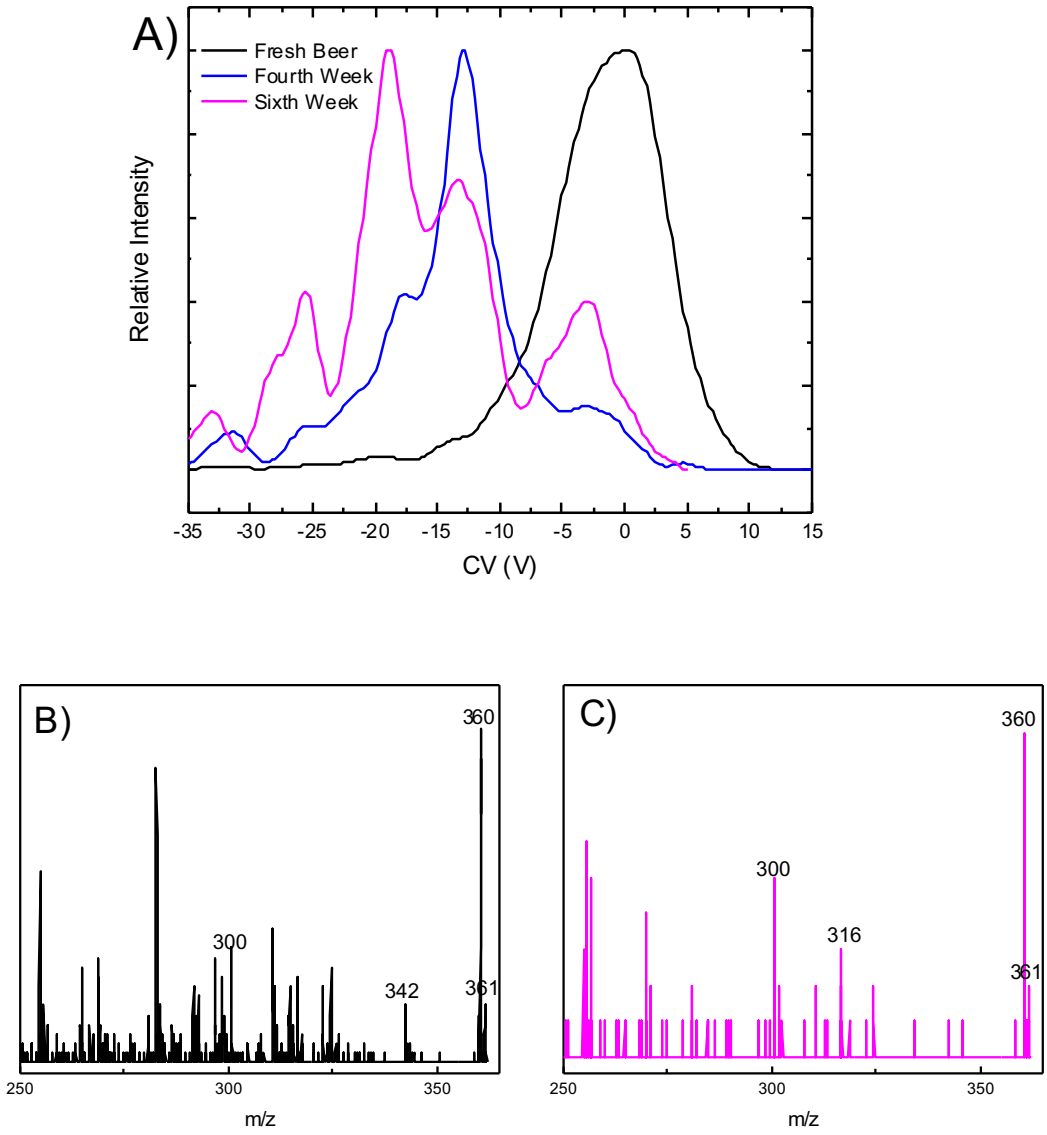

Figure A3.5. (A). The ionogram of Inn Oslainte (In) at 18 °C (black) when heated to 37 °C for four weeks (blue), and six weeks (pink). The beer was diluted to 100 ng/mL in 1:1 MeOH/H_2O solvent. Measurements were acquired in an N_2 environment seeded with 1.5% (mol ratio) IPA with SV = 3500 V. **(B).** The mass spectra associated with fresh beer. **(C).** The mass spectra associated with sixth week beer.